

25656



National Library of Canada

Bibliothèque nationale du Canada

CANADIAN THESES ON MICROFICHE

THÈSES CANADIENNES SUR MICROFICHE

NAME OF AUTHOR/NOM DE L'AUTEUR Claude LASSIGNE

TITLE OF THESIS/TITRE DE LA THÈSE Spin Relaxation and Molecular Motion in Liquid
CH₃Br, Hg(CH₃)₂ and Sn(CH₃)₄ and Deuterium Isotope
Shift for the Series Sn(CH₃)_{4-n}(CD₃)_n

UNIVERSITY/UNIVERSITÉ Simon Fraser University

DEGREE FOR WHICH THESIS WAS PRESENTED/
 GRADE POUR LEQUEL CETTE THÈSE FUT PRÉSENTÉE Doctor of Philosophy

YEAR THIS DEGREE CONFERRED/ANNÉE D'OBTENTION DE CE DEGRÉ 1975

NAME OF SUPERVISOR/NOM DU DIRECTEUR DE THÈSE Dr. E.J. Wells

Permission is hereby granted to the NATIONAL LIBRARY OF CANADA to microfilm this thesis and to lend or sell copies of the film.

L'autorisation est, par la présente, accordée à la BIBLIOTHÈQUE NATIONALE DU CANADA de microfilmer cette thèse et de prêter ou de vendre des exemplaires du film.

The author reserves other publication rights, and neither the thesis nor extensive extracts from it may be printed or otherwise reproduced without the author's written permission.

L'auteur se réserve les autres droits de publication; ni la thèse ni de longs extraits de celle-ci ne doivent être imprimés ou autrement reproduits sans l'autorisation écrite de l'auteur.

DATED/DATÉ 23/1/75 SIGNED/SIGNÉ

PERMANENT ADDRESS/RÉSIDENCE FIXÉE

SPIN RELAXATION AND MOLECULAR MOTION IN LIQUID

CH_2Br , $\text{Hg}(\text{CH}_3)_2$ AND $\text{Sn}(\text{CH}_3)_4$

AND

DEUTERIUM ISOTOPE SHIFT FOR THE SERIES $\text{Sn}(\text{CH}_3)_{4-n}(\text{CD}_3)_n$

by

CLAUDE R.G. LASSIGNE

B.Sc., California State College at Long Beach, 1970

A THESIS SUBMITTED IN PARTIAL FULFILMENT OF

THE REQUIREMENTS FOR THE DEGREE OF

DOCTOR OF PHILOSOPHY

in the Department

of

Chemistry

© CLAUDE R.G. LASSIGNE, 1975

SIMON FRASER UNIVERSITY

January, 1975

All rights reserved. This thesis may not be reproduced in whole or in part, by photocopy or other means, without permission of the author.

APPROVAL

Name: Claude R. G. Lassigne

Degree: Doctor of Philosophy

Title of Thesis: Spin Relaxation and Molecular Motion in Liquid
 CH_3Br , $\text{Hg}(\text{CH}_3)_2$ and $\text{Sn}(\text{CH}_3)_4$ and Deuterium
Isotope Shift for the Series $\text{Sn}(\text{CH}_3)_{4-n}(\text{CD}_3)_n$

Examining Committee:

Chairman: Dr. Lionel B. Funt

Dr. E. J. Wells
Senior Supervisor

Dr. J. Walkley

Dr. J.M. D'Auria

Dr. E.D. Crozier

Dr. R.R. Sharp
External Examiner
Associate Professor
University of Michigan

Date Approved: Jan 16, 1975

PARTIAL COPYRIGHT LICENSE

I hereby grant to Simon Fraser University the right to lend my thesis or dissertation (the title of which is shown below) to users of the Simon Fraser University Library, and to make partial or single copies only for such users or in response to a request from the library of any other university, or other educational institution, on its own behalf or for one of its users. I further agree that permission for multiple copying of this thesis for scholarly purposes may be granted by me or the Dean of Graduate Studies. It is understood that copying or publication of this thesis for financial gain shall not be allowed without my written permission.

Title of Thesis/Dissertation:

Spin Relaxation and Molecular Motion in Liquid CH₃Br,
Hg(CH₃)₂ and Sn(CH₃)₄ and Deuterium Isotope Shift for
the Series Sn(CH₃)_{4-n}(CD₃)_n

Author:

(signature)

Claude Lassigne

(name)

23/1/75

(date)

ABSTRACT

Spin-lattice relaxation times of ^1H , ^2D , ^{13}C , ^{119}Sn and ^{199}Hg have been measured over a wide temperature range in liquid CH_3Br , $\text{Hg}(\text{CH}_3)_2$, $\text{Sn}(\text{CH}_3)_4$ and their isotopic modifications. These measurements have allowed the separation of the relaxation mechanisms. It was found that the spin-rotation interaction mechanism contributes to ^1H and ^{13}C relaxation; and for both nuclei this mechanism is dominated by motion about the molecular figure axis. Estimates are given for the ^1H , ^{13}C , ^{119}Sn and ^{199}Hg spin-rotation constants. It is concluded that molecular reorientation about the symmetry axis is not well-described by molecular diffusion. Reorientation of the methyl group about the symmetry axis is much faster than reorientation of the symmetry axis for all molecules studied. It also shows that spin-rotation is the dominant mechanism for ^{119}Sn and ^{199}Hg relaxation and that the interaction becomes more important for the higher Z nuclei. The scalar relaxation mechanisms of ^1H and ^{13}C in methyl bromide allowed the estimation of several previously unreported scalar coupling constants. We found, $J_{^1\text{H}-^{79}\text{Br}} = 13 \pm 4$ Hz, $J_{^1\text{H}-^{81}\text{Br}} = 14 \pm 4$ Hz ; $J_{^{13}\text{C}-^{79}\text{Br}} = 30 \pm 4$ Hz and $J_{^{13}\text{C}-^{81}\text{Br}} = 32 \pm 4$ Hz.

The members of the series $\text{Sn}(\text{CH}_3)_{4-n}(\text{CD}_3)_n$ were prepared to study the effect of changes in the moments of inertia upon

the spin-rotation dominated T_1 of the ^{119}Sn nucleus. The results demonstrated that the spin-rotational relaxation time varies directly as $I^{\frac{1}{2}}$ and thus in the rotational diffusion limit molecular reorientation times vary as $I^{\frac{1}{2}}$. The preparation of these compounds allowed us to study the successive deuterium isotope effects on the ^1H , ^{13}C and ^{119}Sn chemical shifts and spin-spin coupling constants. The ratio $J_{\text{X-H}} / J_{\text{X-D}}$ (where $X = ^1\text{H}$, ^{13}C and ^{119}Sn) is always very close to the value predicted from the gyromagnetic ratios ($\gamma_{\text{H}} / \gamma_{\text{D}} = 6.5144$). On the average the values of $J_{\text{X-H}}$ are slightly higher than $6.5144 J_{\text{X-D}}$; however they are within the range of experimental error. All chemical shifts (^1H , ^{13}C and ^{119}Sn) were upfield on successive deuteration through the series. Proton isotope shifts were 0.017-0.030 ppm, carbon-13 isotope shifts were 0.088-0.352 ppm for secondary and 0.700 ppm for primary effects, while tin-119 isotopic shifts were 0.8-2.9 ppm. The size of this isotopic shift reflects the chemical shift range for the particular nucleus. This chemical shift range is the paramagnetic contribution to the total shielding constant. Since the paramagnetic term increases roughly as the $4/3$ power of Z the tin-119 nucleus will have the largest chemical shift range (2000 ppm) and is thus more sensitive to changes brought on by deuteration. The T_1 's and chemical shifts of a variety of tin compounds have been surveyed. The results show the very large chemical

shift range for tin-119 and the rather short T_1 values. There is a trend from our data which shows a correlation of $T_1^{SR}(^{119}\text{Sn})$ with the paramagnetic term of the shielding tensor for the tin-119 nucleus. A series of ^{119}Sn resonances has also been observed when anhydrous SnCl_4 is dissolved in water. Tentative assignments have been made for the possible $\text{Sn}(\text{Cl})_{6-n}(\text{OH})_n^-$ species present in solution.

We have observed differential T_1 's for the inner and outer components of the ^{13}C quartet in $\text{Hg}(\text{CH}_3)_2$. We attribute this to probable symmetry effects in the dipole-dipole dominated T_1 of the carbon-13 spin.

To my parents

ACKNOWLEDGEMENT

The author wishes to sincerely thank Dr. E.J. Wells for his interest and constant approachability during the period this research was done. This work owes much to the guidance and inspiration of Dr. E.J. Wells.

I should also like to thank Dr. J. Walkley, Dr. J. D'Auria, Dr. E.D. Crozier and Dr. P.P. Sharp for their time serving as members of my dissertation committee.

Thanks also go to Dr. D. Maharajh for his helpful advice on the designing of the apparatus employed for degassing of samples.

The assistance of Mr. P. Hatch, Mr. R. Morgan and Mr. A. Cutteridge in the construction of the glass apparatus is also acknowledged.

Thanks also go to my colleagues in the laboratory for their many stimulating discussions and enjoyable fishing and hunting expeditions.

Last but not least, I want to express my thanks to my wife, Wendy, for her support and understanding.

TABLE OF CONTENTS

Examining Committee Approval	ii
Abstract	iv
Dedication	.vii
Acknowledgements	viii

CHAPTER	PAGE
1. MECHANISM OF SPIN-LATTICE RELAXATION	1
A. Spectral Density and Auto-Correlation Functions	2
B. Dipole-Dipole Relaxation	5
1. Intramolecular dipole-dipole	5
2. Intermolecular dipole-dipole	6
C. Quadrupolar Relaxation	8
D. Chemical Shift Anisotropy	9
E. Spin-Rotation Relaxation	10
F. Relaxation by Scalar Coupling	11
2. ANISOTROPIC MOLECULAR REORIENTATION IN LIQUID	
METHYL BROMIDE	13
A. Introduction	13
B. Experimental	19
C. Results and Analysis	23
1. General Approach	23
2. Anisotropic rotational reorientation tensor	
for CD ₃ Br	28

3. Proton relaxation	35
a. Translational diffusion	37
b. Proton intramolecular dipole-dipole	39
c. Proton scalar relaxation	40
4. ^{13}C Spin-lattice relaxation	45
5. Proton Spin-rotation interaction	56
3. ANISOTROPIC ROTATIONAL DIFFUSION IN $\text{Hg}(\text{CH}_3)_2$	62
A. Introduction	62
B. Experimental	63
1. Measurement of relaxation times	63
2. Synthesis of $\text{Hg}(\text{CD}_3)_2$	66
3. Spin-spin coupling constants and chemical shifts in $\text{Hg}(\text{CH}_3)_2$ and $\text{Hg}(\text{CD}_3)_2$	68
C. Results and Analysis	70
1. Proton relaxation	73
2. Anisotropic rotational diffusion tensor for $\text{Hg}(\text{CD}_3)_2$	74
3. ^{199}Hg spin-lattice relaxation	81
D. Discussion	83
1. Proton-proton intermolecular relaxation	83
2. ^{199}Hg spin-rotation constant	85
3. Absolute shielding scale of ^{199}Hg	88
4. MAGNETIC RELAXATION STUDIES OF $\text{Sn}(\text{CH}_3)_4$	92
A. Experimental	92
1. Measurement of relaxation times	92
2. Synthesis of $\text{Sn}(\text{CD}_3)_4$ and $\text{Sn}(\text{CH}_3)_{4-n}(\text{CD}_3)_n$	95

B. Relaxation Studies	96
1. ^{13}C and ^2D spin-lattice relaxation	96
2. ^1H relaxation	103
3. ^{119}Sn relaxation in $\text{Sn}(\text{CH}_3)_4$	110
4. ^{119}Sn relaxation in the series $\text{Sn}(\text{CH}_3)_{4-n}$ $(\text{CD}_3)_n$	115
5. Carbon-13 spin-rotation interaction	119
6. Proton spin-rotation interaction	121
5. DEUTERIUM ISOTOPE EFFECTS IN THE ^1H , ^{13}C AND ^{119}Sn NMR SPECTRA FOR THE SERIES $\text{Sn}(\text{CH}_3)_{4-n}(\text{CD}_3)_n$	123
A. Introduction	123
B. Experimental	124
C. Results	133
1. Proton NMR	133
2. ^{13}C NMR	135
3. ^{119}Sn NMR	140
6. HIGH RESOLUTION ^{119}Sn NMR STUDIES BY PULSE FOURIER TRANSFORM	145
A. Survey of Chemical Shifts and T_1 's	145
B. Results and Discussion	146
1. Chemical shifts	146
2. Linewidths or T_2 relaxation	147
3. Spin-lattice relaxation times (T_1)	150
C. Study of Hydrolysis Equilibria Products of $\text{Sn}(\text{IV})\text{Cl}_4$ by ^{119}Sn NMR	153

1. Hydrolysis	153
2. Characterization of the species	156
D. Further Work	164
7. SYMMETRY EFFECTS IN ^{13}C T ₁ RELAXATION IN METHYL GROUPS	165
A. Results	165
B. Discussion	171
APPENDIX A	176
APPENDIX B	177
BIBLIOGRAPHY	179

LIST OF TABLES

TABLE	PAGE
2-1. R_1 relaxation data for liquid methyl bromide	25
2-2. Density and viscosity data for liquid CH_3Br	31
2-3. Theoretical and experimental values for $T_{1\text{inter}}^{\text{H-H}}$	38
2-4. Geometric parameters and moments of inertia for methyl bromide	41
2-5. Contributions to the ^{13}C relaxation time in pure CH_3Br at $+5^\circ\text{C}$.	48
2-6. Contributions* to the ^1H relaxation time in pure CH_3Br at $+5^\circ\text{C}$.	61
3-1. Nuclear spin-spin coupling constants in $\text{Hg}(\text{CH}_3)_2$ and $\text{Hg}(\text{CD}_3)_2$	69
3-2. R_1 relaxation data for liquid $\text{Hg}(\text{CH}_3)_2$ - $\text{Hg}(\text{CD}_3)_2$ mixtures	71
3-3. Geometric parameters and moments of inertia for $\text{Hg}(\text{CH}_3)_2$	79
3-4. Density and viscosity data for liquid $\text{Hg}(\text{CH}_3)_2$	84
3-5. Theoretical and Experimental values for $T_{1\text{inter}}^{\text{H-H}}$	85
4-1. ^{13}C and ^2D relaxation for tetramethyltin	98
4-2. Geometric parameters and moments of inertia for $\text{Sn}(\text{CH}_3)_4$	99
4-3. ^1H and ^{119}Sn relaxation data for liquid $\text{Sn}(\text{CH}_3)_4$	105
4-4. Comparison of computed σ'_p and observed chemical shifts in $\text{Sn}(\text{CH}_3)_4$, SnCl_4 and SnI_4	114

4-5.	Moments of inertia for the molecules of the series $\text{Sn}(\text{CH}_3)_{4-n}(\text{CD}_3)_n$	116
4-6.	$T_1(^{119}\text{Sn})$ for the molecules $\text{Sn}(\text{CH}_3)_{4-n}(\text{CD}_3)_n$	117
4-7.	Spin-rotation constants of ^{119}Sn for the series $\text{Sn}(\text{CH}_3)_{4-n}(\text{CD}_3)_n$	118
4-8.	Values used to calculate the proton spin-rotation constants at 313°K	122
5-1.	^1H chemical shifts and spin-spin coupling constants	134
5-2.	^{13}C chemical shifts for the $\text{Sn}(\text{CH}_3)_{4-n}(\text{CD}_3)_n$ series of compounds.	137
5-3.	J 's involving ^{13}C in the series $\text{Sn}(\text{CH}_3)_{4-n}(\text{CD}_3)_n$	138
5-4.	^{119}Sn chemical shifts coupling constants for the series $\text{Sn}(\text{CH}_3)_{4-n}(\text{CD}_3)_n$	141
6-1.	^{119}Sn chemical shifts, T_1 's and T_2 's	152
6-2.	Assigned chemical shifts and linewidths for the various $^{119}\text{SnCl}_n(\text{OH})_{6-n}^-$ species	158

LIST OF FIGURES

FIGURE	PAGE
1-1. The spectral density function $J(\omega)$ of a random fluctuation with an exponentially decaying autocorrelation function and a mean square value of one	4
2-1. High resolution 60 MHz proton spectra of 57.7% ^{13}C enriched methyl bromide	22
2-2. Experimental and derived relaxation times for ^1H in methyl bromide	26
2-3. Rotation rate constants (D_{\parallel}, D_{\perp}) for CD_3Br	32
2-4. ^2D spin-lattice relaxation rate in CD_3Br	33
2-5. Separation of the proton intramolecular relaxation in CH_3Br into its intramolecular dipole-dipole and spin-rotation rates.	42
2-6. ^{79}Br and ^{81}Br spin-lattice relaxation times calculated from dielectric results	44
2-7. Separation of ^{13}C intramolecular relaxation rate of CH_3Br into $R_{1\text{intra}}^{\text{dd}}$, R_1^{SR} , and $R_1^{\text{SC}}(^{79}\text{Br})$	47
2-8. Temperature dependence of the $R_1^{\text{SC}}(^{79}\text{Br})$ and $R_1^{\text{SC}}(^{81}\text{Br})$ contributions to the carbon-13 relaxation rate	58

2-9.	Relocation of the proton from the z-axis to the y-axis to obtain θ value necessary for the calculation of the spin-rotation contribution from the proton nucleus which lies <u>off</u> the principal axis	58
3-1.	^1H spectrum of neat liquid $\text{Hg}(\text{CH}_3)_2$ at 60 MHz	65
3-2.	Experimental relaxation rates for ^1H in $\text{Hg}(\text{CH}_3)_2$	72
3-3.	Separation of $R_{1\text{inter}}^{\text{H-H}}$ from $R_{1\text{intra}}^{\text{dd}}$ for the proton relaxation rate in $\text{Hg}(\text{CH}_3)_2$	75
3-4.	^2D spin-lattice relaxation rate in $\text{Hg}(\text{CD}_3)_2$	76
3-5.	Rotational rate constants (D_{\parallel}, D_{\perp}) for $\text{Hg}(\text{CD}_3)_2$	80
3-6.	^{199}Hg spin-lattice relaxation rate in $\text{Hg}(\text{CH}_3)_2$	82
3-7.	Temperature dependent ellipses at 313 and 238 $^{\circ}\text{K}$ of C_{\parallel} and C_{\perp} for ^{199}Hg in $\text{Hg}(\text{CH}_3)_2$	90
3-8.	^{199}Hg shielding scales (experimental and theoretical)	91
4-1.	High resolution 60 MHz ^1H spectrum of $\text{Sn}(\text{CH}_3)_4$	94
4-2.	Carbon-13 spin-lattice relaxation of $\text{Sn}(\text{CH}_3)_4$ and its separation into R_1^{dd} and R_1^{SR}	100
4-3.	^2D spin-lattice relaxation rate in $\text{Sn}(\text{CD}_3)_4$	101
4-4.	Temperature dependence of $\tau_c(^2\text{D})$ and $\tau_c(^{13}\text{C-H})$	102
4-5.	Experimental and derived proton relaxation rates in tetramethyl tin	106
4-6.	Temperature dependence of τ_{θ} and τ_M in $\text{Sn}(\text{CH}_3)_4$	107

4-7.	Separation of the proton intramolecular and spin-rotation rates	109
4-8.	^{119}Sn spin-lattice relaxation in $\text{Sn}(\text{CH}_3)_4$	111
5-1.	Simulated (transparency) and experimental ^{13}C NMR spectra at 15.063710 MHz of a mixture of $\text{Sn}(\text{CH}_3)_4$ and $\text{Sn}(\text{CD}_3)_4$	125
5-2.	Simulated (transparency) and experimental ^{13}C NMR spectra at 15.063710 MHz of $\text{Sn}(\text{CH}_3)_3(\text{CD}_3)$	126
5-3.	Simulated (transparency) and experimental ^{13}C NMR spectra at 15.063710 MHz of $\text{Sn}(\text{CH}_3)_2(\text{CD}_3)_2$	127
5-4.	Simulated (transparency) and experimental ^{13}C NMR spectra at 15.063710 MHz of $\text{Sn}(\text{CH}_3)(\text{CD}_3)_3$	128
5-5.	Experimental ^{119}Sn NMR spectra at 15.044368 MHz of a mixture of $\text{Sn}(\text{CH}_3)_4$ and $\text{Sn}(\text{CD}_3)_4$	129 ^l
5-6.	Simulated (transparency) and experimental ^{119}Sn NMR spectra at 15.044368 MHz of $\text{Sn}(\text{CH}_3)_3(\text{CD}_3)$	130
5-7.	Simulated (transparency) and experimental ^{119}Sn NMR spectra at 15.044368 MHz of $\text{Sn}(\text{CH}_3)_2(\text{CD}_3)_2$	131
5-8.	Simulated (transparency) and experimental ^{119}Sn NMR spectra at 15.044368 MHz of $\text{Sn}(\text{CH}_3)(\text{CD}_3)_3$	132
5-9.	Plot of $\delta(^{13}\text{C})$ vs n in $\text{Sn}(\text{CH}_3)_{4-n}(\text{CD}_3)_n$	139
5-10.	Plot of $\delta(^{119}\text{Sn})$ vs n in $\text{Sn}(\text{CH}_3)_{4-n}(\text{CD}_3)_n$	142
6-1.	High resolution ^{119}Sn NMR spectra at 15.05 MHz of 5M $\text{Sn}(\text{CH}_3)_3\text{Cl}$ in CCl_4	148

6-2.	Possible cis and trans isomers of the dichloro, trichloro and tetrachlorohydroxo tin species	155
6-3.	Typical ^{119}Sn NMR spectra of the chlorohydroxo tin species	157
7-1.	Plot of $180^\circ\text{-}\tau\text{-}90^\circ$ pulse sequence in the proton undecoupled ^{13}C quartet of natural abundance $^{13}\text{CH}_3\text{CN}$	167
7-2.	Plot of $180^\circ\text{-}\tau\text{-}90^\circ$ pulse sequence in the proton undecoupled ^{13}C quartet of natural abundance $\text{Hg}(^{13}\text{CH}_3)(\text{CH}_3)$	168
7-3.	Plot of $180^\circ\text{-}\tau\text{-}90^\circ$ sequence for $\tau = 8.5$ sec in the ^{13}C quartet of $\text{Hg}(\text{CH}_3)_2$ (1000 scans)	169
7-4.	Plot of $180^\circ\text{-}\tau\text{-}90^\circ$ sequence for $\tau = 8.7, 8.8$ and 9.0 sec in the ^{13}C quartet of $\text{Hg}(\text{CH}_3)_2$	170
7-5.	Sketch showing the possible processes for energy transfer to the lattice in a) CH_3CN and b) $\text{Hg}(\text{CH}_3)_2$	172
7-6.	I-Spin resonance quartet	174

CHAPTER 1

MECHANISM OF SPIN-LATTICE RELAXATION

When an ensemble of nuclear spins is placed in a strong magnetic field \vec{H}_0 , it will show a resulting equilibrium macroscopic magnetization given by,

$$(1-1) \quad \vec{M}_0 = \frac{N\gamma^2 \hbar^2 I(I+1)}{3kT} \vec{H}_0$$

At thermal equilibrium there is only a magnetization component parallel to the external magnetic field \vec{H}_0 , but no perpendicular components. However if we then apply a perturbation such as an rf field, $\vec{H}_1(t)$ to this equilibrium state and later remove it we can create an instantaneous magnetization $\vec{M}(t)$ which has both parallel and perpendicular components with respect to \vec{H}_0 . The evolutions of these components may often be characterized by the time constants T_1 and T_2 .

As described above the instantaneous magnetization $\vec{M}(t)$ has two components. The longitudinal component's (i.e. parallel to H_0) usual exponential recovery towards its equilibrium value is described by a characteristic value T_1 called the spin-lattice relaxation time which involves the transfer of energy between a spin and its surroundings (lattice). On the other hand the

perpendicular or transverse component has a decay described by a time constant called the spin-spin relaxation time (T_2) because it involves the transfer of energy from one spin to another within the spin system. These relaxation processes have been described by Bloch (1946) in terms of first order differential equations, which serve as phenomenological definitions of T_1 and T_2 .

$$(1-2) \quad \frac{dM_z}{dt} = - \frac{M_z - M_0}{T_1}$$

$$(1-3) \quad \frac{dM_{x,y}}{dt} = - \frac{M_{x,y}}{T_2}$$

A. Spectral density and auto-correlation functions

When some random function $f(t)$ with average value zero fluctuates in some time interval, then the time dependence of the statistical average is described by the autocorrelation function $G(\tau)$, which serves as a "memory function" of the fluctuation, averaged over the ensemble.

$$(1-4) \quad G(\tau) = \overline{f(t+\tau)f(t)}$$

$\tau \rightarrow 0$ then $G(\tau) \rightarrow \overline{|f(t)|^2}$ and conversely when τ becomes very large $G(\tau)$ approaches zero. Frequently $G(\tau)$ may be approximated as

an exponential decay with a correlation time τ_c ; then the auto-correlation function is assumed to have the form

(Carrington and Mc Lachlan 1967)

$$(1-5) \quad G(\tau) = \overline{f^*(t)f(t)} e^{-|\tau|/\tau_c}$$

The auto-correlation function $G(\tau)$ is related to the spectral density function $J(\omega)$ by a Fourier transformation (Carrington and Mc Lachlan 1967),

$$(1-6) \quad J(\omega) = \int_{-\infty}^{+\infty} G(\tau) e^{i\omega\tau} d\tau$$

Exponential correlation functions give only a crude description of most relaxation experiments in liquids. Nuclear magnetic relaxation experiments in the extreme narrowing limit $\omega_0\tau_c \ll 1$ yield only $\int_0^{\infty} G(\tau) d\tau$ and are thus unable to delineate possible finite structure in the autocorrelation functions; this effect may lead to incorrect conclusions when based on assumed exponentiality for $G(\tau)$. However faster time scale methods such as IR and Raman band contour analysis may be able to give detailed information about the shape of the auto-correlation function (Rothschild 1970).

If we assume an exponential decay for $G(\tau)$ we have

$$(1-7) \quad J(\omega) = \frac{2\tau_c}{1 + \omega^2\tau_c^2} \overline{f^*(t)f(t)}$$

The spectrum for this function is shown in Figure 1-1 (Poole and Faracah 1971).

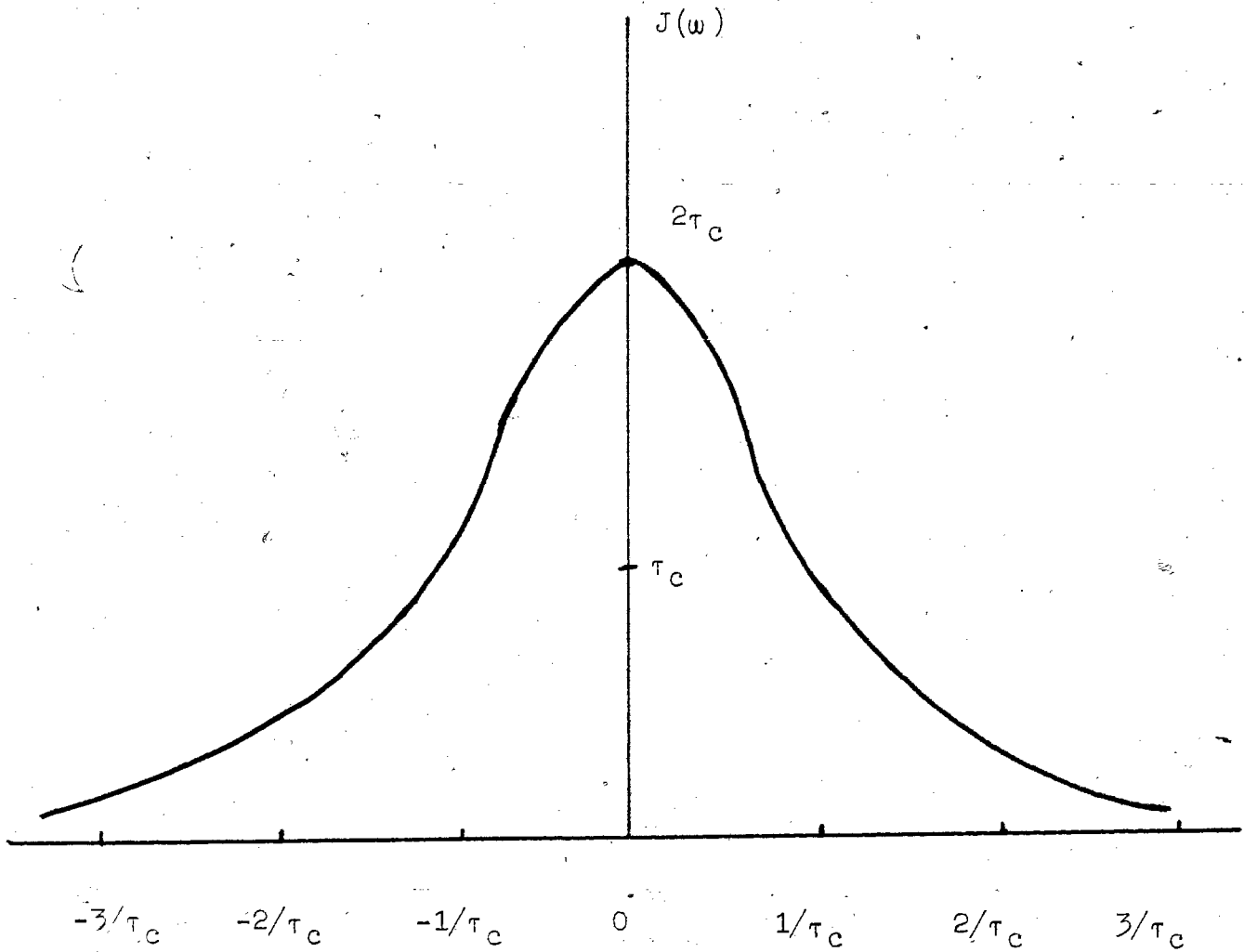


Figure 1-1 The spectral density function $J(\omega)$ of a random fluctuation with an exponentially decaying auto-correlation function and a mean square value of one.

B. Dipole-dipole relaxation

When the classical expression for the interaction energy of two magnetic dipoles is written in operator form, the interaction Hamiltonian is, in Cartesian tensor form:

$$(1-8) \quad \mathcal{H}_{dd}(t) = \sum_{i < j} \vec{I}(i) \cdot \vec{D}_{ij}(t) \cdot \vec{I}(j)$$

where $\vec{I}(i)$ and $\vec{I}(j)$ are the spin vector operators of the two nuclei. $\vec{D}_{ij}(t)$ is the dipolar interaction tensor between nuclei i and j , with components which depend on \vec{r} and the external field. The tensor components are time dependent in a coordinate system fixed by the external field, because of two reasons: i) if the two nuclei belong to the same molecule the distance \vec{r} is fixed but θ varies according to the rotation of the molecule, ii) if the nuclei belong to different molecules the relative translational motion makes \vec{r} also time dependent.

1. Intramolecular dipole-dipole

For rotational motion, which is all that is necessary for intramolecular dipole-dipole interactions, for like spins the longitudinal relaxation rate of magnetization of I spins is given by (Abragam 1961),

$$(1-9) \quad (R_1^I)_{\text{rot}} = (1/T_1)_{\text{rot}} = \frac{2\gamma^4 \hbar^2}{5r^6} I(I+1) \left[\frac{\tau_c}{1 + \omega_0^2 \tau_c^2} + \frac{4\tau_c}{1 + 4\omega_0^2 \tau_c^2} \right]$$

where γ is the gyromagnetic ratio of nuclei with spin I , ω_0 is the angular precession frequency of nuclei I and τ_c is the molecular correlation time. In mobile liquids where the relation $\omega_0 \tau_c \ll 1$ holds,

$$(1-10) \quad R_{1_{\text{rot}}} = \frac{2\gamma^4 \hbar^2}{r^6} I(I+1) \tau_c$$

This situation is called the extreme narrowing condition. For selective experiments on the I spins with dipole interaction between unlike spins (I and S) in the extreme narrowing limit, it is given as

$$(1-11) \quad (R_1^I)_{\text{rot}} = \frac{4}{3} \frac{\hbar^2 \gamma_I^2 \gamma_S^2}{r^6} S(S+1) \tau_c$$

Thus, the dipolar interaction is related to molecular geometry via the rapid r dependence. However the correlation time is difficult to determine and will be discussed in more detail in a later section.

2. Intermolecular dipole-dipole

The intermolecular contribution depends on the same motions as those for intramolecular dipole-dipole as well as on the relative translational motions. Since these motions have different correlation times they lead to somewhat different expressions for the contribution of dipolar relaxation to R_1 .

Bloombergen, Purcell and Pound (1948) showed that the spin-lattice relaxation of a single nuclear spin ($I=1/2$) in a liquid is induced by the fluctuating local magnetic field of its neighbouring spins (assuming all nuclei are identical)

$$(1-12) \quad R_{1\text{trans}} = \frac{\pi \gamma^4 \hbar^2 N}{4aD_s}$$

where a is the molecular radius and D_s is the liquid's self-diffusion constant. Their results have now been generalized to systems with many nuclei by Gutowsky and Woessner (1956),

$$(1-13) \quad R_{1\text{trans}} = \frac{\pi \hbar^2 \gamma_i^2 N}{a^2} \left[6\gamma_i^2 \sum_j \frac{1}{r_{ij}} + \frac{16\gamma_f^2 I_f(I_f+1)}{3} \sum_f^* \frac{1}{r_{if}} \right] \tau_t$$

where γ is the gyromagnetic ratio of the nucleus, r is the internuclear distance, N is the number of molecules per unit volume and a is an average spherical molecular radius. The summation Σ is over nuclei of the same type as i and Σ^* over all others. The translational relaxation time in Eq. (1-13) is given by

$$(1-14) \quad \tau_t = a^2 / 12 D_s$$

These self-diffusion constants may be known or can be estimated

using Gierer and Wirtz's (1953) formula for the translational diffusion constant of a spherical molecule with radius r_0 in a spherical solvent of radius r_s and viscosity η ,

$$(1-15) \quad D_{\text{trans}} = kT / \beta_t$$

β_t is the translational friction constant.

$$(1-16) \quad \beta_t = 6\pi\eta r_0 f_t$$

where f_t is the translational microviscosity factor.

$$(1-17) \quad f_t = \left(\frac{3}{2}(r_s/r_0) + \frac{1}{(1 + r_s/r_0)} \right)^{-1}$$

Although these formulas were derived for spheres they are commonly used and work well for non-spherical molecules.

C. Quadrupolar relaxation

Nuclei with spin I greater than $1/2$ possess electric quadrupole moments eQ . The interaction of the quadrupole moment with the molecule-fixed electric field gradients provides a very efficient relaxation path. In this case the interaction Hamiltonian is given by,

$$(1-18) \quad \mathcal{H}_A(t) = \vec{I} \cdot \vec{A}(t) \cdot \vec{I}$$

the tensor \vec{A} of rank 2 is time dependent because of the rotation of the molecule. The translational motion is not important because the field gradients arise from charge distributions within the molecule to which the nucleus belongs. For the case of molecular reorientation and in the limit that $\omega_0 \tau_c \ll 1$, it can be shown that (Abragam 1961),

$$(1-19) \quad R_{1Q} = \frac{3\pi^2(2I+3)}{10 I^2(2I-1)} \left(1 + \frac{\eta^2}{3}\right) (e^2qQ/h)^2 \tau_c$$

where I is the spin for the nucleus, η is the field gradient asymmetry [$\eta = (a_{xx} - a_{yy})/a_{zz}$], (e^2qQ/h) is the quadrupole coupling constant in Hz and τ_c is the molecular correlation time.

D. Chemical shift anisotropy

It is well known that a nucleus does not experience the laboratory applied magnetic field H_0 but instead a local field,

$$(1-20) \quad \vec{H}_{local} = \vec{H}_0(1 - \vec{\sigma})$$

where $\vec{\sigma}$ is called the shielding tensor. The interaction Hamiltonian may be written as,

$$(1-21) \quad \mathcal{H}_{CSA} = \gamma \vec{H}_0 \cdot \vec{\sigma} \cdot \vec{I}$$

The amount of shielding depends on the orientation of the molecule but in isotropic liquids and gases the average value σ is detected as a field or frequency shift

$$(1-22) \quad \sigma = \frac{1}{3} (\sigma_{xx} + \sigma_{yy} + \sigma_{zz})$$

The nucleus on the average sees a chemical shift given by σ , however on a shorter time scale it sees fluctuations in the local magnetic field. Therefore if $\sigma_{xx}, \sigma_{yy}, \sigma_{zz}$ are not equal (i.e. anisotropic), this provides a relaxation mechanism. The magnitude of this mechanism is,

$$(1-23) \quad R_{1\text{csa}} = \left(\frac{1}{15} \right) \gamma^2 H_0^2 (\sigma_{\parallel} - \sigma_{\perp})^2 \left[\frac{2\tau_c}{1 + \omega_0^2 \tau_c^2} \right]$$

in the limit $\omega_0 \tau_c \ll 1$

$$(1-24) \quad R_{1\text{csa}} = \left(\frac{2}{15} \right) \gamma^2 H_0^2 (\sigma_{\parallel} - \sigma_{\perp})^2 \tau_c$$

E. Spin-rotation relaxation

This is the interaction of a nuclear magnetic moment with the magnetic field produced at the position of the nucleus by the rotation of the molecule containing the nucleus. The interaction Hamiltonian can be written as,

$$(1-25) \quad \mathcal{H}_{\text{sr}} = \vec{I} \cdot \vec{C}(t) \cdot \vec{J}(t)$$

where \vec{I} is the nuclear spin operator, \vec{J} is the molecular angular momentum operator and \vec{C} is the spin-rotation tensor consisting of ranks 0, 1 and 2. For liquids undergoing isotropic molecular reorientation by rapid rotational diffusion, the relaxation rate is given by (Hubbard 1963)

$$(1-26) \quad R_1^{SR} = \frac{8\pi^2 I k T}{h^2} C_{\text{eff}}^2 \tau_w$$

where $C_{\text{eff}}^2 = \frac{1}{3}(2C_{\perp}^2 + C_{\parallel}^2)$ and τ_w is the angular momentum correlation time which is a measure of the time a molecule spends in any given angular momentum state.

F. Relaxation by scalar coupling

Scalar coupling is the intramolecular nuclear magnetic coupling found in multiplet splitting of high resolution NMR. This coupling is a source of relaxation for spin I if either the coupling constant A or spin S are time dependent. The hyperfine coupling Hamiltonian is given by,

$$(1-27) \quad \mathcal{H}_{\text{scalar}} = \vec{I} \cdot \vec{R}(t) \cdot \vec{S}(t)$$

R can be time dependent as a result of chemical exchange and S can also be time dependent if S relaxes rapidly, for this second case the splitting of S on I is not observed. The relaxation rate due to scalar coupling of

spin I modulated by relaxation of S is given by Abragam (1961)

$$(1-28) \quad R_1^{SC} = \frac{2}{3} A^2 S(S+1) \left[\frac{T_{2S}}{1 + (\omega_I - \omega_S)^2 T_{2S}^2} \right]$$

$$(1-29) \quad R_2^{SC} = \frac{1}{3} A^2 S(S+1) \left[T_{1S} + \frac{T_{2S}}{1 + (\omega_I - \omega_S)^2 T_{2S}^2} \right]$$

where $A = 2\pi J$, T_{1S} and T_{2S} are the longitudinal and transverse relaxation times of nucleus S, ω_I and ω_S are the Larmor frequencies of nucleus I and S. From this equation we can see that unless T_{2S} is of the same order as $(\omega_I - \omega_S)$ and $2\pi J$ is large the R_1^{SC} contribution will be negligibly small.

CHAPTER 2

ANISOTROPIC MOLECULAR REORIENTATION IN LIQUID
METHYL BROMIDE

A. Introduction

A considerable amount of work, both experimental and theoretical, has been devoted over the past decade to the problems of molecular reorientation and molecular collision dynamics in liquids and dense gases (Gordon 1968). An increasing number of experimental techniques are being brought to bear on these problems, and now include IR and Raman band shape contours (Gordon 1966, Rothschild 1969, 1970, 1972, and Goldberg and Pershan 1973), neutron scattering (Egelstaff et al. 1971), dielectric relaxation (Poole and Farach 1970), and magnetic relaxation (Poole and Farach 1970). An important dynamic parameter which is obtained from these methods is the molecular orientation correlation time $\tau_{e,l}$, which is a measure of the orientation memory time of an individual molecule against space-fixed axes. Here l denotes the order of the spherical harmonic of the relevant interaction; $l = 1$ for reorientation of a vector such as the electric dipole moment appropriate to the IR lineshape and dielectric relaxation problems, whereas $l = 2$ for the tensor reorientations applying to Raman lineshapes or magnetic relaxation dominated by dipole-dipole or quadrupole interactions.

A second parameter of interest which relates to the microscopic dynamics is the correlation time τ_w of the molecular angular momentum or angular velocity. This has been considerably more difficult to monitor, but may in suitable cases be obtained from magnetic relaxation due to spin-rotation interaction. Classically this interaction arises from the coupling of a nuclear magnetic dipole with the magnetic field produced by the rotation of a molecular electric quadrupole. If independent information (from, for example, molecular beam studies) is available on the magnitude of the coupling constant, then measurement of the nuclear spin-lattice relaxation time leads fairly directly to a value for τ_w . Such studies are exemplified by the elegant work on liquid ClO_2F by Maryott et al. (1971).

The importance of simultaneous measurement of $\tau_{\theta, \ell}$ and τ_w is that the relationship between these microscopic parameters is model-dependent, and thus together they give insight to the state of molecular motion. Early workers assumed an isotropic hydrodynamic model (Debye 1929), the so-called ~~rotational~~ rotational diffusion model, in which the angular velocity changes rapidly ($\tau_w \ll \tau_{\theta, \ell}$) and the orientation changes by a succession of small Brownian steps. In this limit

$$(2-1) \quad \tau_{\theta, 1} = 3\tau_{\theta, 2}$$

and the autocorrelation function for angular position decays

exponentially. Hubbard (1963) later showed that in the same limit $\tau_{\theta, \ell}$ and τ_w are inversely related

$$(2-2) \quad \tau_{\theta, \ell} \tau_w = \frac{I}{[\ell(\ell+1)]kT}$$

The limiting case of isotropic rotational diffusion has been extended into the gas-like region (Bloom 1967) where $\tau_w \equiv \tau_{\theta}$ may become comparable to $\tau_{\theta, \ell}$, but where the intermolecular torques represented by τ_{θ} act impulsively. This extended diffusion model was applied by Gordon (1966) to linear molecules, and further to spherical molecules by McClung (1969) and Fixman and Rider (1969). A feature of these theories is that a distinction can be made between J-diffusion, wherein both the magnitude and direction of the angular momentum is randomized upon collision, and M-diffusion, where only the orientation of the molecular angular momentum is randomized. In those few cases where a critical experimental test has been made to date, weakly or non-polar linear or quasi-spherical molecules in the liquid phase outside the rotational diffusion limit appear to obey J-diffusion dynamics [ClO_3F (Maryott et al. 1971, CCl_4 (Gillen et al. 1972), CS_2 (Spriss et al. 1971, Pines et al. 1971), CCl_2F (Gillen et al. 1972)]. Very recently the entire treatment of isotropic molecular dynamics in liquids has been unified (Kivelson and Keyes 1972) by relaxation of the impulsive torque condition to include long duration torques but impulsive changes in the torques.

This limit corresponds to the solid-like cell theory of liquids yielding torsional oscillations in the molecular orientation, and is the one appropriate to Ivanov's (1964) description of reorientation in the liquid phase, later used by O'Reilly (1968,1971,1972) and Atkins (1969).

The rotational diffusion model of a liquid views the reorientational motion of a molecule as proceeding slowly via a large number of small angular steps, whereas in the free-gas and solid-like models large incoherent angular changes may take place during infrequent "collisions".

In this large angle step case, Eq.(2-1) evolves into $\tau_{\theta,1} \approx \tau_{\theta,2}$, Eq. (2-2) becomes invalid, and the autocorrelation function of θ approximates a gaussian decay. Nuclear magnetic relaxation studies of $\tau_{\theta,t}$ alone have limitations in probing such details of the microdynamics, for in the "extreme narrowing" limit, $\omega_0 \tau_{\theta} \ll 1$ (appropriate to dense gases and liquids) only the area of the angular correlation function is normally determined, and not its shape. Faster time-scale methods, such as IR and Raman lineshape studies, are preferable in this respect, but it now appears (Goldberg and Pershan 1973) that some of the earlier work (Rothschild 1969,1970,1972) along these lines is suspect because of neglect of vibration-rotation interaction. The picture that is emerging is that small symmetric non-polar molecules in their neat liquids [CH_4 and CD_4 (Bloom 1967), benzene axial

rotation (Gillen and Griffiths 1972), cyclohexane (O'Reilly et al. 1972), UF_6 (Bull and Jonas 1970), AsH_3 (Burnett and Zeltmann 1972)] undergo molecular reorientation that is not in the rotational diffusion limit, but rather in the so-called "inertial region" between rotational diffusion and the quantized free rotator. On the other hand, the presence of a moderate electric dipole in a (necessarily) asymmetric molecule sends the reorientation of the dipole axis into the diffusion limit (Goldberg and Pershan 1973, Gillen and Noggle 1970), even for a molecule as small as NH_3 (Atkins et al. 1969, Gillen and Noggle 1970). Moderately anisotropic molecules of intermediate size such as toluene (Kivelson and Keyes 1972) and chlorobenzene (O'Reilly 1971, Bull and Jonas 1970) may be in the solid-like cell-theory limit, which may also apply to liquids under high pressure (Bull and Jonas 1970, Van der Hart 1973).

The above theories of molecular reorientation are isotropic, whereas the normal experimental situation is one of anisotropic molecular geometries, motions and interactions. The anisotropic motional problem has been solved in the rotational diffusion limit by Huntress (1968, 1970), and the anisotropic spin-rotation interaction problem in the same limit by Bender and Zeidler (1971). The anisotropic symmetric top theory has been given very recently by McClung (1972) into the extended diffusion or inertial region, and for random anisotropic large angle jumps (O'Reilly 1972, Cukier and Lakatos-Lindenberg 1972).

The solutions are found to be of similar form to those of the anisotropic small-step case. However the connection between the two models is made only if the anisotropy of the diffusion tensor can be attributed to the anisotropy of the inertia tensor. This difference between the anisotropic rotational diffusion and extended diffusion cases relates to the assumption in rotational diffusion, of complete lack of correlation between different molecule-fixed components of angular velocity; in the gas-like inertial region of extended diffusion the angular momentum is taken as a constant of the motion between collisions and its components are correlated by precession. McClung's treatment indicates that changes in the anisotropy of the diffusion tensor with τ_w could account for the difference in the apparent activation energies of $D_{||}$ and D_{\perp} which have been observed in CH_3I (Gillen et al. 1971), CD_3CN , VOCl_3 (Gillen and Noggle 1970) and in our studies on CH_3Br .

The present investigation is a study, by nuclear relaxation methods, of the small polar symmetric top molecule CH_3Br and its various isotopic modifications, in the neat liquid phase over the temperature range 223 to 315°K. By analogy with related CH_3I (Goldberg and Pershan 1973, Gillen et al. 1971) and CH_3CN (Bopp 1967, Woessner et al. 1968) the motion of the polar axis ("tumbling") may be taken to be in the rotational diffusion limit, with $\tau_{0,1}$ given by dielectric relaxation

data. Then measurement of ^1H , ^2D and ^{13}C T_1 's as a function of temperature allows separation of the competing relaxation mechanisms and derivation of the temperature dependence of the two reorientational motions. Also the effects of unobserved ^{79}Br and ^{81}Br can be estimated. Due to the chance near-degeneracy of the Zeeman splitting of ^{13}C and ^{79}Br the ^{13}C spins in the species $^1\text{H}_2^{13}\text{C}^{79}\text{Br}$ suffer a significant scalar T_1 relaxation from ^{79}Br , which is in turn passed on as a T_2 broadening to the ^1H spins scalar-coupled to the ^{13}C . In addition the ^1H spins experience a direct T_2 scalar relaxation from both ^{79}Br and ^{81}Br , so that all scalar coupling constants to Br isotopes can be obtained.

Spin-rotation effects at ^{13}C and ^1H can be accounted for, and estimates obtained for the ^1H spin-rotation coupling constants. The derived values for τ_w allow estimation of the mean angular reorientation between collisions.

B. Experimental

The proton spin-lattice relaxation times T_1 were measured by the saturation recovery method (Van Geet and Hume 1965) and rapid adiabatic passage with sampling (Parker and Jonas 1970) on a Varian A56/60 high resolution NMR spectrometer at 60 MHz. The ^2D spin-lattice relaxation times were measured at 15.4 MHz by rapid adiabatic passage with sampling on a Varian XI-100 spectrometer.

The ^{13}C relaxation times were measured indirectly by the modified selective pulse rotary echo method (Wells and Abramson 1969, Chan 1969) on the proton multiplet components of ^{13}C enriched methyl bromide. $R_{2r} (\equiv T_{2r}^{-1})$ for protons was obtained at 60 MHz with the modified A56/60 spectrometer. The relaxation rate in the rotating frame is given by,

$$(2-3) \quad R_{2r} = \frac{1}{2}(R_{1H} + R_{2H})$$

Therefore a selective rotary echo experiment on the central proton signal due to $^{12}\text{CH}_3\text{Br}$ yields

$$(2-4) \quad R_{2r}^I = \frac{1}{2}(R_{1H}^I + R_{2H}^I)$$

where $R_{2H}^I = R_{1H}^I + R_{2H}^{\text{scalar}}$, and R_{2H}^{scalar} is the contribution to R_{2r}^I due to the unresolved coupling between ^1H and $^{79,81}\text{Br}$. Further, a selective rotary echo experiment on either member of the proton doublet due to $^{13}\text{CH}_3\text{Br}$ gives (Figure 2-1),

$$(2-5) \quad R_{2r}^{II} = \frac{1}{2}(R_{1H}^{II} + R_{2H}^{II})$$

where $R_{1H}^{II} = R_{1H}^I + R_{1H}^{1\text{H}-^{13}\text{C}}$ and $R_{1H}^{1\text{H}-^{13}\text{C}}$ is the intramolecular dipole-dipole contribution from the interaction between the protons and the carbon-13 spin. Also $R_{2H}^{II} = R_{1H}^{II} + R_{2H}^{\text{scalar}} + R_1(^{13}\text{C})$ where R_{2H}^{scalar} is the same as that previously

described for Eq. (2-4) and $R_1(^{13}\text{C})$ is the carbon-13 contribution to the proton R_2 in the limit of slow ^{13}C relaxation ($R_1(^{13}\text{C}) \ll 2\pi J_{^{13}\text{C}-^1\text{H}}$) which is well satisfied here.

Therefore using these two selective rotary echo experiments along with $R_{^1\text{H}}^{^1\text{H}-^{13}\text{C}}$ we can indirectly obtain averaged values for $R_1(^{13}\text{C})$. Expected differential ^{13}C relaxation in the two species $\text{H}_3^{13}\text{C}^{79}\text{Br}$ and $\text{H}_3^{13}\text{C}^{81}\text{Br}$ could not be experimentally resolved.

$$(2-6) \quad \Delta R_{2r} = R_{2r}^{\text{II}} - R_{2r}^{\text{I}} = R_{^1\text{H}}^{^1\text{H}-^{13}\text{C}} + \frac{1}{2}R_1(^{13}\text{C})$$

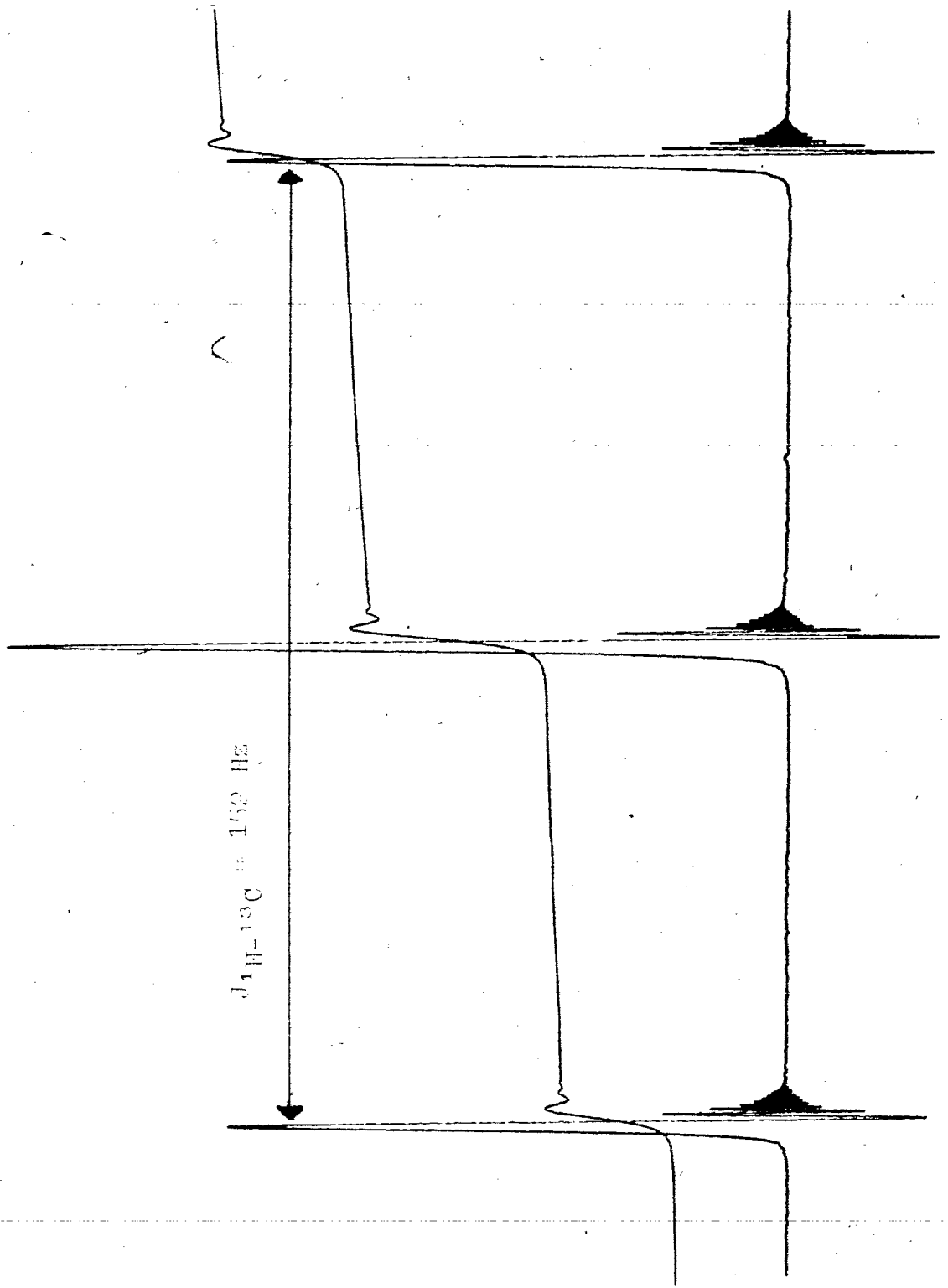
Overhauser complications in the relaxation of the ^{13}C which may cause non-exponentiality of the ^{13}C relaxation are negligible because the total dipole-dipole contribution to the ^{13}C T_1 is small.

For the mixtures of CH_3Br and CD_3Br there was no evidence of any mixed species such as CH_2DBr or CHD_2Br , so that in the separation of the various mechanisms, possible H-D exchange could be neglected.

Temperature control below room temperature was accomplished by using the Varian V-6040 variable temperature NMR probe accessory. Temperatures were measured by using a copper constantan thermocouple; temperature readings were accurate to $\pm 1^\circ\text{C}$. Experiments could not be carried out at temperatures

FIGURE 2-1

High resolution 60 MHz ^1H spectra of (57.7%) ^{13}C
enriched CH_3Br



above 315° K because of severe refluxing problems inside the sample tube. This refluxing problem was kept to a minimum at and above room temperature by the use of a pressure cap on the NMR probe. This cap minimized thermal gradients in a vertical direction along the sample tube.

The ^{13}C enriched methyl bromide (57.7% ^{13}C) obtained from Merck, Sharp and Dohme of Canada was several years old and had a pinkish tinge possibly due to slight decomposition of the sample; however this does not appear to have affected our ^{13}C T_1 measurements which are in good agreement with the reported values of Farrar et al. (1972). CD_3Br (99.8% ^2D) was also obtained from Merck, Sharp and Dohme of Canada. The samples were degassed in 5 mm tubes by the usual freeze-pump-thaw cycles under vacuum. The mole fraction mixtures of CD_3Br and CH_3Br were determined by weight with the use of a Rota-flo valve which allowed the degassed sample to be removed from the vacuum system without the danger of oxygen entering into the sample.

C. Results and Analysis

1. General Approach

For most spin $\frac{1}{2}$ nuclei the relaxation rate $(T_1)^{-1} = R_1$ is caused by a combination of mechanisms,

$$(2-7) \quad (R_1)_{\text{total}} = R_{1\text{inter}}^{\text{DD}} + R_{1\text{intra}}^{\text{DD}} + R_1^{\text{SR}} + R_1^{\text{CSA}} + R_1^{\text{SC}}$$

where the first two terms are due to inter- and intra-molecular magnetic dipolar coupling, R_1^{SR} is the spin-rotational interaction term, R_1^{CSA} is due to chemical shift anisotropy and R_1^{SC} is a scalar coupling contribution of the second kind. The proton T_1 relaxation data in Table 2-1 and curves (a), (b) and (c) of Figure 2-2 indicate the presence of several mechanisms in the relaxation rate.

The chemical shift anisotropy contribution in a mobile liquid has the form,

$$(2-8) \quad R_1^{CSA} = \frac{2}{15} \gamma^2 H_0^2 (\sigma_{\parallel} - \sigma_{\perp})^2 \tau_c$$

where H_0 is the applied field ($\sim 1.4 \times 10^4$ Gauss) and $(\sigma_{\parallel} - \sigma_{\perp})$ is the chemical shift anisotropy, 1.3 ± 0.6 ppm (Caesar and Bailey 1969) for protons in methyl bromide. Since the correlation time, τ_c is of the order of 10^{-12} sec a rough estimate shows $R_1^{CSA} = 10^{-8}$ sec $^{-1}$, which is completely negligible. For ^{13}C in $^{13}\text{CH}_3\text{Br}$ the chemical shift anisotropy has been measured to be -10 ± 5 ppm (Dailey and Bhattacharyya 1973), which makes $R_1^{CSA} = 10^{-7}$ sec $^{-1}$ also completely negligible.

For protons the scalar contribution to R_1 is shown to be negligible in Section 3c. However for ^{13}C there is a scalar contribution between $^{13}\text{C}-^{79}\text{Br}$ and $^{13}\text{C}-^{81}\text{Br}$ which must be taken into account, as discussed in section 4.

TABLE 2-1

R_1 RELAXATION DATA FOR LIQUID METHYL BROMIDE

^1H of 100% CH_3Br ^1H of 64.8% CH_3Br ^1H of 31.7% CH_3Br

T(°K)	$R_1(\text{sec}^{-1})$	$R_1(\text{sec}^{-1})$	$R_1(\text{sec}^{-1})$
315	0.073 ± 0.003	0.071 ± 0.003	0.070 ± 0.003
278	0.079 ± 0.003	0.076 ± 0.003	0.073 ± 0.003
264	0.083 ± 0.003	0.080 ± 0.003	0.074 ± 0.003
249	0.093 ± 0.004	0.086 ± 0.003	0.079 ± 0.003
238	0.100 ± 0.004	0.092 ± 0.004	0.086 ± 0.004
223	0.122 ± 0.005	0.107 ± 0.004	0.093 ± 0.004

^2D of CD_3Br

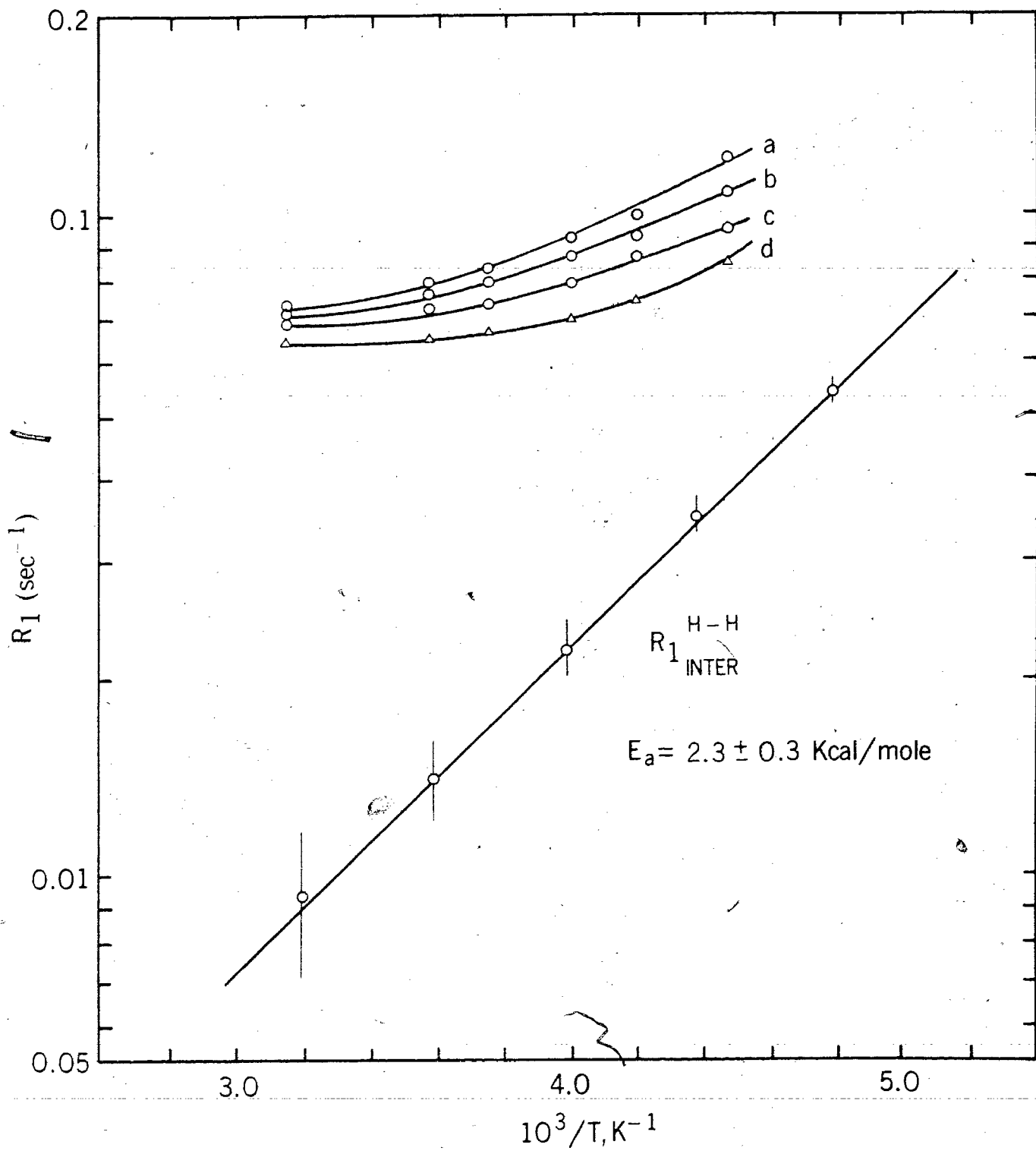
T(°K)	$R_1(\text{sec}^{-1})$
312	0.131 ± 0.004
301	0.135 ± 0.004
262	0.191 ± 0.007
245	0.223 ± 0.009
233	0.250 ± 0.010
223	0.294 ± 0.012

^{13}C of $^{13}\text{CH}_3\text{Br}$

T(°K)	$R_1(\text{sec}^{-1})$
315	0.109 ± 0.011
284	0.095 ± 0.010
260	0.081 ± 0.008
253	0.081 ± 0.008
247	0.089 ± 0.009
235	0.078 ± 0.008
225	0.079 ± 0.008

FIGURE 2-2

Experimental and derived relaxation times for ^1H in methyl bromide; (a) pure CH_3Br ; (b) 64.8% CH_3Br in CD_3Br ; (c) 31.7% CH_3Br in CD_3Br ; (d) $R_{\text{intra}}^{\text{H}}$.



Standard extrapolation (Bonera and Rigamonti 1965) of our dilution data of CH_3Br in CD_3Br allows the separation of intermolecular dipole-dipole effects from intramolecular mechanisms for protons. In the ^{13}C relaxation in liquid methyl bromide it is safe to assume that the intermolecular dipole-dipole relaxation rate is insignificant (Kuhlmann, Grant and Harris 1970) because of the much increased intermolecular nuclear separation. We are thus left with separating the various intramolecular contributions for both ^1H and ^{13}C . The method (Gillen et al. 1971) used involves the calculation of the dipolar contribution from theoretical equations for intramolecular dipole-dipole relaxation rates. These theoretical equations require known internuclear parameters and correlation times for the reorientation of the particular dipole interaction.

In the case of ^{13}C , the correlation time for reorientation of the intramolecular C-H bond directions is easily obtained from the ^2D quadrupolar relaxation times, since the latter depend upon the reorientation of the same C-D bond directions assuming that the electric field gradient at the deuteron is aligned along the C-D bond axis. For protons the analysis is not as easy; in order to obtain the needed correlation time for the direction connecting two protons in the methyl group, we must know both components of the molecule's rotational reorientation tensor. Therefore this must first

be determined in order to separate the intramolecular dipolar contribution from other intramolecular contributions.

2. Anisotropic rotational reorientation tensor for CD₃Br

The usual method of obtaining the anisotropic reorientational tensor of a symmetric top molecule involves the measurement of the relaxation time of two quadrupolar nuclei which have different bond angles with respect to the symmetry axis of the molecule (Gillen and Noggle 1970; Bopp 1967; Woessner et al. 1968; Jonas and Di Gennaro 1969; Allerhand 1970). Thus in our case we might wish to determine the reorientational tensor for CD₃Br from quadrupolar relaxation of both ²D and ^{79,81}Br. The necessary equations (Huntress 1968) that relate the measured relaxation rate of a nucleus to the reorientational tensor components and the relative orientation of this tensor to the electric field gradient tensor are*:

$$(2-9) \quad (R_{-1})_Q = \frac{3\pi^2(2I+3)}{10I^2(2I-1)} \left(\frac{e^2qQ}{h} \right) \tau_c$$

$$(2-10) \quad \tau_c = \frac{\frac{1}{2}(3\cos^2\theta-1)^2}{6D_{\perp}} + \frac{3 \sin^2\theta \cos^2\theta}{5D_{\perp} + D_{\parallel}} + \frac{(\frac{3}{4})\sin^4\theta}{2D_{\perp} + 4D_{\parallel}}$$

* Eqs. (2-9) and (2-10) were first derived (Huntress 1968) in the rotational diffusion model, but apply in addition to

the extended diffusion (McClung 1972) and random large angle jump models (Cukier and Lakatos-Lindenberg 1972); there the D 's should be interpreted as generalized reorientational rate constants. Independent NMR data from two symmetrically different relaxing quadrupoles, whose coupling constants are accurately known, then suffice to obtain D_{\parallel} and D_{\perp} , independent of the models. The choice between models can then be based on temperature dependence or other criteria.

where I is the spin of the quadrupolar nucleus, (e^2qQ/h) the quadrupole coupling constant in Hz, D_{\parallel} is the rate constant for rotation about the top axis and D_{\perp} the rate constant for rotation about an axis perpendicular to the molecule's symmetry axis, θ is the angle between the symmetry axis of the molecule and the z-axis of the molecular coordinate system which diagonalizes the field gradient tensor at the nucleus.

Since the ^{79}Br and ^{81}Br lie exactly on the molecule's symmetry axis the angle $\theta=0$ and thus the $^{79,81}\text{Br}$ relaxation time will depend only on D_{\perp} . The difficulty is that the ^{79}Br and ^{81}Br quadrupole coupling constants (Gordy et al. 1953) (550 and 460 MHz respectively, intermediate values between gaseous and solid state), are extremely large making the Zeeman line widths extremely broad. Thus we are unable to directly measure the relaxation times of either Br nucleus. We must therefore find an alternate way to determine D_{\perp} .

The perpendicular reorientation of CH_3I (Goldberg and Pershan 1973; Gillen et al. 1971) and CH_3CN (Bopp 1967; Woessner et al. 1968) is known to be in the rotational diffusion limit, and we shall assume this to be the case also for CH_3Br . Then the dielectric relaxation time τ_{diel} gives us D_{\perp} because in the diffusion limit (Carrington and McLachlan 1967),

$$(2-11) \quad D_{\perp} = (2 \tau_{\text{diel}})^{-1}$$

No dielectric relaxation time values have been reported in the literature for liquid methyl bromide. However Vuks and Chernyavska (1962) have measured the dielectric relaxation time for the series of normal alkyl bromides from ethyl bromide to n-decyl bromide. From this series a value of $\tau_{\text{diel}} = 2.8$ psec has been extrapolated for methyl bromide at 20°C . The dielectric relaxation for this series has also been measured at 1°C and 25°C (Higasi et al. 1960), from which we extrapolate for methyl bromide 3.5 psec and 2.6 psec respectively. The activation energy for D_{\perp} is calculated to be (1.7 ± 0.2) kcal/mole from these dielectric results.

Gillen and Noggle (1970) have shown that the energy of activation for D_{\perp} of polar symmetric top molecules can be estimated quite well from the energy of activation calculated from hydrodynamic diffusion constants. For pure liquids the microviscosity diffusion constant D_{\perp} is given by the equation,

$$(2-12) \quad D_{\mu} = 1.15 \times 10^8 \frac{T\rho}{M_w \eta}$$

where M_w is the molecular weight, ρ the density and η the viscosity. The assumptions on which Gierrer and Wirtz (1953) based their calculation of the microviscosity correction factor 6.125 from the classical hydrodynamic theory and which have been carried into Eq. (2-12), have been criticized recently by O'Reilly (1972a). Nevertheless, microviscosity theory apparently works well for the polar reorientational motion of small polar molecules (Gillen and Noggle 1970). Using the data in Table 2-2 along with Eq. (2-12), we obtain an activation energy of (1.7 ± 0.1) kcal/mole for D_{μ} , and this temperature dependence is plotted in Figure 2-3.

TABLE 2-2

DENSITY AND VISCOSITY DATA FOR LIQUID CH_3Br

T(°K)	ρ (g/ml)	η (cP)
273	1.73265	0.3767
263	1.75676	0.4139
253	1.78077	0.4585
243	1.80488	0.5115

Ref: R.R. Dreisbach, Physical Properties of Chemical Compounds, 1955.

FIGURE 2-3

Rotational rate constants for CD_3Br . D_{\perp} was placed from extrapolated dielectric relaxation data at 1° , 20° and 25°C as described in the text, with temperature dependence identical to that of the microviscosity diffusion constant D_{μ} calculated from literature values of η and ρ over the temperature range -30°C to 0°C . Absolute values of D_{μ} are plotted for comparison. Values of D_{\parallel} at a given temperature were then obtained from D_{\perp} and the measured ^2D relaxation rate using Eq. (2-10).

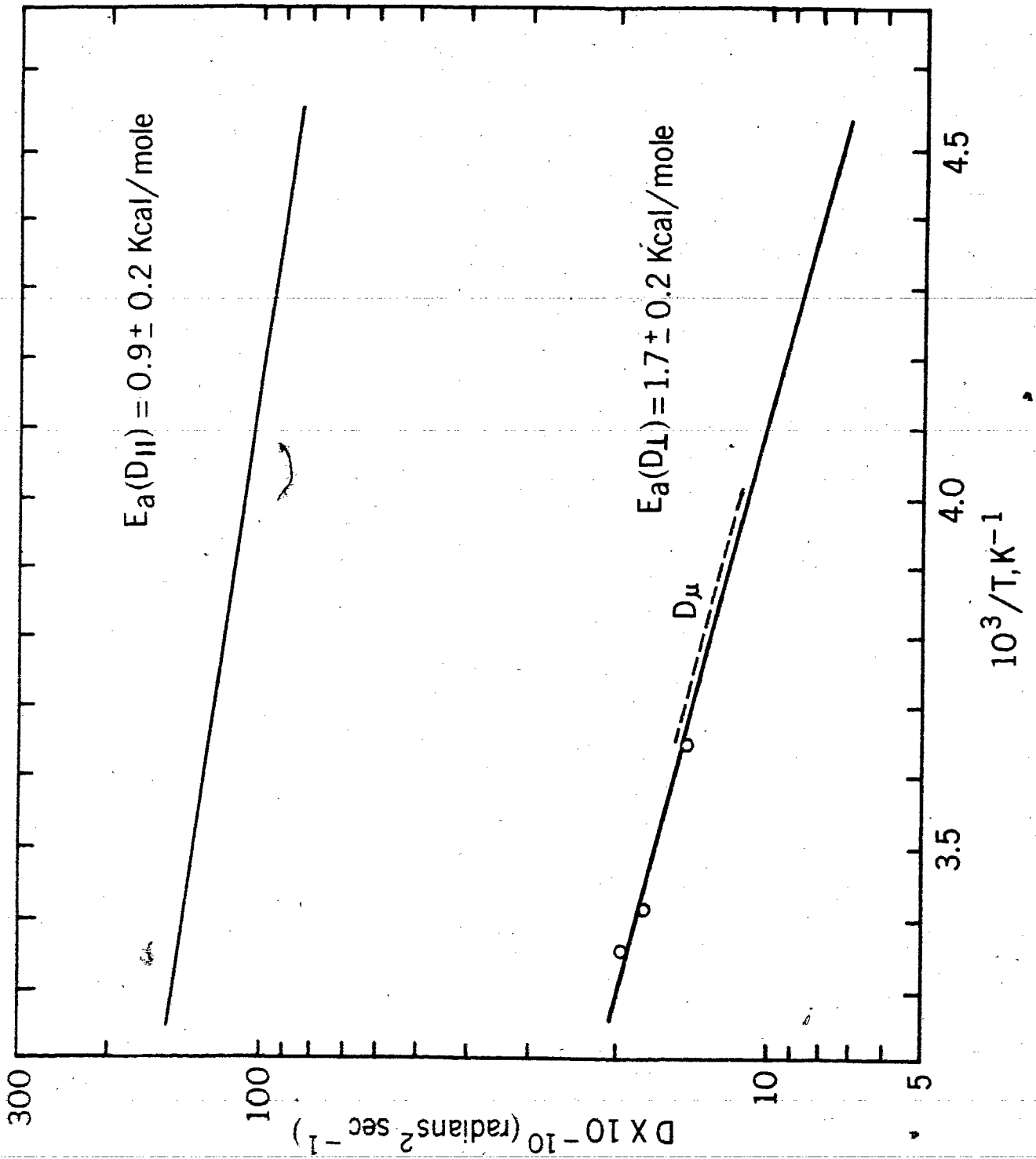
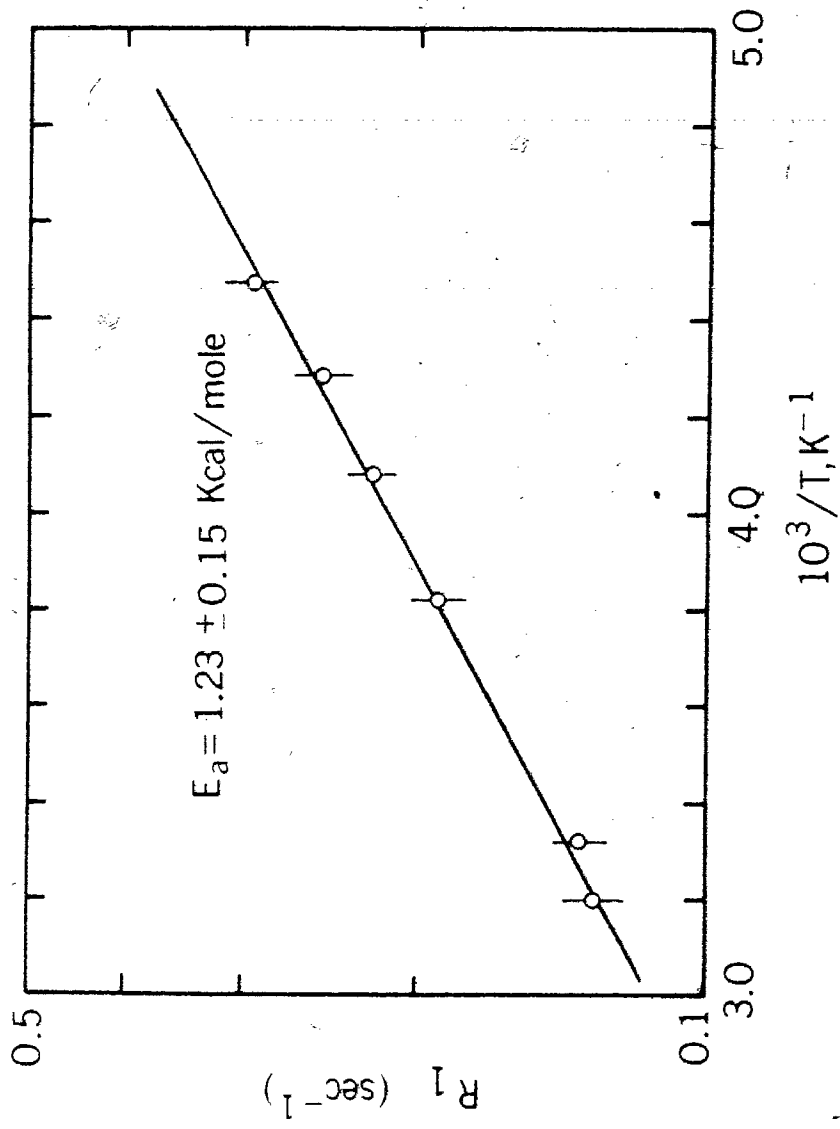


FIGURE 2-4

Deuteron spin-lattice relaxation rate in CD_3Br



For comparison the three dielectric values of D_{\perp} are indicated, and are seen to agree well with D_{μ} .

Now making use of D_{\perp} along with the 2D relaxation times (Figure 2-4, Table 2-1), the measured 2D quadrupole coupling constant (Caspary et al. 1969) of 171 ± 4 KHz in oriented liquids, the D-C-Br angle and Eqs. (2-9) and (2-10), D_{\parallel} and its temperature dependence are obtained. We find $E_a(D_{\parallel})$ to be (0.9 ± 0.2) kcal/mole, and that reorientation about the figure axis is about eight times faster than reorientation of the figure axis at 25°C .

The derived values of D_i yield reorientational correlation times $\tau_{\theta 2i} = (6D_i)^{-1}$ that can be compared with the classical free rotor reorientational time about the same axis $\tau_{fi} = (3/5)(I/kT)^{\frac{1}{2}}$ in the so-called χ -test (Gillen and Noggle 1970). Thus

$$(2-13) \quad \chi_i = \tau_{\theta 2i} / \tau_{fi} = 5 / (18D_i)(kT/I)^{\frac{1}{2}}$$

and $\chi_i \gg 1$ for the rotational diffusion model to apply.

We find χ_{\perp} ranges over values from 3 to 10 for the temperature range $+40$ to -64°C , indicating that this motion does indeed tend to the rotational diffusion limit, as was earlier assumed. On the other hand, χ_{\parallel} values of 1.1 to 1.3 are found over the same temperature range, indicating this motion to be in the intermediate region between diffusion and the inertial region. This is not a surprising result,

for the molecule has a very small moment of inertia about the figure axis, because the motion requires no reorientation of the dipole, and because the angular dependence of the intermolecular potential is expected to be small. The liquid microdynamics of CH_3Br are then similar to CH_3I (Gillen et al. 1971) and CH_3CN (Bopp 1967).

3. Proton Relaxation

All theoretical calculations of the intermolecular dipole-dipole interaction involve many questionable assumptions (Hertz 1967). It is assumed that (a) the relaxation of spin I is due to the uncorrelated motion of all its intermolecular spin pairs, (b) only relative translation changes the intermolecular dipole vector i.e. the effect of rotations is neglected, (c) the molecules are spherical and have a single distance of closest approach independent of relative orientations. A typical theoretical expression for $R_{\text{Inter}}^{\text{dd}}$ is (Mitchell and Eisner 1960),

$$(2-14) \quad R_{\text{inter}}^i = \frac{2\pi\gamma_i^2 h^2 N \tau}{a^2} \left\{ 4\gamma_i^2 I_i(I_i+1) \sum_j \frac{1}{d_{ij}^3} + \frac{8}{3} \sum_f \gamma_i^2 I_f(I_f+1) \frac{1}{d_{if}^3} \right\}$$

for the i 'th dipolar nucleus due to the intermolecular coupling to all other dipoles in the sample. The sum over j includes all nuclei of the same type as i ; the sum over f includes all non-identical nuclei on neighbouring molecules.

The d^0 is the distance of closest approach; N is the number of molecules per unit volume, a is the radius of the assumed spherical molecule and τ_t is the translational correlation time.

The temperature dependent proton relaxation times are shown in Figure 2-2 for pure CH_3Br and for mixtures containing 31.7 and 64.8 per cent mole fraction CH_3Br in CD_3Br . For these CH_3Br - CD_3Br mixtures the intermolecular relaxation rate is,

$$(2-15) \quad R_{1\text{inter}}^{\text{H}} = R_{1\text{inter}}^{\text{H-H}} + R_{1\text{inter}}^{\text{H-D}} + R_{1\text{inter}}^{\text{H-Br}}$$

Since $\gamma_{\text{H}}^2 = 42.5 \gamma_{\text{D}}^2$ and the spin values are different, the deuterium in CD_3Br will contribute $1/24$ as much to the intermolecular relaxation as the hydrogens in CH_3Br . The total proton relaxation is then,

$$(2-16) \quad R_{1\text{total}}^{\text{H}} = \frac{23C + 1}{24} R_{1\text{inter}}^{\text{H-H}} + R_{1\text{inter}}^{\text{H-Br}} + R_{1\text{intra}}^{\text{dd}} + R_{1\text{SR}}$$

where C is the mole fraction of protonated methyl bromide.

A plot of $R_{1\text{total}}^{\text{H}}$ vs. $23C/24$ gives,

$$(2-17) \quad \text{slope} = R_{1\text{inter}}^{\text{H-H}}$$

$$\text{and intercept} = \frac{1}{24} R_{1\text{inter}}^{\text{H-H}} + R_{1\text{inter}}^{\text{H-D}} + R_{1\text{intra}}^{\text{dd}} + R_{1\text{SR}}$$

Now we can proceed to eliminate R_{1inter}^{H-Br} if we assume that d_{H-Br}° equals d_{H-H}° (in fact, d_{H-Br}° will be actually greater than d_{H-H}°), whence

$$(2-18) \quad R_{1inter}^{H-Br} \cong 0.07 R_{1inter}^{H-H}$$

We are then left with separating R_{1intra}^{dd} from R_1^{SR} .

3a. Translational Diffusion

The translational correlation time τ_t is given by the liquid's self-diffusion coefficient D_s by (Mitchell and Eisner 1960),

$$(2-19) \quad \tau_t = a^2/12D_s$$

$$(2-20) \quad R_{1inter}^{H-H} = \frac{3\pi^{\dagger}h^2\gamma_H^4 N}{2D_s d_{H-H}^{\circ}}$$

D_s is given by the Stokes formula as $kT/6\pi\eta a$, in which it is assumed that a spherical 'solute' particle of radius "a" moves in a continuous 'solvent' medium of viscosity η . Gierer and Wirtz (1953) have extended Stokes' theory by introducing a translational microviscosity term f_t , to account for the finite size of the solvent molecules. For a pure liquid

$$f_t = \frac{1}{2}.$$

$$(2-21) \quad D_s = \frac{kT}{6\pi\eta a f_t} = \frac{kT}{3\pi\eta a}$$

Therefore,

$$(2-22) \quad R_{H-H}^{1inter} = \frac{9\pi^2 \hbar^2 \eta \gamma_H^4 N a}{2kT d_{H-H}^{\circ}}$$

Now for $d_{H-H}^{\circ} = 2a$

$$(2-23) \quad R_{H-H}^{1inter} = \frac{9\pi^2 \hbar^2 \eta \gamma_H^4 N}{4kT}$$

which can be directly compared with experimental values (Table 2-3). From this we see that the theoretical results are in surprisingly good agreement with the experimentally obtained values. From theory the energy of activation is 2.1 kcal/mole and from experiment it is (2.3 ± 0.3) kcal/mole.

TABLE 2-3

THEORETICAL AND EXPERIMENTAL VALUES FOR T_{H-H}^{1inter}

T (°K)	Theory (from η ; Eq. 2-20)	Exp. (from data and Eq 2-14)
273	72 sec	66 sec
263	62 sec	56 sec
253	53 sec	47 sec
243	45 sec	41 sec

3b. Proton intramolecular dipole-dipole interaction

Separation of $R_{\text{intra}}^{\text{dd}}$ from R_{SR} can be accomplished using the theoretical equations for $R_{\text{intra}}^{\text{dd}}$ given by Powles (1963), which assumes independent pairwise interactions and neglects symmetry effects:

$$(2-24) \quad R_{\text{intra}}^{\text{H-H}} = \frac{3}{2} \hbar^2 \gamma_{\text{H}}^4 \cdot \frac{2}{n} \left(\sum_{i < j}^n r_{ij}^{-6} \right) \tau_c(\text{H-H})$$

where n is the number of protons in the molecule. For the interaction between the protons and the bromine it is;

$$(2-25) \quad R_{\text{intra}}^{\text{H-Br}} = \frac{4}{3} \hbar^2 \gamma_{\text{H}}^2 \gamma_{\text{Br}}^2 I_{\text{Br}} (I_{\text{Br}} + 1) r_{\text{H-Br}}^{-6} \tau_c(\text{H-Br})$$

$\tau_c(\text{H-H})$ is the effective correlation time for reorientation of the proton internuclear vector and can be calculated using D_{\perp} and D_{\parallel} with $\theta=90^\circ$ because the pertinent proton relaxation interaction occurs in the plane of the methyl hydrogens.** This plane is normal to the major axis.

** The values of D_{\parallel} and D_{\perp} appropriate to CD_3Br have been corrected for the calculations on the CH_3Br case. The difference between D_{\perp} for CD_3Br and CH_3Br is negligible but the difference in D_{\parallel} is large since the parallel moments of inertia differ by a factor of 2. This large difference in D_{\parallel} however is not very important since the correlation time

τ_c is not affected much by changes in $D_{||}$ (~9 per cent difference if we use $D_{||}$ for CD_3Br instead of $D_{||}$ for CH_3Br).

For $\tau_c(H-Br)$ $\theta = 25.0^\circ$; using the appropriate internuclear distances given in Table 2-4, we obtain the following:

for $^{12}CH_3^{79}Br$

$$(2-26) \quad R_{1\text{intra}}^{dd} = 4.92 \times 10^{10} \tau_c(H-H) + 7.15 \times 10^8 \tau_c(H-^{79}Br)$$

for $^{12}CH_3^{81}Br$

$$(2-27) \quad R_{1\text{intra}}^{dd} = 4.92 \times 10^{10} \tau_c(H-H) + 7.11 \times 10^8 \tau_c(H-^{81}Br)$$

The resulting $R_{1\text{intra}}^{dd}$ is shown in Figure 2-5.

3c. Proton Scalar Relaxation

The fast relaxation of the bromine nucleus induces rapidly fluctuating magnetic fields at the protons under observation, through the indirect scalar coupling, J_{H-C-Br} . This mechanism is called a type II scalar interaction by Abragam (1961). The contributions to the relaxation processes for the spin I by this interaction are:

$$(2-28) \quad R_1^{SC} = \frac{2(2\pi J)^2}{3} S(S+1) \left[\frac{T_{2S}}{1 + (\omega_I - \omega_S)^2 T_{2S}^2} \right]$$

$$(2-29) \quad R_2^{SC} = \frac{2(2\pi J)^2}{3} S(S+1) \left[T_{1S} + \frac{T_{2S}}{1 + (\omega_I - \omega_S)^2 T_{2S}^2} \right]$$

TABLE 2-4

GEOMETRIC PARAMETERS AND MOMENTS OF INERTIA FOR CH₃Br

$r_{\text{C-H}}$	1.096 Å*
$r_{\text{H-H}}$	1.806 Å
$r_{\text{C-Br}}$	1.93 Å**
$r_{\text{H-Br}}$	2.50 Å
$\angle \text{H-C-H}$	110°58' *
$\angle \text{Br-C-H}$	107°56' *
$\angle \text{C-Br-H}$	25.0°
$I_{\perp}, 10^{-40} \text{g.cm}^2$	87.7**
$I_{\parallel}, 10^{-40} \text{g.cm}^2$	5.51**

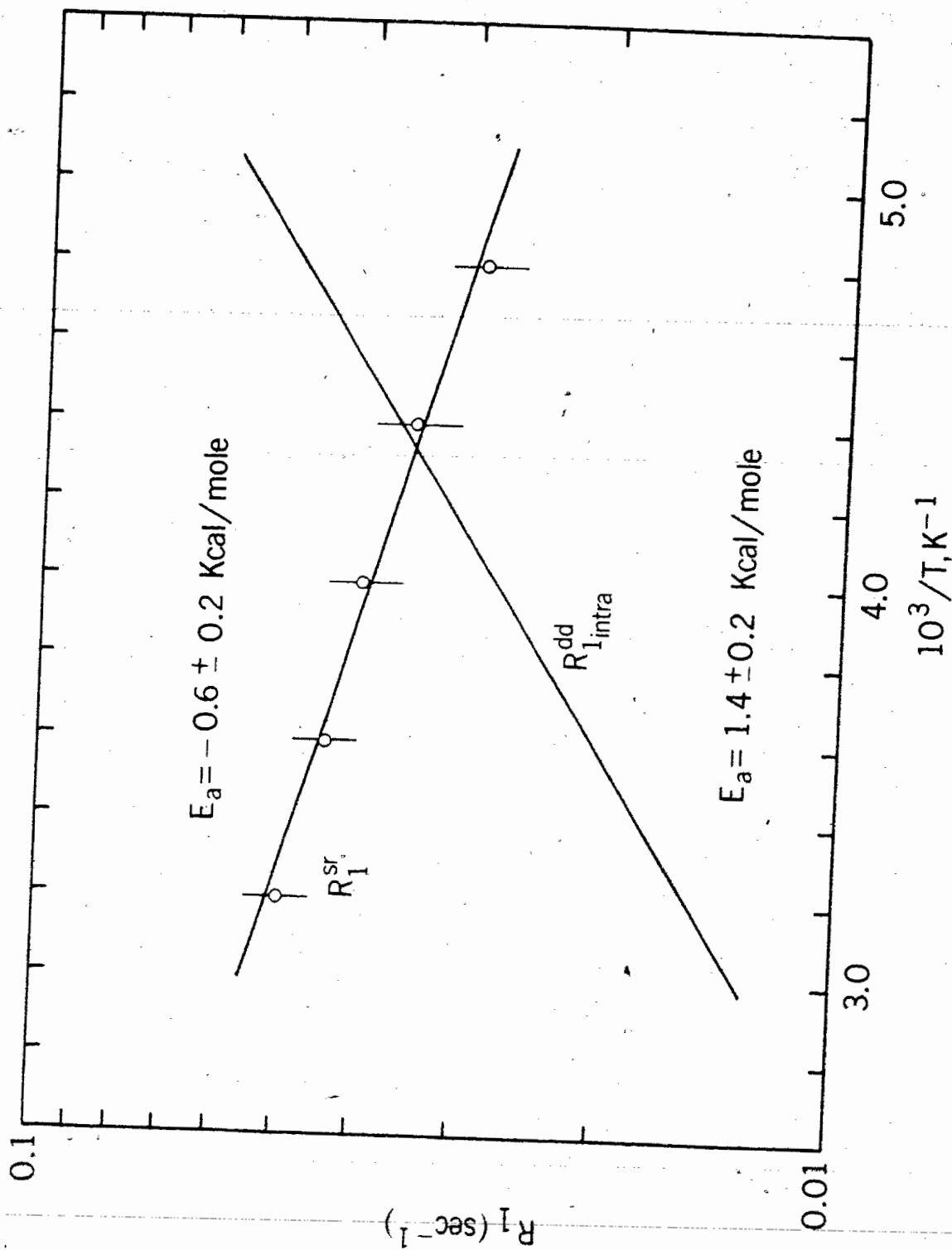
All values obtained from references below, otherwise calculated.

* T.L. Barnett and T.H. Edwards, J. Mol. Spect., 20, 352(1966).

** W. Gordy, J.W. Simmons and A.G. Smith, Phys. Rev., 72, 344 (1947):

FIGURE 2-5

Separation of the proton intramolecular relaxation rate in CH_3Br into its intramolecular dipole-dipole and spin-rotation rates.



where J is the scalar coupling constant between spins I and S , ω_I and ω_S are the resonant angular frequencies of the nuclei with spins I and S , and T_{2S} is the transverse relaxation time of the quadrupole nucleus, which is in the liquid state equal to the spin-lattice relaxation time

T_{1S} .

Since $(\omega_H - \omega_{Br})^2 T_{2Br}^2 \gg 1 \gg T_{1Br}$, T_{2Br} , this mechanism contributes only to R_{2H} , and not to R_{1H} . Therefore the selective measurement of R_{1H} and R_{2rH} (selective for the species $^{12}CH_3Br$) can be used to determine this scalar contribution and thus the spectrally unobservable J_{H-Br} coupling constant. R_{1H} was measured by adiabatic fast passage. Values for $T_1(^{79}Br)$ and $T_1(^{81}Br)$ (Figure 2-6) were obtained from the extrapolated D_1 values of Figure 2-3 based on the dielectric results, together with literature values (Gordy et al. 1953) for the isotopic quadrupole coupling constants. R_{2rH} was obtained by the rotary echo method on the $^{12}CH_3Br$ resonance. Since distinct R_{2r} decays from the equally abundant species $^{12}CH_3^{79}Br$ and $^{12}CH_3^{81}Br$ were not experimentally resolved, it was assumed that the observed experimental decay gave mean values of the individual decay constants.

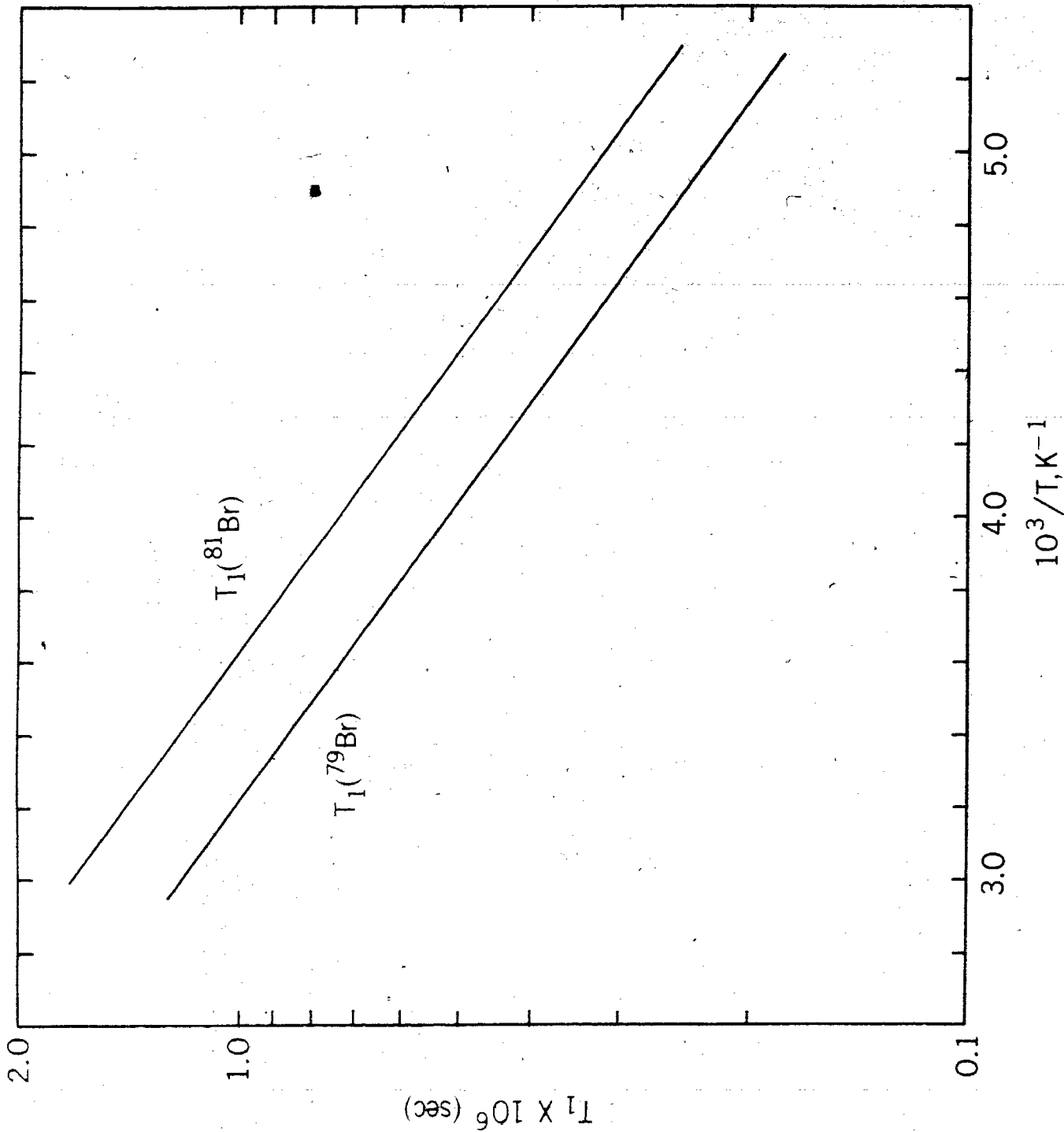
The J values were then resolved by noting that the ratio

$$\frac{J_{^1H-^{79}Br}}{J_{^1H-^{81}Br}} = \frac{\gamma_{^{79}Br}}{\gamma_{^{81}Br}}. \quad \text{The extracted values were}$$

$$\frac{J_{^1H-^{79}Br}}{J_{^1H-^{81}Br}} = 13 \pm 4 \text{ Hz and } J_{^1H-^{81}Br} = 14 \pm 4 \text{ Hz.}$$

FIGURE 2-6

^{79}Br and ^{81}Br spin-lattice relaxation times
calculated from dielectric results.



4. ^{13}C Spin-lattice Relaxation

For the ^{13}C relaxation in a methyl group it is safe to assume that the intermolecular dipole-dipole relaxation is insignificant as previously mentioned. Therefore the T_1 's of ^{13}C in liquid methyl bromide (Figure 2-7) come from a combination of intramolecular dipole-dipole, spin-rotation and scalar relaxation of the second kind resulting from scalar coupling of ^{13}C to either the ^{79}Br or ^{81}Br nucleus. This efficient scalar relaxation between ^{13}C and $^{79,81}\text{Br}$ has been observed for a number of systems: bromomethanes (Farrar et al. 1972; Iyerla et al. 1971), p-bromobenzonitrile (Freeman and Hill 1971) and bromobenzene (Levy 1972). The total relaxation expression for ^{13}C can then be written as,

$$(2-30) \quad R_{\text{total}}^{13\text{C}} = R_{\text{intra}}^{\text{dd}} + R_{\text{SR}} + R_{\text{SC}}$$

The dipolar contribution is given theoretically as,

$$(2-31) \quad R_{\text{intra}}^{\text{dd}} = \frac{3\gamma_{\text{H}}^2 \gamma_{^{13}\text{C}}^2 h^2}{r_{\text{C-H}}^6} \tau_{\text{C}}(\text{C-H}) + \frac{5\gamma_{^{13}\text{C}}^2 \gamma_{^{79,81}\text{Br}}^2 h^2}{r_{\text{C-Br}}^6} \tau_{\text{C}}(\text{C-Br})$$

Using the appropriate values for the constants and intermolecular distances,

$$(2-32) \quad R_{1\text{intra}}^{\text{dd}} = 6.52 \times 10^{10} \tau_c(\text{C-H}) + 1.33 \times 10^{10} \tau_c(\text{C-}^{79}\text{Br})$$

$$(2-33) \quad R_{1\text{intra}}^{\text{dd}} = 6.52 \times 10^{10} \tau_c(\text{C-H}) + 1.43 \times 10^{10} \tau_c(\text{C-}^{81}\text{Br})$$

$\tau_c(\text{C-Br})$ is the correlation time for reorientation perpendicular to the symmetry axis and is equal to $(6D_{\perp})^{-1}$. The tensor axis whose reorientation is represented by $\tau_c(\text{C-H})$ is the same as that from the ^2D relaxation.** The calculated contributions are listed in Table 2-5 for 5°C and are plotted in Figure 2-7.

Recently Kuhlmann, Grant and Harris (1970, 1971) have shown that evaluation of the $^{13}\text{C}\{-^1\text{H}\}$ nuclear Overhauser effect (NOE) in conjunction with nuclear spin-lattice relaxation times (T_1) allows a separation of the dipolar mechanism from other T_1 processes. Farrar, Druck, Shoup and Becker (1972) have measured this for liquid methyl bromide at 30°C and 15.1 MHz; they obtained $\eta_{\text{I}\{-\text{S}\}} = \frac{1}{2} \frac{\gamma_{\text{S}} R_1^{\text{dd}}}{\gamma_{\text{I}} R_{1\text{total}}}$ = 0.29 (this is the ratio of the change in the total intensity of the spin I resonance during double resonance to the single resonance intensity); and $T_1(^{13}\text{C}) = 8.8$ sec, which gives an $R_{1\text{intra}}^{\text{dd}} = 0.017 \text{ sec}^{-1}$ in very good

** This is a good approximation even though $D_{\parallel}(\text{CD}_3\text{Br})$ is very different from $D_{\parallel}(\text{CH}_3\text{Br})$. This is shown in the calculation of $R_{1\text{intra}}^{\text{dd}}(^{13}\text{C})$ using $\tau_c(\text{C-D})$ instead of $\tau_c(\text{C-H})$.

FIGURE 2-7

Separation of carbon-13 intramolecular
relaxation rate of CH_3Br into $R_{1\text{intra}}^{\text{dd}}$,
 $R_{1\text{SR}}$, and $R_{1\text{SC}}^{79\text{Br}}$.

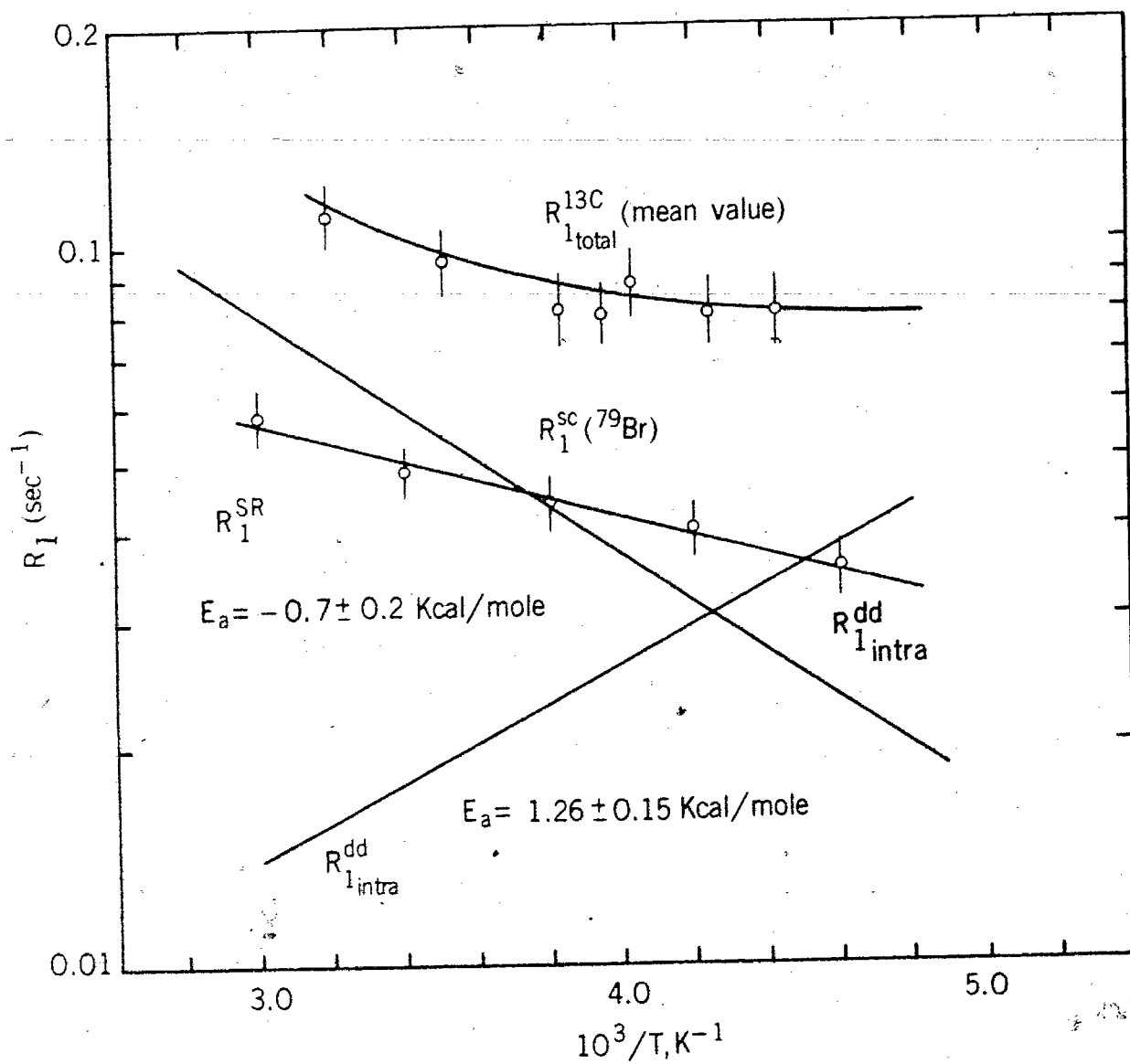


TABLE 2-5

CONTRIBUTIONS TO THE ^{13}C RELAXATION TIME IN PURE CH_3Br
AT 5°C

a) $^{13}\text{CH}_3^{79}\text{Br}$

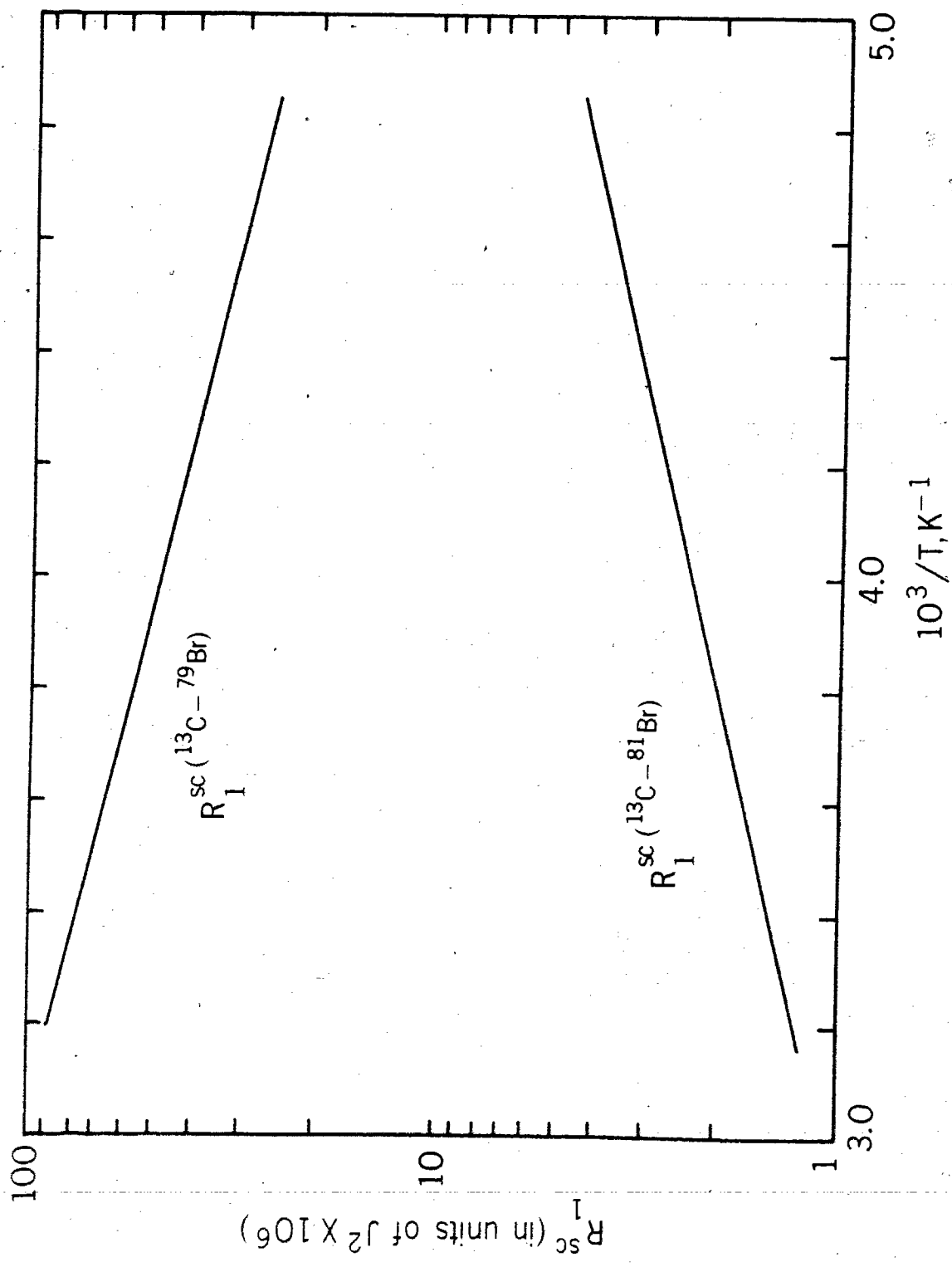
T_1	Mechanism	Relaxation Rate (sec^{-1})	Relaxation Time (sec)
T_1	total	0.126	7.9
T_1	$^1\text{H}-^{13}\text{C}$ 1 intra	0.019	53
T_1	SR	0.047	22
T_1	SC	0.060	16.7
T_1	$^{13}\text{C}-^{79}\text{Br}$ 1 intra	0.00015	~6700

b) $^{13}\text{CH}_3^{81}\text{Br}$

T_1	Mechanism	Relaxation Rate (sec^{-1})	Relaxation Time (sec)
T_1	total	0.068	14.7
T_1	$^1\text{H}-^{13}\text{C}$ 1 intra	0.019	53
T_1	SR	0.047	22
T_1	SC	0.0018	~560
T_1	$^{13}\text{C}-^{81}\text{Br}$ 1 intra	0.00016	~6300

FIGURE 2-8

Temperature dependence of the $R_1^{SC}(^{79}\text{Br})$ and $R_1^{SC}(^{81}\text{Br})$ contributions to the carbon-13 relaxation rate.



agreement with our theoretical $R_{1\text{intra}}^{\text{dd}}$ (Figure 2-7). It appears therefore that the dipolar contribution to ^{13}C in liquid methyl bromide is small, at least at the higher temperatures.

We are left with separating R_1^{SR} from R_1^{SC} for ^{13}C . The problem is that the scalar contribution is not the same for both bromine isotopes; in fact as shown later it is the ^{79}Br isotope which contributes to R_1^{SC} and the ^{81}Br contribution is quite small (see Figure 2-8).

The spin-rotation interaction constant for the ^{13}C spin in CH_3Br has not been reported. However it can be estimated from the average paramagnetic shielding of ^{13}C by a method due to Deverell (1970). From an 'atom in a molecule' approach he finds the modified Ramsey paramagnetic shielding σ'_p to be for a nucleus on the axis of a symmetric top molecule,

$$(2-34) \quad \sigma'_p = \sigma_{\text{tot}} - \sigma'_d = (2\pi/3\hbar g_I)(M_p/m_e)(2C_{\perp}I_{\perp} + C_{\parallel}I_{\parallel})$$

where σ'_d represents the atomic diamagnetic shielding, taken to be a constant, and can be calibrated from the observed nuclear shielding of a molecule whose isotropic spin-rotation constant $C_{\text{av}} = \frac{1}{3} \text{Tr } C$ has been measured from molecular beam data. Eq. (2-34) then forms the basis of an absolute chemical shift scale for nucleus I. The constants in Eq. (2-34)

have their usual meaning, with g_I being the nuclear g-factor of spin I, and the units of C being in Hz and I in gm-cm².

Using the value of C = -32.59 kHz for ¹³C¹⁶O (Ozier, Crapo and Ramsey 1968) along with Eq. (2-34) we can establish a ¹³C shift scale based on ¹³CO as the reference,

$\sigma'_p = -256.3$ ppm for ¹³CO. The measured shift of ¹³CH₃Br is 172.3 ppm upfield from ¹³CO therefore $\sigma'_p = -84.0$ ppm for ¹³CH₃Br.

If we now make use of the following two equations,

$$(2-35) \quad \sigma'_p = \frac{1}{3}(2\sigma_{\perp} + \sigma_{\parallel})$$

$$(2-36) \quad \Delta\sigma = \sigma_{\parallel} - \sigma_{\perp}$$

along with $\sigma'_p = -84.0$ ppm and $\Delta\sigma = -10 \pm 5$ ppm (Dailey and Bhattacharyya 1973) for ¹³CH₃Br we obtain σ_{\parallel} and σ_{\perp} . Now by equating Eq. (2-34) with (2-35) we obtain,

$$(2-37) \quad 2\sigma_{\perp} + \sigma_{\parallel} = 7.78 \times 10^{30} (2I_{\perp}C_{\perp} + I_{\parallel}C_{\parallel})$$

and therefore

$$(2-38a,b) \quad \sigma_{\perp} = 7.78 \times 10^{30} I_{\perp}C_{\perp} \quad \text{and} \quad \sigma_{\parallel} = 7.78 \times 10^{30} I_{\parallel}C_{\parallel}$$

from which we obtain $C_{\perp} = + 1.20$ kHz and $C_{\parallel} = + 21.2$ kHz.

These results are in agreement with Lyerla, Grant and Wang's (1971) comment that the (IC) tensor for carbon-13 spins in many non-linear molecules is near isotropic i.e. $(IC)_t \cong I_{\parallel} C_{\parallel} \cong I_{\perp} C_{\perp}$. This is true only for the cases where $\Delta\sigma$ is small compared to σ'_p .

Spin-rotation interactions in small molecules have been the subject of many studies (Gillen et al. 1971, 1974; Woessner et al. 1968; Sawyer and Powles 1971; Litchman and Alei 1972). An expression for R_1^{SR} for symmetric top molecules is given by (Bender and Zeidler 1971; Lyerla Jr. et al. 1971),

$$(2-39) \quad R_1^{SR} = \frac{8\pi^2 kT}{3h^2} \left[(I_{\parallel} C_{\parallel})^2 \frac{\tau_{\omega_{\parallel}}}{I_{\parallel}} + 2(I_{\perp} C_{\perp})^2 \frac{\tau_{\omega_{\perp}}}{I_{\perp}} \right]$$

The terms $I_{\perp} C_{\perp}$ and $I_{\parallel} C_{\parallel}$ refer to the sets of longitudinal and transverse components of moment of inertia and spin-rotational coupling constant with respect to the symmetry axis.

The values obtained for C_{\parallel} and C_{\perp} in $^{13}\text{CH}_3\text{Br}$ are nearly the same values as obtained for $^{13}\text{CH}_3\text{I}$ (Gillen et al. 1971). Both of these molecules are symmetric tops consisting of a methyl group and have nearly the same $(IC)_t$ for the ^{13}C spins, but in methyl bromide this is masked by the large scalar contribution from the bromine. We will assume the same T_1^{SR} for the carbon-13 spin for the more complex case of $^{13}\text{CH}_3\text{Br}$. It has been shown for the molecules $^{13}\text{CH}_3\text{CN}$ (Gillen et al. 1974) and $^{13}\text{CH}_3\text{I}$ (Gillen et al. 1971), that the ^{13}C spin-rotation

relaxation is dominated by reorientation about the figure axis, i.e. $\tau_{\omega\perp}/I_{\perp} \ll \tau_{\omega\parallel}/I_{\parallel}$, so that this term can be neglected in Eq. (2-39). We then obtain $\tau_{\omega\parallel} = 0.22$ psec at 30° C for the methyl bromide geometry. This correlation time can be identified with the time between collisions that interrupt the angular velocity about the axis, and may then be compared with the period for free rotation through one radian given by the equipartition principle,

$$(2-40) \quad \tau_{\parallel,f} = (I_{\parallel}/kT)^{\frac{1}{2}} = 0.11 \text{ psec}$$

with the result that the molecule makes about a 100° jump for the parallel motion. However this value should not be taken as a quantitative measure of this angle jump since it is based on an assumed value of 18 sec for T_1^{SR} , but we can say that the angle jump is large. Hubbard's relationship (1963),

$$(2-41) \quad \tau_{\theta,2} \tau_{\omega} = \frac{I}{6kT}$$

may not be used to calculate $\tau_{\omega\parallel}$ because this motion is not in the rotational diffusion limit but instead in the inertial region. However for the perpendicular motion the Hubbard relationship should hold, and we may use it to calculate $\tau_{\omega\perp}$.

For the perpendicular motion we obtain $\tau_{\omega_{\perp}} = 0.039$ psec and $\tau_{\perp,f} = 0.46$ psec. This means that for this motion the molecule moves through an angle of about 5° . These results are in agreement with those found by Bartoli and Litovitz (1972) using Raman scattering techniques and the results of Laulicht and Meriman (1973) who obtained a value of $\langle\theta\rangle = 3 \pm 1^{\circ}$.

At this time we can check the statement made about the spin-rotation interaction in ^{13}C being dominated by the orientation about the figure axis. If we substitute the values for R_1^{SR} , I_{\parallel} , I_{\perp} , C_{\parallel} , C_{\perp} , $\tau_{\omega_{\parallel}}$, $\tau_{\omega_{\perp}}$ into Eq. (2-39) we see that the reorientation about the figure axis contributes 98 % while the other 2 per cent comes from the perpendicular motion.

The derived R_1 values for ^{13}C are a mean value because we have two isotopic species $^{13}\text{CH}_3^{79}\text{Br}$ and $^{13}\text{CH}_3^{81}\text{Br}$ which have different R_1^{SC} contributions. Again, this experimental problem is that of decomposing a double exponential in the proton rotary echo envelope decays for the $^{13}\text{CH}_3\text{Br}$ resonances. However deviation from single exponential recovery was not observed, at least through the first decade; this indicates that the ratio $R_{2\text{rH}}(^{13}\text{CH}_3^{79}\text{Br})/R_{2\text{rH}}(^{13}\text{CH}_3^{81}\text{Br}) \leq 1.5$ and $R_1(^{13}\text{CH}_3^{79}\text{Br})/R_1(^{13}\text{CH}_3^{81}\text{Br}) \leq 2$ (see Experimental section).

Therefore within ~5% error the derived observed value of the $R_1(^{13}\text{C})$ can be expressed as,

$$(2-42) \quad R_{1\text{obs}}(^{13}\text{C}) \approx \frac{R_1(^{13}\text{CH}_3^{79}\text{Br}) + R_1(^{13}\text{CH}_3^{81}\text{Br})}{2}$$

using $R_{1\text{obs}}(^{13}\text{C})$ at 30°C and the estimated value of T_1^{SR} at the same temperature we can calculate the R_1^{SC} contribution at 30°C and thus the coupling constants $J_{^{13}\text{C}-^{79}\text{Br}}$ and $J_{^{13}\text{C}-^{81}\text{Br}}$ (30 ± 4 Hz and 32 ± 4 Hz correspondingly). Using these coupling constants along with the temperature dependence of the Br T_1 values in Figure 2-6 and Eq. (2-28) applied to the C-Br pairs, we obtain the temperature dependence of R_1^{SC} contribution, leaving finally in Eq. (2-30), the temperature dependence of the R_1^{SR} contribution. The results are plotted in Figure 2-7.

It should be pointed out that usually R_1^{SC} is small but in this case the proximity of the γ 's of ^{13}C and $^{79,81}\text{Br}$ coupled with the very short $T_{2\text{Br}}$ makes this contribution quite significant. From these results we see that the ^{79}Br isotope is the one which contributes significantly to the R_1^{SC} while the ^{81}Br isotope contributes only a very small amount.

The experimental activation energy of the spin-rotation interaction relaxation is found to be (-0.7 ± 0.2) kcal/mole. This value can be compared with the E_a for D_{\parallel} , which is (0.9 ± 0.2)

kcal/mole; the values agree within experimental errors. Thus although the motion about the symmetry axis is not in the diffusion limit, as discussed in Section 2, we now find that the activation energies are related as though the diffusion model applies. This result is at variance with the correlated inertial model of McClung (1969,1972) but is in agreement with earlier data (Gillen et al. 1971; Woessner et al. 1968) for CH_3I and CH_3CN . The equal and opposite temperature dependences of D_{\parallel} and $\tau_{w\parallel}$ have been taken in the past as evidence for methyl group reorientation as the source of the large spin-rotation interaction.

5. Proton Spin-Rotation Interaction

Since $R_1^{SC}(\text{H-Br})$ is negligible, the spin-rotation contribution is all that remains of Eq. (2-17) and by subtraction its contribution is also shown in Figure 2-5. Its energy of activation is (-0.6 ± 0.2) kcal/mole. The errors are from uncertainty in Eq. (2-17) because of possible errors in the dilution extrapolation.

The ^1H spin-rotation constants for CH_3Br have not been reported; however we may estimate the averaged spin-rotational constant by Deverell's method (1970). From molecular beam data it was found for CH_4 that $C_{\parallel} = -1.58$ kHz and $C_{\perp} = +16.54$ kHz (Wofsy et al. 1970) ; since the chemical shift of CH_3Br is 2.3 ppm downfield from CH_4 we obtain,

$$\bar{C} = \frac{(2C_{\perp} I_{\perp} + C_{\parallel} I_{\parallel})}{\frac{1}{3}(2I_{\perp} + I_{\parallel})} = + 2.30 \text{ kHz}$$

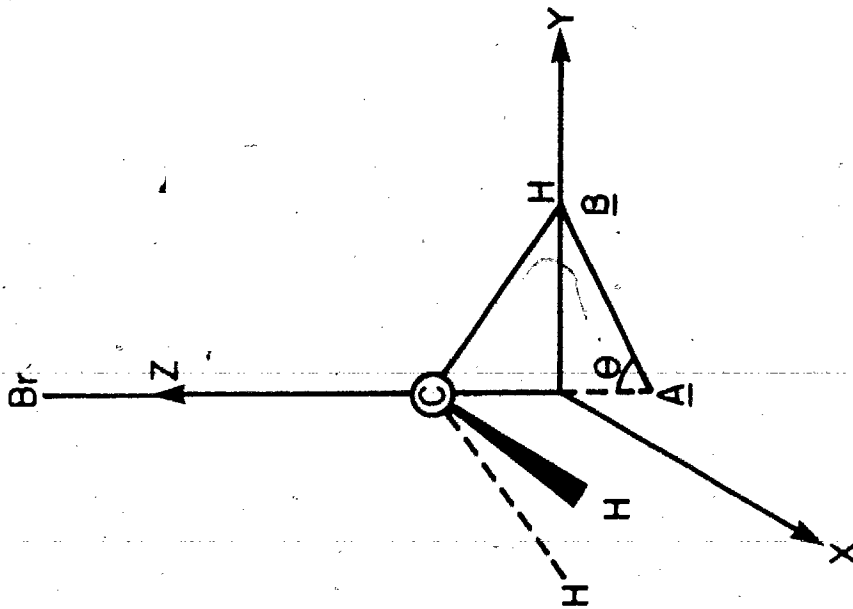
Eq. (2-39) is only applicable when the resonant nucleus is located along the principal symmetry axis, as is the case for the carbon-13 spin in $^{13}\text{CH}_3\text{Br}$, however this equation does not apply for a nucleus off the principal axis i.e. the protons in methyl bromide. The expression for the spin-rotation contribution to T_1 has been explicitly obtained for the resonant nucleus located off the symmetry axis for spherical-top and symmetric-top molecules (Wang 1973). He first assumes that the C-H bond in a molecule such as methyl bromide lies along the z-axis with the proton along the z-axis at some point A at which the C tensor for the proton is diagonalized (i.e. $C_{xx} = C_{yy} = C_{\perp}$ and $C_{zz} = C_{\parallel}$), he then relocates the proton to its final position at the y-axis on the x-y plane by a rotation about the carbon through an angle θ (see Figure 2-9). As a result the C-tensor element for the proton after the transformation is given by,

$$C = \begin{pmatrix} C_{\perp} - \beta \sin^2 \theta & 0 & \beta \sin \theta \cos \theta \\ 0 & C_{\perp} & 0 \\ \beta \sin \theta \cos \theta & 0 & C_{\parallel} + \beta \sin^2 \theta \end{pmatrix}$$

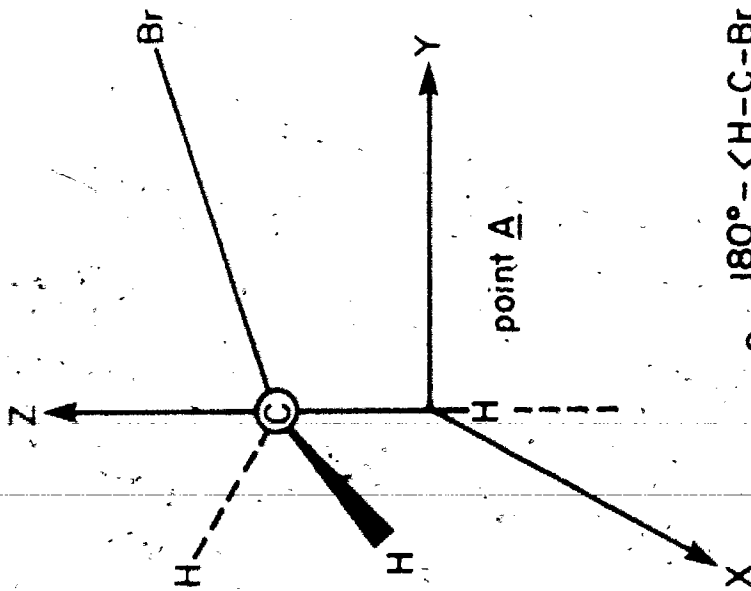
where $\beta = C_{\perp} - C_{\parallel}$.

FIGURE 2-9

Relocation of the proton from the z-axis to the y-axis to obtain θ value necessary for the calculation of the spin-rotation contribution from the proton nucleus which lies off the principal axis.



Rotation
About C Atom



$$\theta = \frac{180^\circ - \angle \text{H-C-Br}}{2} = 36^\circ$$

Wang then obtains the expression for R_1^{SR} ,

$$(2-43) \quad R_1^{SR} = \frac{8\pi^2 kT}{3\hbar^2} \left[I_{\parallel} (C_{\parallel} + \beta \sin^2 \theta)^2 \left(\frac{\tau_{w\parallel}}{1 + 2D_{\perp} \tau_{w\parallel}} \right) \right. \\ \left. + I_{\perp} (\beta^2 \sin^2 \theta \cos^2 \theta) \left(\frac{\tau_{w\perp}}{1 + 2D_{\perp} \tau_{w\perp}} + \frac{\tau_{w\parallel}}{1 + (D_{\perp} + D_{\parallel}) \tau_{w\parallel}} \right) \right. \\ \left. + I_{\perp} (C_{\perp} - \beta \sin^2 \theta)^2 \left(\frac{\tau_{w\perp}}{1 + (D_{\perp} + D_{\parallel}) \tau_{w\parallel}} \right) \right]$$

in the limit $D_{\perp} \tau_{w\perp}, D_{\perp} \tau_{w\parallel} \ll 1$ reduces to

$$(2-44) \quad R_1^{SR} = \frac{8\pi^2 kT}{3\hbar^2} \left[I_{\parallel} (C_{\parallel} + \beta \sin^2 \theta)^2 \tau_{w\parallel} + I_{\perp} \beta^2 \sin^2 \theta \cos^2 \theta \right. \\ \left. \left(\tau_{w\perp} + \frac{\tau_{w\parallel}}{1 + D_{\parallel} \tau_{w\parallel}} \right) + I_{\perp} [(C_{\perp} - \beta \sin^2 \theta)^2 + C_{\perp}^2] \tau_{w\perp} \right]$$

Now we may use the value for \bar{C} along with Eq. (2-44) and the values $\tau_{w\parallel} = 0.22$ psec and $\tau_{w\perp} = 0.039$ psec, $D_{\parallel} = 250 \times 10^{10}$ and the experimental $R_1^{SR} = 0.050 \text{ sec}^{-1}$ and obtain values for C_{\parallel} and C_{\perp} . We obtain two possible solutions: (a) $C_{\perp} = +1.07$ kHz and $C_{\parallel} = -8.95$ kHz, (b) $C_{\perp} = +0.47$ kHz and $C_{\parallel} = +10.18$ kHz.

We may compare these to values obtained as in the ^{13}C calculation using σ'_p and $\Delta\sigma$ for ^1H . From this calculation we have obtained $C_{\perp} = +0.50$ kHz and $C_{\parallel} = +9.17$ kHz in excellent agreement with the second set of solutions.

The various contributions to the proton relaxation time in pure CH_3Br at $+5^\circ\text{C}$ are shown in Table 2-6.

TABLE 2-6

CONTRIBUTIONS TO THE ^1H RELAXATION TIME IN PURE CH_3Br
AT 5°C

T_1 Mechanism	Relaxation Rate (sec^{-1})	Relaxation Time (sec)
T_1 total	0.079	12.7
T_1 H-H inter	0.014	71
T_1 H-Br inter	0.001	~1000
T_1 H-H intra	0.017	59
T_1 H-Br intra	0.0006	~1700
T_1 SR	0.047	21.3

CHAPTER 3

ANISOTROPIC ROTATIONAL DIFFUSION IN DIMETHYLMERCURY

A. Introduction

Nuclear magnetic resonance is a convenient probe for the study of the rotation of molecules in liquids (Abragam 1961) because the nuclear spin-relaxation time depends on the molecular motion although there is still some question as to the validity of the various proposed models. In a molecule in the liquid phase, the more nuclei whose relaxation times can be measured, the more information one can obtain about the motions of that particular molecule (see e.g. Bopp 1967; Zeidler 1965). For nuclei of spin $I \geq 1$ the quadrupolar relaxation is generally the dominant mechanism in the spin-lattice relaxation time. However for nuclei of spin $\frac{1}{2}$ the problem is more complicated because of the various possible mechanisms which may contribute to the total relaxation rate.

In a number of studies involving nuclei of spin $\frac{1}{2}$, ^{13}C (Gillen et al. 1971; Farrar et al. 1972; Grant et al. 1971); ^{19}F (Armstrong and Courtney 1972); ^{31}P (Sawyer and Powles 1971); ^{15}N (Litchman and Alei Jr. 1972); ^{119}Sn (Sharp 1972, 1974) and ^{207}Pb (Hawk 1974) it has been shown that the spin-rotation contribution to the spin-lattice relaxation rate is a dominant mechanism. There appears to be a trend showing that the

spin-rotation interaction ($I \cdot J$) becomes more important for the higher Z nuclei of spin $\frac{1}{2}$, however studies involving these higher Z nuclei have been rarely reported in the literature. If indeed this interaction is large it should be reflected in the value for the spin-rotation constant C for the ^{199}Hg nucleus in dimethylmercury.

Along with the study of the relaxation of the ^{199}Hg nucleus we have also studied the ^1H and ^2D temperature dependence of the spin-lattice relaxation times and thus derived the anisotropic reorientational motion of the dimethylmercury molecule.

B. Experimental

1. Measurement of relaxation times.

The proton spin-lattice relaxation times T_1 were measured by the saturation recovery method (Van Geet 1965) and rapid adiabatic passage with sampling (Parker and Jonas 1970) on a Varian A56/60 high resolution NMR spectrometer operating at 60 MHz. The ^2D spin-lattice relaxation times were measured at 15.4 MHz by rapid adiabatic passage with sampling on a Varian XL-100 NMR spectrometer.

The ^{199}Hg relaxation times were measured indirectly by the modified rotary echo method of Wells and Abramson (1969) on the proton multiplet components. $R_{2r} (\equiv T_{2r}^{-1})$ for protons was obtained at 60 MHz (14.1 kGauss). The relaxation rate in

the rotating frame as mentioned previously is given by,

$$(3-1) \quad R_{2r} = \frac{1}{2}(R_{1H} + R_{2H})$$

Therefore by performing a selective rotary echo experiment on the proton signal due to the dimethylmercury molecules containing non-magnetic Hg (I=0) we obtain,

$$(3-2) \quad R_{2r}^I = \frac{1}{2}(R_{1H}^I + R_{2H}^I)$$

For this case the value of $R_{2r}(H)$ was found to be the same as $R_1(H)$ which means that $R_{1H}^I = R_{2H}^I$.

Also performing a selective rotary echo experiment on either doublet member due to $^{199}\text{Hg}(\text{CH}_3)_2$ (see Figure 3-1) we obtain,

$$(3-3) \quad R_{2r}^{II} = \frac{1}{2}(R_{1H}^{II} + R_{2H}^{II})$$

Where $R_{1H}^{II} = R_{1H}^I$ since both dipole and scalar contributions from ^{199}Hg to ^1H are negligible, and $R_{2H}^{II} = R_{1H}^{II} + R_1(^{199}\text{Hg})$; $R_1(^{199}\text{Hg})$ is the mercury-199 scalar contribution to the proton R_{2H} .

The ^{201}Hg isotope (13.22%, I= 3/2) is scalar coupled to ^1H but collapsed in the spectrum, and affords a scalar R_2 mechanism to the ^1H which is included in with the rotary echo measurement on Hg (I=0) resonance. The effect is negligible as is shown in the calculation in Appendix B.

Figure 3-1

^1H spectrum of neat liquid $\text{Hg}(\text{CH}_3)_2$ at 60 MHz

^{199}Hg

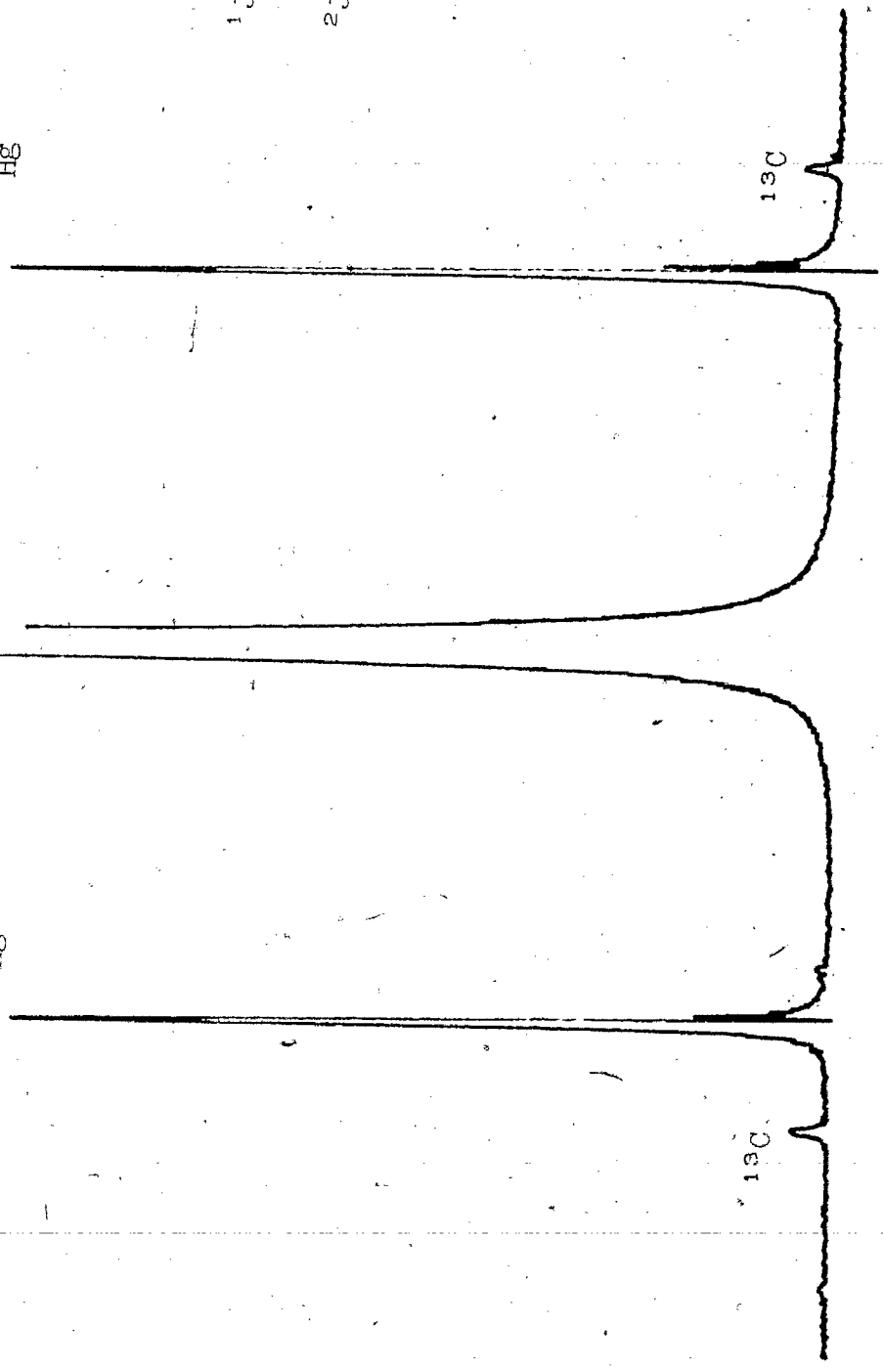
^{199}Hg

$^1J_{\text{H-}^{13}\text{C}} = 129.5 \text{ Hz}$

$^2J_{\text{H-}^{199}\text{Hg}} = 101.5 \text{ Hz}$

^{13}C

^{13}C



Therefore using these two selective rotary echo experiments we can indirectly obtain values of $R_1(^{199}\text{Hg})$.

$$(3-4) \quad R_1(^{199}\text{Hg}) = 2(\Delta R_{2r}) = 2(R_{2r}^{\text{II}} - R_{2r}^{\text{I}})$$

For the mixtures of $\text{Hg}(\text{CH}_3)_2$ and $\text{Hg}(\text{CD}_3)_2$ there was no evidence of any of the mixed species such as $\text{CH}_3\text{-Hg-CH}_2\text{D}$ etc. or $\text{CH}_3\text{-Hg-CD}_3$ so that in the separation of the various mechanisms we did not have to worry about possible H-D or $\text{CH}_3\text{-CD}_3$ exchange.

Temperature control was accomplished using the Varian W-6040 variable temperature NMR probe accessory. Temperatures were measured using a copper constantan thermocouple, temperature readings were accurate to $\pm 1^\circ\text{C}$.

2. Synthesis of $\text{Hg}(\text{CD}_3)_2$

The d_e -dimethylmercury was prepared according to Gilman and Brown's Grignard method (1929) with minor modifications. In a dry 100 cc flask fitted with a reflux condenser and a drying tube filled with "Drierite" was added 2.0 grams of Mg turnings. To this was added 10 cc of dry (absolute) ether and 2.0 grams of dry methyl iodide- d_3 (Merck, Sharp and Dohme of Canada). As soon as the reaction had started, a solution of 8.0 grams CD_3I in 40 cc of dry (absolute) ether was slowly added. An ice bath was used to cool the reaction flask when the reaction proceeded too vigorously. When spontaneous refluxing had ceased, the mixture was further refluxed for

30 minutes to drive the reaction to completion.

The Grignard reagent was carefully decanted from the excess Mg into a 500 cc flask fitted with a condenser and heated until refluxing had begun. To this is attached a Soxhlet extractor containing 7.15 grams of mercuric chloride and 75 cc of dry (absolute) ether is added to the flask. This was allowed to reflux for 3 days to improve the yield of dimethylmercury- d_6 .

After three days of refluxing the solution was cooled in ice and the excess Grignard reagent was destroyed by the addition of about 25 cc of water through the condenser. The water had to be carefully added to keep the reaction from becoming too vigorous. Next the ether layer was separated and the aqueous layer extracted with 20 cc of dry (absolute) ether. The combined ether extract was washed with 25 cc of water, separated and dried over $CaCl_2$. The ether was carefully distilled off using a "spiral" column. The remaining traces of ether were separated out using preparative vapor phase chromatography. The yield was 3.92 grams of $Hg(CD_3)_2$ (57% yield); B.P. 88-89°C (uncorrected).

The $Hg(CH_3)_2$ was obtained from Alfa Inorganics. The samples were degassed in 5 mm tubes by the usual freeze-pump-thaw cycles under vacuum. The viscosity and density were measured by standard methods.

3. Spin-Spin coupling constants and chemical shifts in
Hg(CH₃)₂ and Hg(CD₃)₂.

We have measured the various nuclear spin-spin coupling constants for Hg(CH₃)₂ and Hg(CD₃)₂ using ¹H and ¹³C NMR. These values are tabulated in Table 3-1.

The first four coupling constants are in excellent agreement with the results of Dean and McFarlane(1967). The last two coupling constants have never been previously reported. The value of $J_{1H-2D} = 1.9 \pm 0.1$ Hz indicates that the $\langle H-C-D$ is very close to 109.5° since the geminal coupling constant is very sensitive to small changes in the $\langle H-C-H$ (Karplus, Grant and Gutowsky 1959).

The ratio J_{C-H}/J_{C-D} is always very close to the value predicted by the gyromagnetic ratios $\gamma_H/\gamma_D = 6.5144$ (Wimmett 1953) so that we may thus calculate the value for $J_{C-H} - 6.5144J_{C-D} = +0.6 \pm 4.0$ Hz. Thus it appears that the isotope effect on coupling constants is negligible. These results are in agreement with those observed by Colli, Gold and Pearson (1973) for a variety of deuterated organic compounds.

We have also measured the deuterium isotopic shift in both ¹³C and ¹H NMR of Hg(CH₃)₂ and modified species. The values obtained are $\delta_{isot} (^{13}C) = 0.95 \pm 0.07$ ppm upfield and $\delta_{isot} (^1H) (CH_3-CHD_2) = 0.040 \pm 0.003$ ppm also upfield. The isotopic difference in the ¹H and ¹³C is representative of the differences of ranges in chemical shifts (¹³C ~ 600 ppm and ¹H ~ 20 ppm).

TABLE 3-1

NUCLEAR SPIN-SPIN COUPLING CONSTANTS IN $\text{Hg}(\text{CH}_3)_2$ AND $\text{Hg}(\text{CD}_3)_2$

$^1J_{\text{H}-^{13}\text{C}}$	$= 129.5 \pm 0.2$ Hz	(^1H spectrum)
$^2J_{\text{H}-^{199}\text{Hg}}$	$= 101.5 \pm 0.2$ Hz	(^1H spectrum)
$^1J_{^{13}\text{C}-^{199}\text{Hg}}$	$= 684.6 \pm 0.3$ Hz	(^{13}C - $\{^1\text{H}\}$ decoupled)
$^4J_{\text{H}-^1\text{H}}$	$= 0.43 \pm 0.03$ Hz	(^1H spectrum)
$^1J_{\text{H}-^2\text{D}}$	$= 1.9 \pm 0.1$ Hz	(^1H spectrum)
$^1J_{^{13}\text{C}-^2\text{D}}$	$= 19.8 \pm 0.6$ Hz	(^{13}C undecoupled spectrum)

Note: ^1H spectrum obtained on Varian A56/60 at 60 MHz and
 ^{13}C spectrum obtained on XL-100 operating at 25.1 MHz
in FT mode.

C. Results and Analysis

As mentioned previously for most nuclei of spin $\frac{1}{2}$ the relaxation is caused by a combination of mechanisms: intermolecular and intramolecular dipolar coupling, spin-rotation and possibly chemical shift anisotropy. The proton relaxation data in Table 3-2 and Figure 3-2 indicate the presence of several mechanisms in the relaxation rate.

As described earlier the form of the chemical shift anisotropy contribution is $R_1^{CSA} = \frac{2}{15} \gamma^2 H_0^2 (\sigma_{\parallel} - \sigma_{\perp})^2 \tau_c$ since $(\sigma_{\parallel} - \sigma_{\perp}) \approx 1-5$ ppm and $\tau_c \approx 10^{-12}$ sec for protons usually, $R_1^{CSA} \approx 10^{-9}$ for protons is negligible. For ^{199}Hg the chemical shift anisotropy $(\sigma_{\parallel} - \sigma_{\perp})$ has not been measured; however if we assumed a value of even ~ 3000 ppm, $R_1^{CSA} \approx 10^{-2} \text{ sec}^{-1}$ which would still be completely negligible.

Extrapolation from data by standard type of dilution studies (Bonera and Rigamonti 1965) of $\text{Hg}(\text{CH}_3)_2$ in $\text{Hg}(\text{CD}_3)_2$ allows the separation of intermolecular dipole-dipole effects from intramolecular mechanisms for protons. In the ^{199}Hg relaxation in dimethylmercury it is safe to assume that the intermolecular dipole-dipole relaxation rate is insignificant as in the ^{13}C relaxation (Kuhlmann, Grant and Harris 1970) because of the much increased intermolecular nuclear separation. Thus we are left with the separation of the intramolecular contributions to both the ^1H and ^{199}Hg relaxation rates.

TABLE 3-2

R_1 RELAXATION DATA FOR LIQUID $\text{Hg}(\text{CH}_3)_2$ - $\text{Hg}(\text{CD}_3)_2$ MIXTURES

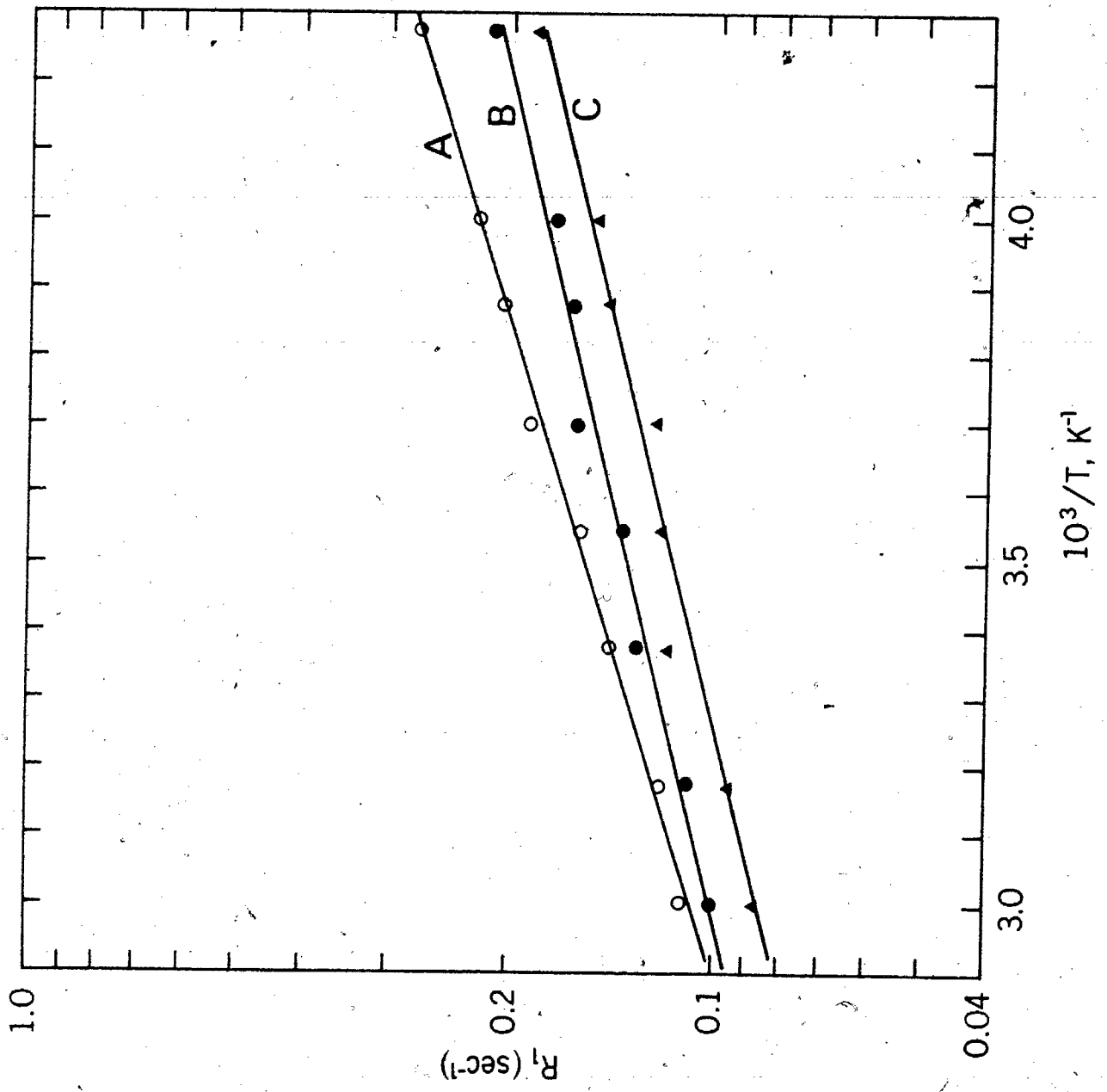
^1H of 100% $\text{Hg}(\text{CH}_3)_2$	^1H of 60% $\text{Hg}(\text{CH}_3)_2^*$	^1H of 27% $\text{Hg}(\text{CH}_3)_2^*$	
T(°K)	$R_1(\text{sec}^{-1})$	$R_1(\text{sec}^{-1})$	$R_1(\text{sec}^{-1})$
333	0.109	0.099	0.085
315	0.118	0.108	0.093
296	0.139	0.128	0.114
282	0.156	0.135	0.117
270	0.183	0.157	0.120
258	0.203	0.160	0.143
250	0.220	0.170	0.148
234	0.271	0.211	0.182

* in $\text{Hg}(\text{CD}_3)_2$. Error in measured relaxation rates is $\pm 5\%$

^2D in $\text{Hg}(\text{CD}_3)_2$		^{199}Hg in $\text{Hg}(\text{CH}_3)_2$	
T(°K)	$R_1(\text{sec}^{-1})$	T(°K)	$R_1(\text{sec}^{-1})$
333	0.410	333	1.150
311	0.422	315	0.970
298	0.459	296	0.850
267	0.557	282	0.780
263	0.570	270	0.774
245	0.641	258	0.670
240	0.684	250	0.600
234	0.743	234	0.571
219	0.828		

Figure 3-2

Experimental relaxation rates for ^1H in dimethylmercury
(A) neat $\text{Hg}(\text{CH}_3)_2$; (B) 60 per cent $\text{Hg}(\text{CH}_3)_2$ in $\text{Hg}(\text{CD}_3)_2$;
(C) 27 per cent $\text{Hg}(\text{CH}_3)_2$ in $\text{Hg}(\text{CD}_3)_2$



1. Proton relaxation

The temperature dependent proton relaxation times are shown in Figure 3-2 for pure $\text{Hg}(\text{CH}_3)_2$ and for mixtures containing 27 and 60 per cent mole fraction $\text{Hg}(\text{CH}_3)_2$ in $\text{Hg}(\text{CD}_3)_2$ respectively. Using the same method as for the methyl bromide case (Chapter 2) the relaxation rate for the mixtures is,

$$(3-5) \quad R_{1\text{inter}}^{\text{H}} = R_{1\text{inter}}^{\text{H-H}} + R_{1\text{inter}}^{\text{H-D}} + R_{1\text{inter}}^{\text{H-}^{199}\text{Hg}}$$

Since $\gamma_{\text{H}}^2 = 42.5 \gamma_{\text{D}}^2$ and the spin values are different, the deuterium in dimethylmercury- d_6 will contribute 1/24 as much to the intermolecular relaxation as the hydrogens in dimethylmercury- h_6 . The total proton relaxation is then,

$$(3-6) \quad R_{1\text{total}}^{\text{H}} = \frac{23C + 1}{24} R_{1\text{inter}}^{\text{H-H}} + R_{1\text{inter}}^{\text{H-}^{199}\text{Hg}} + R_{1\text{intra}}^{\text{dd}} + R_{1\text{SR}}$$

where C is the mole fraction of dimethylmercury- h_6 . Once again as described in Chapter 2, a plot of $R_{1\text{total}}^{\text{H}}$ vs. $23C/24$ yields,

$$(3-7) \quad \text{slope} = R_{1\text{inter}}^{\text{H-H}}$$

and

$$(3-8) \quad \text{intercept} = \frac{1}{24} R_{1\text{inter}}^{\text{H-H}} + R_{1\text{inter}}^{\text{H-}^{199}\text{Hg}} + R_{1\text{intra}}^{\text{dd}} + R_{1\text{SR}}$$

We may eliminate $R_{1\text{inter}}^{\text{H-}^{199}\text{Hg}}$ if we assume that $d^{\circ}_{\text{H-Hg}}$ equals

$d^{\circ}_{\text{H-H}}$ (in fact $d^{\circ}_{\text{H-Hg}}$ will actually be greater than $d^{\circ}_{\text{H-H}}$),

we must also keep in mind that ^{199}Hg is only 16.86 per cent.

natural abundance, whence

$$(3-9) \quad R_{1\text{inter}}^{\text{H-}^{199}\text{Hg}} \approx 0.024 R_{1\text{inter}}^{\text{H-H}}$$

We are then left with separating $R_{1\text{intra}}^{\text{dd}}$ from R_1^{SR} . If we notice the plots in Figure 3-2 we see that they show no curvature, which would normally be present if we had a mixture of intramolecular dipole-dipole and spin-rotation interactions since these two mechanisms have opposite temperature dependence. It appears safe to assume that at least over the temperature range studied that the spin-rotation contribution is negligible for protons and that the only relaxation mechanisms present are those due to inter and intramolecular dipole-dipole interactions. The separation of these two mechanisms is shown in Figure 3-3. For the intermolecular interaction the energy of activation is 2.3 ± 0.3 Kcal/mole and for the intramolecular dipole-dipole it is 0.9 ± 0.1 Kcal/mole. The data indicates the intramolecular dipole-dipole mechanism to be the predominant at the higher temperatures.

2. Anisotropic rotational diffusion tensor for $\text{Hg}(\text{CD}_3)_2$

The usual method of obtaining the anisotropic rotational diffusion tensor of a symmetric top molecule involves the measurement of the relaxation time of two quadrupolar nuclei which have different bond angles with respect to the symmetry axis of the molecule (Woessner et al. 1968; Jonas and Di Gennaro

Figure 3-3

Separation of $R_{\text{inter}}^{\text{H-H}}$ from $R_{\text{intra}}^{\text{dd}}$ for the
 ^1H relaxation rate in $\text{Hg}(\text{CH}_3)_2$.

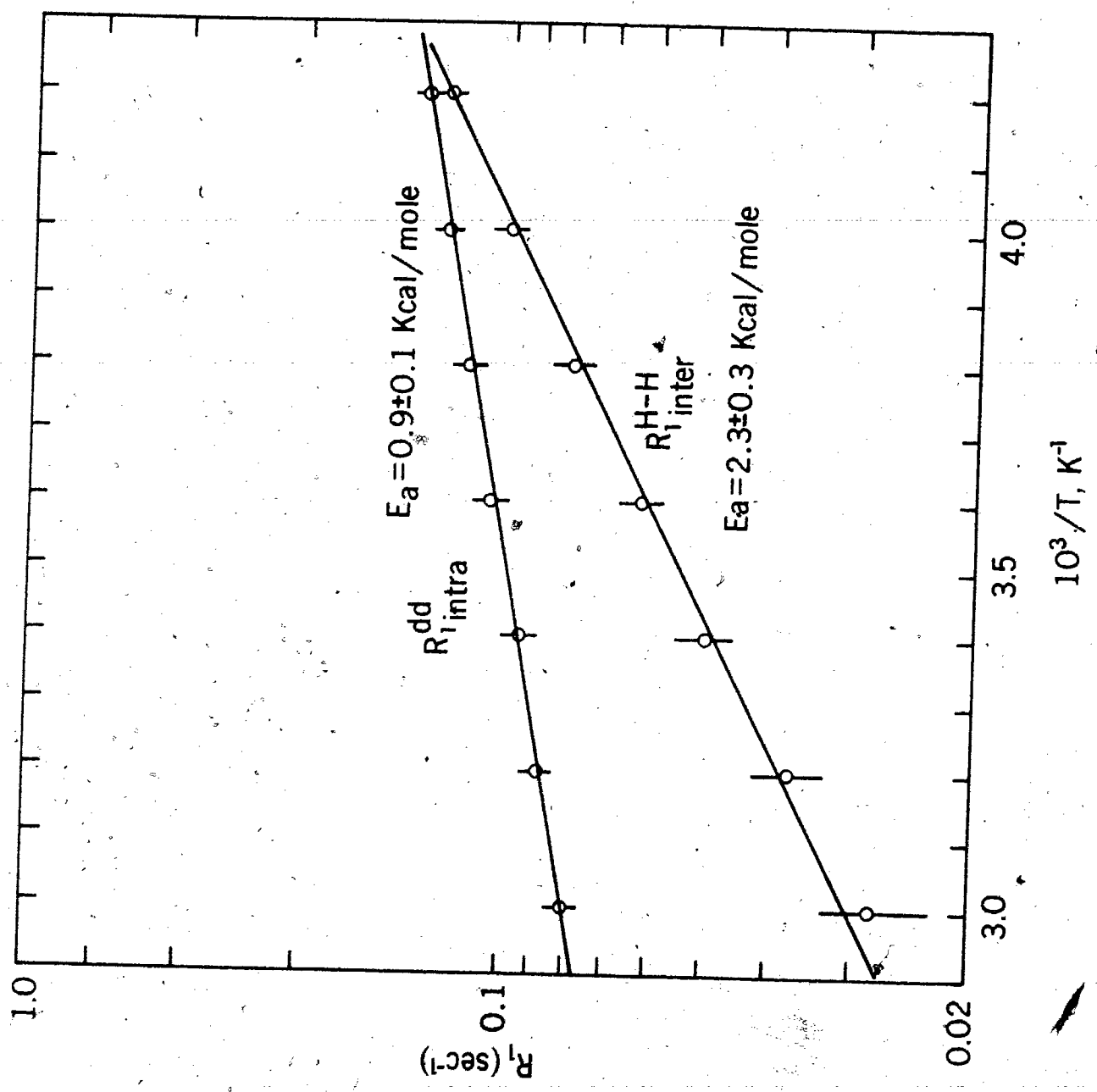
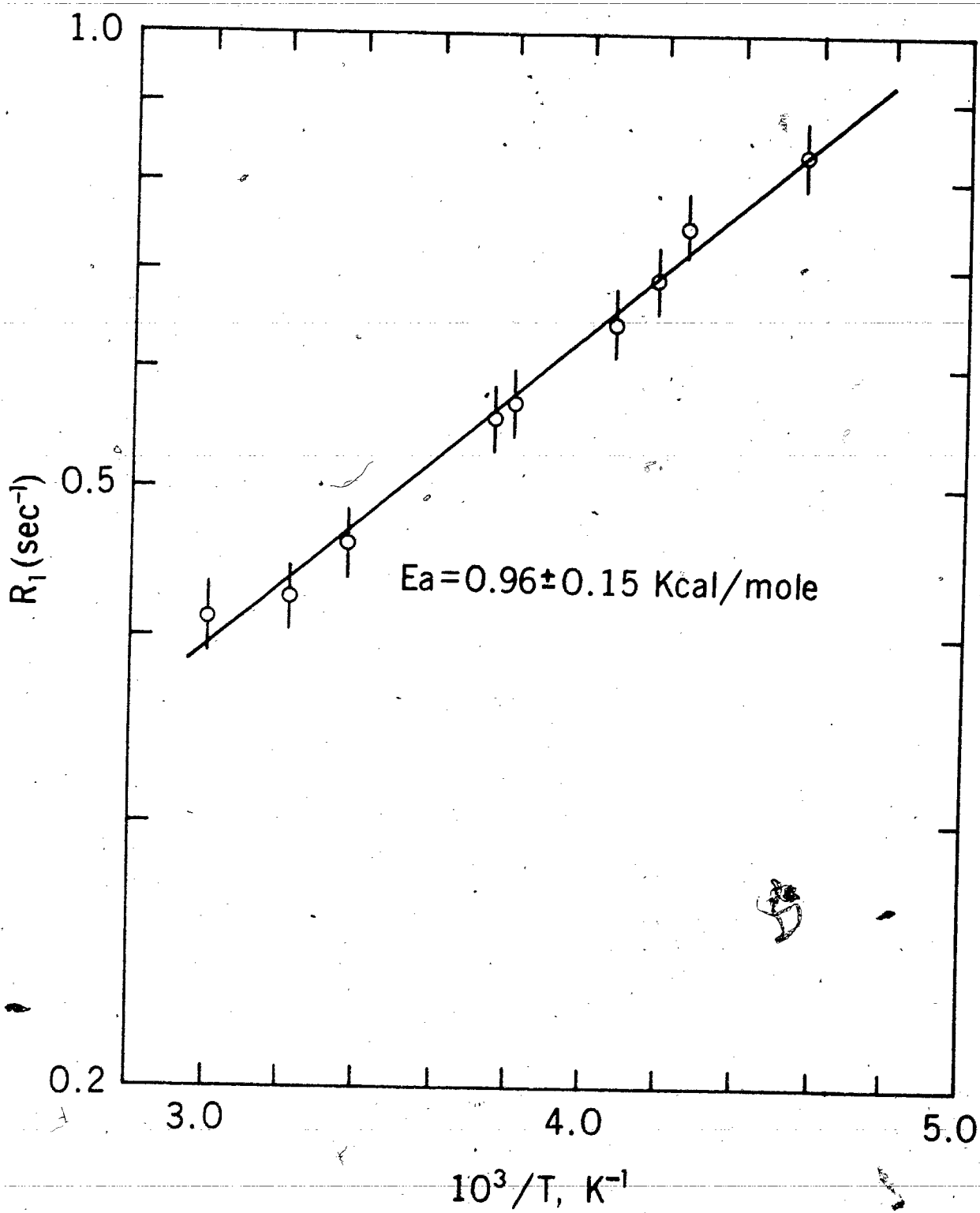


Figure 3-4

^2D spin-lattice relaxation rate in $\text{Hg}(\text{CD}_3)_2$



1969; Allerhand 1970; Gillen and Noggle 1970). Thus in our molecule we could determine the anisotropic rotational diffusion tensor for dimethylmercury- d_6 from quadrupolar relaxation of both 2D and ^{201}Hg . As before the equations (Huntress 1965) that relate the measured relaxation rate of a nucleus to the diffusion tensor components and the relative orientation to the electric field gradient are:

$$(3-10) \quad R_{1Q} = \frac{3\pi^2(2I+3)}{10I^2(2I-1)} (e^2qQ/h)^2 \tau_c$$

$$(3-11) \quad \tau_c = \frac{\frac{1}{4} (3\cos^2\theta - 1)^2}{6D_{\perp}} + \frac{3\sin^2\theta\cos^2\theta}{5D_{\perp} + D_{\parallel}} + \frac{(3/4)\sin^4\theta}{2D_{\perp} + 4D_{\parallel}}$$

The problem is that the ^{201}Hg resonance is not observable either directly or indirectly because of its very short relaxation time due to its presumably large quadrupole coupling constant (see Appendix B). We must therefore find a different method of obtaining D_{\perp} and D_{\parallel} . First we use the 2D relaxation times of Figure 3-4, the approximate 2D quadrupole coupling constant for molecules containing methyl groups (165 kHz) and Eq. (3-10) to obtain $\tau_c(D)$. We then assume that D_{\parallel} and D_{\perp} will not differ greatly in going from the $Hg(CH_3)_2$ to the $Hg(CD_3)_2^{**}$ species and use Powles' equation (1963),

$$(3-12) \quad R_{1\text{intra}}^{H-H} = \frac{3\gamma_H^4 \hbar^2}{r_{H-H}^6} \tau_c(H-H)$$

(which assumes independent pairwise interactions and neglects symmetry effects) to obtain $\tau_c(\text{H-H})$. This is the effective correlation time for reorientation of the proton internuclear vector. For this correlation time $\theta=90^\circ$ because the pertinent proton relaxation interaction occurs in the plane of the methyl hydrogens. This plane is normal to the major axis. Using the appropriate values for the constants and $r_{\text{H-H}}$ (from Table 3-3) in Eq. (3-12) we obtain,

$$(3-13) \quad R_1^{\text{H-H}} \text{intra} = 4.86 \times 10^{10} \tau_c(\text{H-H})$$

Using Eq. (3-11), the experimental values for $\tau_c(\text{H-H})$, $\tau_c(\text{D})$, $\theta=90^\circ$ for $\tau_c(\text{H-H})$ and $\theta=109^\circ 28'$ for $\tau_c(\text{D})$ we can solve for the temperature dependence of both D_\perp and D_\parallel . These are given in Figure 3-5. We find E_a for D_\perp is 0.85 ± 0.15 Kcal/mole and for D_\parallel , $E_a = 1.30 \pm 0.60$ Kcal/mole. Also the reorientation about the figure axis is about forty times faster than orientation of the figure axis. The values for D_\parallel have a great uncertainty because as mentioned below both $\tau_c(\text{D})$ and $\tau_c(\text{H-H})$

** This is quite reasonable for D_\perp but not D_\parallel since there is a factor of 2 difference between $I_\parallel(\text{Hg}(\text{CD}_3)_2)$ and $I_\parallel(\text{Hg}(\text{CH}_3)_2)$. However this does not matter much since in the calculation of $\tau_c(\text{H-H}) \sim 90\%$ comes from the first term in Eq. (3-11) which is solely dependent on D_\perp . Also in the calculation of $\tau_c(\text{D}) \sim 70\%$ comes from the first term in Eq. (3-11).

TABLE 3-3

GEOMETRIC PARAMETERS AND MOMENTS OF INERTIA FOR $\text{Hg}(\text{CH}_3)_2$

$r_{\text{C-H}}$	1.096 \AA	*
$r_{\text{H-H}}$	1.81	*
$r_{\text{Hg-C}}$	2.094	**
$r_{\text{Hg-H}}$	2.62 (calculated)	
$\angle \text{H-C-H}$	109.5°	*
$\angle \text{C-Hg-C}$	180°	**

$$I_1 = 11.0 \times 10^{-40} \text{ gm-cm}^2$$

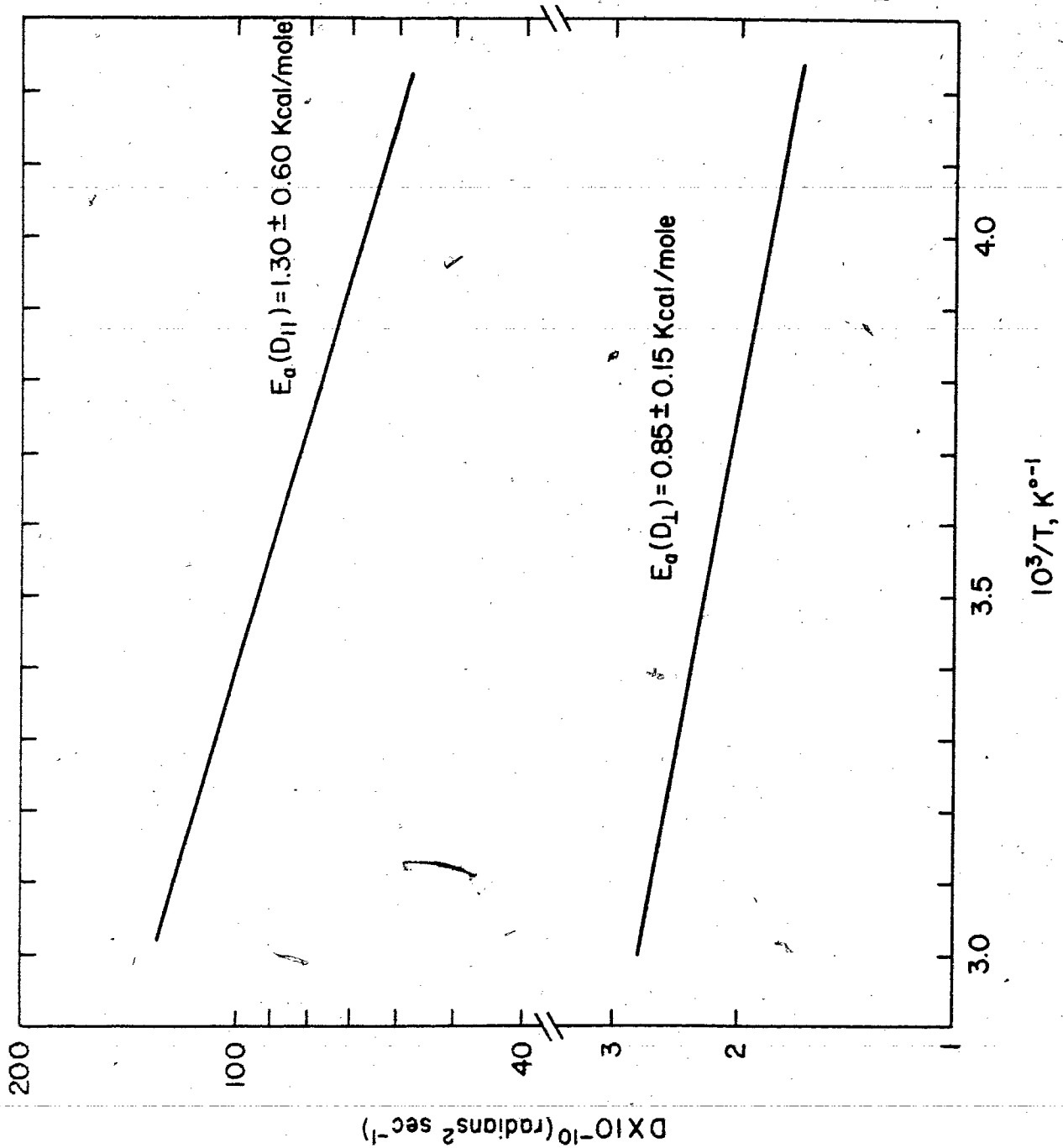
$$I_2 = 240.8 \times 10^{-40} \text{ gm-cm}^2 \quad **$$

* Typical values of average $-\text{CH}_3$ group

** K. Suryanarayana Rao, B.P. Stoicheff, and R. Turner,
Can. J. Phys., 38, 1516(1960)

Figure 3-5

Rotational rate constants (D_{\parallel} , D_{\perp}) for $\text{Hg}(\text{CD}_3)_2$



are largely dependent on the value of D_{\perp} ; however large changes in D_{\parallel} have very little effect on either $\tau_c(D)$ or $\tau_c(H-H)$. The value of $E_a(D_{\parallel}) = 1.30 \pm 0.6$ Kcal/mole would appear a bit high since in most cases involving methyl group reorientation $E_a(D_{\parallel}) = \sim 0.8$ Kcal/mole (Bopp 1967; Woessner *et al.* 1968; Jonas and Di Gennaro 1969; Gillen *et al.* 1971; Chapter 2 of this thesis), however a value of 0.8 Kcal/mole is within the uncertainty of our measurement.

Since Eqs. (3-10) and (3-11) are derived from the assumption of rotational diffusion, we can test the results by the so-called χ -test (Gillen and Noggle 1970) to check that this method is a good approximation of the reorientations. The χ test consists of calculating the ratio of the reorientational correlation time about a particular axis to the theoretical free gas reorientational time about the same axis. If χ is large compared to one, the rotational diffusion limit applies. For dimethylmercury application of the χ -test to the perpendicular motion gives values ranging from 15-22 indicating rotational diffusion for this motion. However for the parallel motion the range of χ_{\parallel} is 1.4-3.0 indicating possible inertial effects due to the much smaller moment of inertia about this axis.

3. ^{199}Hg Spin-lattice relaxation

For the ^{199}Hg relaxation it is safe to assume that the intermolecular dipole-dipole relaxation is insignificant as previously mentioned. Therefore the T_1 's of ^{199}Hg in $\text{Hg}(\text{CH}_3)_2$

Figure 3-6

^{199}Hg spin-lattice relaxation rate in $^{199}\text{Hg}(\text{CH}_3)_2$

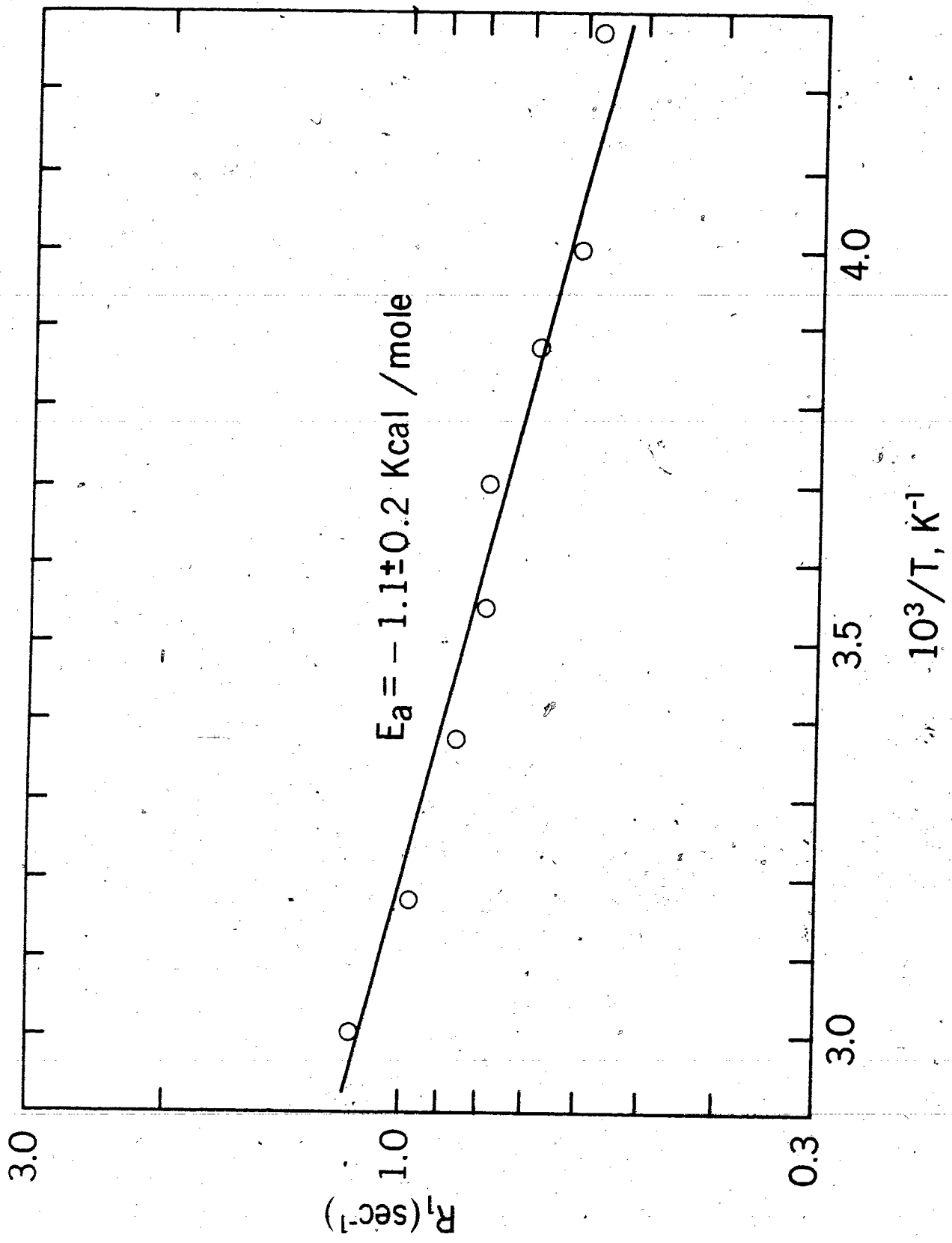


(Figure 3-6) come from intramolecular interactions. The dipolar contribution can be written as (powles 1963),

$$(3-14) \quad R_{1\text{intra}}^{\text{dd}} = \frac{6\gamma_{\text{H}}^2 \gamma_{\text{Hg}}^2 \hbar^2}{r_{\text{H-Hg}}^6} \tau_c(\text{Hg-H})$$

Using the appropriate values for the constants and intermolecular distances (Table 3-3) we obtain,

$$(3-15) \quad R_{1\text{intra}}^{\text{dd}} = 3.36 \times 10^8 \tau_c(\text{Hg-H})$$

$\tau_c(\text{Hg-H})$ can be calculated using equation (3-11) along with D_{\perp} , D_{\parallel} and $\theta=23.5^\circ$. The calculated contribution at $+40^\circ\text{C}$ is $R_{1\text{intra}}^{\text{dd}} = 0.0014 \text{ sec}^{-1}$ which is negligible, the dominant reason being the large Hg-H separation. We are thus left with the conclusion that the only operative spin-lattice relaxation mechanism is that due to the spin-rotation interaction. This conclusion is supported by the experimental temperature dependence (see Figure 3-6) as this is the only mechanism which shows this particular temperature dependence. It shows an Arrhenius behaviour with an energy of activation of -1.1 ± 0.2 Kcal/mole.

D. Discussion

1. Proton-proton intermolecular relaxation times

The proton-proton intermolecular relaxation times (see Figure 3-3) compare very well to those calculated from Eq.(2-20) Using the same treatment as for the methyl bromide proton-

proton intermolecular relaxation time we obtain the result,

$$(3-16) \quad R_{1\text{inter}}^{\text{H-H}} = \frac{9\pi^2 h^2 \gamma^4 \eta N}{2kT}$$

where all symbols have the previously mentioned meanings.

Using Eq. (3-16) along with the measured values for density and viscosity (Table 3-4) we obtain the theoretical $R_{1\text{inter}}^{\text{H-H}}$.

TABLE 3-4

DENSITY AND VISCOSITY FOR LIQUID $\text{Hg}(\text{CH}_3)_2$

T(°K)	ρ (g/ml)	η (cP)
273	3.1403	1.308
288	3.0903	1.115
298	3.0787	1.040
308	3.0620	0.956

These theoretical values can be compared with experimental values (Table 3-5). The theoretical results are in surprisingly good agreement with the experimentally obtained values again, although perhaps fortuitous in view of the questionable assumptions in its derivation. From theory the energy of activation is 2.2 Kcal/mole and from experiment E_a is 2.3 ± 0.3 Kcal/mole.

TABLE 3-5

THEORETICAL AND EXPERIMENTAL VALUES FOR $T_1^{\text{H-H}}_{\text{inter}}$

T(°K)	Theory	Experiment
273	13.9 sec	15.1 sec
288	17.5 sec	18.9 sec
298	19.6 sec	21.7 sec
308	22.2 sec	24.6 sec

2. ^{199}Hg Spin-rotation constant

Since we have established that the relaxation of the ^{199}Hg nucleus in dimethylmercury is due strictly to the spin-rotation interaction we should be able to obtain the spin-rotation constant (C_{Hg}). The angular momentum correlation time τ_w has been related to the tumbling reorientational correlation time τ_c by Hubbard (1963) in the diffusion limit

$$(3-17) \quad \tau_c \tau_w = \frac{\bar{I}}{6kT}$$

where $\bar{I} = \frac{1}{3}(I_{\parallel} + 2I_{\perp})$.

The classical diffusion model was extended by Gordon (1965,1966). In the extended diffusion model, molecular re-orientation is described as a stochastic process in which the

molecules are undergoing free rotation interrupted by collisions. After each period of free rotation, τ_w , there occurs a collision which randomizes both the magnitude and direction of the angular momentum vector (J-diffusion) or randomizes only the direction (M-diffusion). McClung (1971, 1972) obtained limiting expressions for spherical top molecules,

$$(3.17a) \quad \tau_c \tau_w = \frac{\alpha I}{6kT}$$

where $\alpha = 1, 3$ in J and M-diffusion respectively.

An expression for R_1^{SR} has been given by Blicharski (1963),

$$(3.18) \quad R_1^{SR} = \frac{8\pi^2 kT}{3h^2} (I_{\parallel} + I_{\perp}) C_{Hg}^2 \tau_w$$

where $C_{Hg} = \left[\frac{1}{3} (C_{\parallel}^2 + 2C_{\perp}^2) \right]^{\frac{1}{2}}$ is the spin-rotation interaction constant:

Since the ^{199}Hg nucleus lies on the main symmetry axis, $\theta = 0$ and therefore its tumbling correlation time is given by $\tau_c = (6D_{\perp})^{-1}$. This indicates that the 'energy of activation' for $R_1^{SR} (^{199}\text{Hg})$ should have the same temperature dependence as D_{\perp} but of opposite sign. The experimental results are in fairly good agreement, $E_a(R_1^{SR}) = -1.1 \pm 0.2$ Kcal/mole and $E_a(D_{\perp}) = +0.85 \pm 0.15$ Kcal/mole.

Using Eq. (3-17a) along with $\tau_c = 6.7 \times 10^{-12}$ sec at 300°K and I we obtain $\tau_w = 1.0 \times 10^{-14}$ sec for J-diffusion and $\tau_w = 3.0 \times 10^{-14}$ sec for M-diffusion. Now using Eq. (3-18) along with τ_w and R_1^{SR} , we obtain $C_{Hg} = 45 \pm 5$ kHz for J-diffusion

and $C_{\text{Hg}} = 28 \pm 5$ kHz for M-diffusion. Since the molecule is highly anisotropic as can be seen from the inertia and diffusion tensors, it is quite plausible that the anisotropy of the spin-rotation tensor ($C_{\parallel} - C_{\perp}$) is quite large. Therefore discrepancies are expected when one uses an isotropic approach for a highly anisotropic molecule. With enough available information the more rigorous anisotropic approach is possible.

Bender and Zeidler (1971) have derived an equation relating the spin-rotation relaxation of a nucleus in symmetric top molecules to the rotational diffusion constants of the molecule. Their result is,

$$(3-19) \quad R_1^{\text{SR}} = \frac{8\pi^2}{3h^2} (I_{\parallel}^2 C_{\parallel}^2 D_{\parallel} + 2I_{\perp}^2 C_{\perp}^2 D_{\perp})$$

where all symbols have their usual meaning. The derivation of this equation is based on the assumption that both diffusion constants are in the rotational diffusion limit, which is reasonable for D_{\perp} but possibly not for D_{\parallel} because of inertial effects for this motion. However with this in mind we will proceed with this treatment.

If the temperature dependent data for D_{\parallel} , D_{\perp} and R_1^{SR} is known, one can obtain the values of C_{\parallel} and C_{\perp} using Eq. (3-19). From equation (3-19) and the necessary values for R_1^{SR} , D_{\parallel} and D_{\perp} we obtain,

$$(3-20a) \quad \text{at } 313^{\circ}\text{K} \quad C_{\parallel}^2 + 19.30 C_{\perp}^2 = 2.70 \times 10^{10}$$

$$(3-20b) \quad \text{at } 238^{\circ}\text{K} \quad C_{\parallel}^2 + 26.30 C_{\perp}^2 = 3.15 \times 10^{10}$$

The values for C_{\parallel} and C_{\perp} are obtained from the intersections of the temperature dependent ellipses plotted in Figure 3-7. The values obtained are:

$$|C_{\parallel}| = 120 \pm 60 \text{ kHz} \quad \text{and} \quad |C_{\perp}| = 26 \pm 3 \text{ kHz}$$

Using these values for C_{\parallel} and C_{\perp} we can calculate $C_{\text{eff}} = [\frac{1}{3}(2C_{\perp}^2 + C_{\parallel}^2)]^{\frac{1}{2}}$, from which we obtain $C_{\text{eff}} = 72 \pm \frac{33}{23} \text{ kHz}$.

This result is in fair agreement with the calculated values for J- and M-diffusion. As mentioned at the beginning of this discussion we must remember that although D_{\perp} is in the rotational diffusion limit D_{\parallel} probably isn't and we must be cautious with the value obtained for C_{eff} according to Bender and Zeidler's treatment. We must be especially careful with the value obtained for C_{\parallel} in view of the large error associated with this value.

3. Absolute shielding scale of ^{199}Hg

The magnetic shielding constant has been related to the spin-rotation constant through the second order paramagnetic term of Ramsey's shielding expression (Ramsey 1950, 1956; Flygare 1964). Deverell (1970) has rewritten this expression for symmetric top molecules,

$$(3-22) \quad \sigma_{\text{ave}} = \sigma_{\text{d}}' + \sigma_{\text{p}}' = \frac{e^2}{3mc^2} \left\{ \langle 0 | \sum_k \frac{1}{r_k} | 0 \rangle - \sum_j (Z_j/r_{ij}) \right\} + \frac{e^2}{6mc^2} \left\{ \frac{\pi}{\mu_N \gamma_I} (2C_{\perp} I_{\perp} + C_{\parallel} I_{\parallel}) \right\}$$

using Deverell's notation. This relation has been used to obtain the absolute chemical shift scale for ^{31}P (Deverell 1970; Gillen 1972); ^{19}F (Deverell 1970); ^{119}Sn (Sharp 1972) and ^{207}Pb (Sharp and Hawk 1974). The above expression suggests that the σ_p' is the only portion of the shielding constant that is sensitive to chemical environment changes and thus changes in the spin-rotation constant (C).

Using the second term of Eq. (3-22) along with the appropriate value for the constants, C_{\parallel} and C_{\perp} , we obtain σ_p' for ^{199}Hg in $\text{Hg}(\text{CH}_3)_2$. We assume σ_p' to be negative in order to have a net deshielding effect and thus there are two solutions for σ_p' :

$$\left. \begin{array}{l} \text{if } C_{\parallel} = -120 \text{ kHz} \\ C_{\perp} = -26 \text{ kHz} \end{array} \right\} \text{ then } \sigma_p' = -5050 \text{ ppm}$$

$$\left. \begin{array}{l} \text{if } C_{\parallel} = +120 \text{ kHz} \\ C_{\perp} = -26 \text{ kHz} \end{array} \right\} \text{ then } \sigma_p' = -4100 \text{ ppm}$$

The average total shielding constant can be calculated from Deverell's formula along with the value of σ_d' for the free atom tabulated by Ramsey (1956). Ramsey gives $\sigma_d' = 9650$ ppm for Hg and therefore $\sigma_{\text{ave}} = 4600$ or 5550 ppm. The shielding scale obtained is shown in Figure 3-8 and shows that the resonances of the non-metallic mercury compounds are found between the resonances of the bare nucleus and the free mercury atom.

Figure 3-7.

Temperature dependent ellipses (---- 313°K and
— 238°K) of $C_{||}$ and C_{\perp} for ^{199}Hg in dimethylmercury.

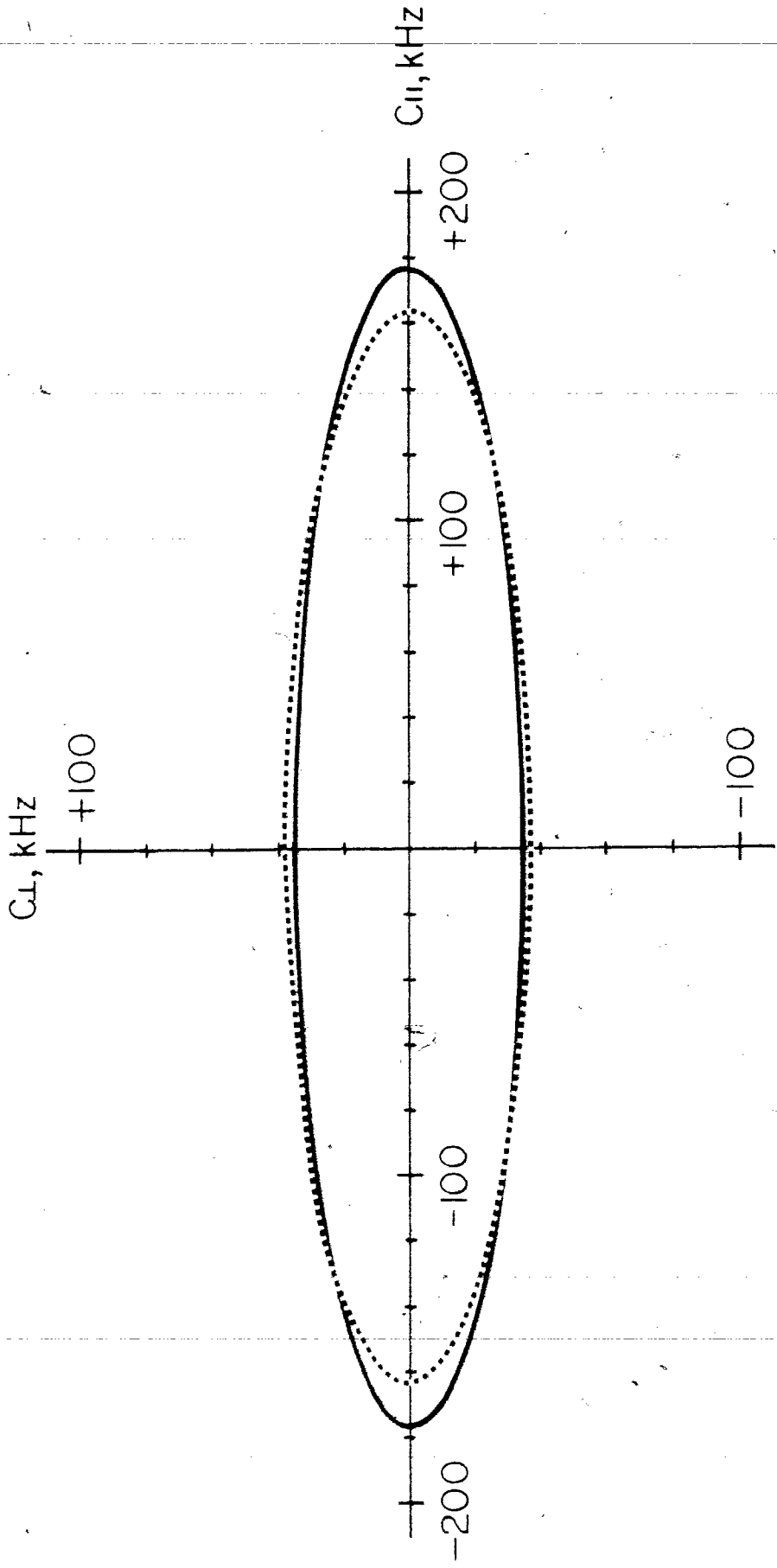
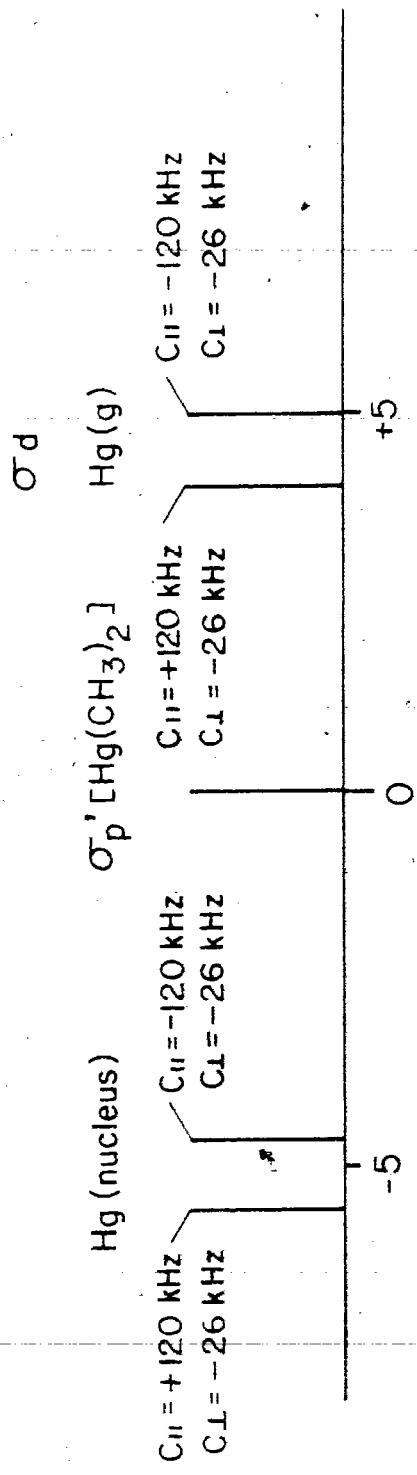


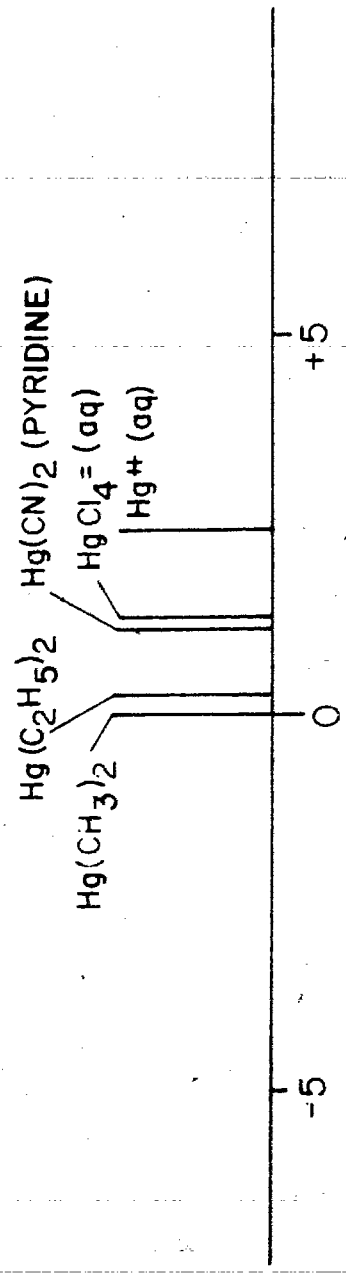
Figure 3-8

^{199}Hg shielding scales. Experimental scale values obtained from the results of Schneider and Buckingham (1962). Theoretical scale derived from experimental values for C_{\perp} and C_{\parallel} along with Eq. (3-22).

THEORETICAL



EXPERIMENTAL



PARTS
10⁻³

CHAPTER 4

MAGNETIC RELAXATION STUDIES OF $\text{Sn}(\text{CH}_3)_4$

This study involves the investigation of the spin-lattice relaxation times of ^1H , ^2D , ^{13}C and ^{119}Sn in tetramethyl tin. Measurement of these times has allowed us to separate the temperature dependences of the various contributions: dipolar and spin-rotation for ^1H , ^{13}C and ^{119}Sn and quadrupolar for the ^2D nucleus. These contributions can be directly related to both the molecular orientational time τ_θ and the molecular angular momentum time τ_ω . These can be used to obtain values for the spin-rotational constants and compared to values obtained from chemical shift data. Our data seems to indicate that the spin-rotational interaction becomes more important as the Z number of the nuclei increases as has been pointed out earlier for the ^{199}Hg case in dimethyl mercury.

A. Experimental

1. Measurement of relaxation times

The proton and deuterium T_1 's were measured in the same manner as for the dimethylmercury case described earlier in Chapter 3.

The ^{13}C spin-lattice relaxation times were measured under proton-noise decoupled conditions using the $180^\circ\text{-}\tau\text{-}90^\circ$ pulse sequence. The nuclear Overhauser enhancement (η) was obtained by dividing the integrated peak intensity in ^1H decoupled cmr spectra by the total integrated peak intensities in the coupled cmr spectra. All of the ^{13}C experiments were performed on a Varian XL-100-15 spectrometer equipped for pulsed Fourier transform (FT) operation at 25.2 MHz.

The ^{119}Sn relaxation times in $\text{Sn}(\text{CH}_3)_4$ were measured indirectly by the previously described rotary echo method (see Chapter 3). Spin-lattice relaxation times (T_1) of the ^{119}Sn for the series $^{119}\text{Sn}(\text{CH}_3)_{4-n}(\text{CD}_3)_n$ were measured by the $180^\circ\text{-}\tau\text{-}90^\circ$ sequence at 15.05 MHz by direct observation of the ^{119}Sn resonance at $+28^\circ\text{C}$. These measurements were made on a modified NMR-Specialties spectrometer with a home-built crossed coil, external H_2O lock probe (Wells *et al.*) equipped with a Nicolet 1082 FT system.

Temperature control was accomplished using the Varian variable temperature NMR probe accessory. Temperatures were measured using a copper constantan thermocouple, temperature readings were accurate to $\pm 1^\circ\text{C}$.

The $\text{Sn}(\text{CH}_3)_4$ was obtained from Aldrich Chemical Co.. The mixtures of $\text{Sn}(\text{CH}_3)_4 + \text{Sn}(\text{CD}_3)_4$ were measured in the same fashion as for the $\text{CH}_3\text{Br}\text{-CD}_3\text{Br}$ mixtures (see Chapter 2). All samples were degassed in 5 mm tubes by the usual freeze-pump-thaw cycles under vacuum.

FIGURE 4-1

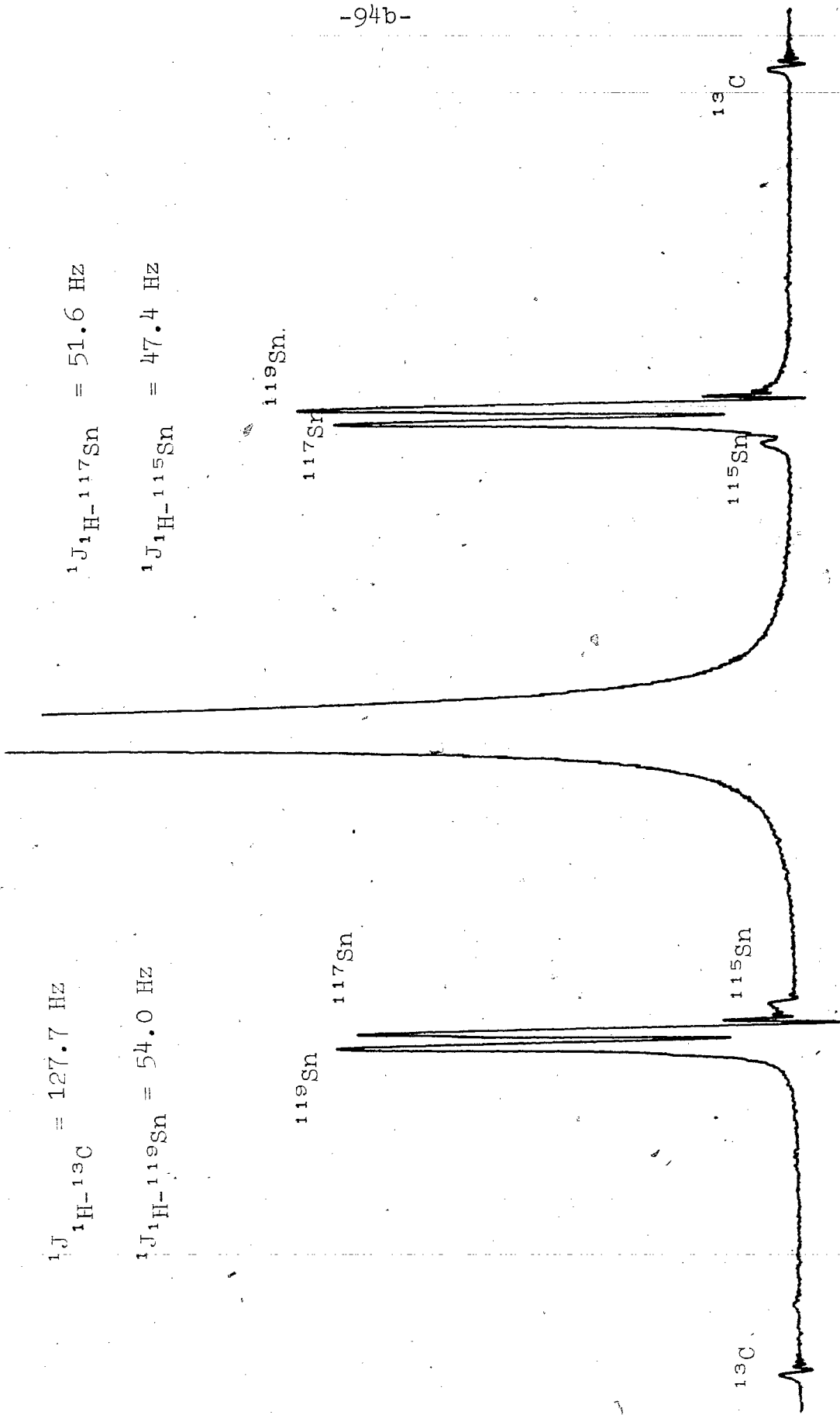
High resolution 60 MHz ^1H spectra of $\text{Sn}(\text{CH}_3)_4$

$^1J_{\text{H-}^{13}\text{C}} = 127.7 \text{ Hz}$

$^1J_{\text{H-}^{119}\text{Sn}} = 54.0 \text{ Hz}$

$^1J_{\text{H-}^{117}\text{Sn}} = 51.6 \text{ Hz}$

$^1J_{\text{H-}^{115}\text{Sn}} = 47.4 \text{ Hz}$



2. Synthesis of $\text{Sn}(\text{CD}_3)_4$ and $\text{Sn}(\text{CH}_3)_{4-n}(\text{CD}_3)_n$

The d_{12} -tetramethyl tin was prepared according to Waring and Horton's Grignard method (1945) with minor modifications. To a 500 cc 3-neck flask was added 3.4 grams of Mg turnings and 50 cc of anhydrous ethyl ether, fitted with a thermometer, dropping funnel and condenser with a drying tube. Into the dropping funnel was added the CD_3I (15.0 grams) and an equal volume of dry ether. The CD_3I solution was slowly added until the reaction began and the remainder added dropwise while the mixture refluxed. It was further refluxed for 30 minutes and allowed to cool to room temperature.

Next was added 5.0 grams of SnCl_4 (anhydrous) dropwise, at this time slow refluxing occurred. After all of the stannic chloride had been added the reaction mixture was refluxed for 24 hrs. The excess Grignard reagent was then destroyed by slow addition of water to the mixture. The aqueous layer was separated from the ether layer. The ether layer was then fractionally distilled off using a "spiral" column. The small traces of residual ether were removed by preparative VPC. The yield was 0.90 grams of $\text{Sn}(\text{CD}_3)_4$ (26 per cent yield); B.P. 76-77°C (uncorrected).

The other members of the series: $\text{Sn}(\text{CH}_3)_3(\text{CD}_3)$, $\text{Sn}(\text{CH}_3)_2(\text{CD}_3)_2$ and $\text{Sn}(\text{CD}_3)_3(\text{CH}_3)$ were prepared in the same manner by reacting the Grignard reagent (CD_3MgI) with the appropriate methyl tin chlorides obtained from Alfa Inorganics.

B. Relaxation results

1. ^{13}C and ^2D spin-lattice relaxation

For the ^{13}C relaxation in a methyl group it is safe to assume that the intermolecular dipole-dipole relaxation is insignificant as mentioned previously. The chemical shift anisotropy contribution for ^{13}C in methyl groups is also negligible (see Chapters 2 and 3). Therefore the T_1 's of ^{13}C in tetramethyl tin given in Table 4-1 and Figure 4-2 come from a combination of intramolecular dipole-dipole and spin-rotation interactions. The dipolar contribution is given as,

$$(4-1) \quad R_{1\text{intra}}^{\text{dd}} = \frac{3\gamma_{\text{H}}^2\gamma_{^{13}\text{C}}^2\hbar^2}{r_{\text{C-H}}^6} \tau_{\text{C}}(^{13}\text{C-H}) + \frac{3\gamma_{^{119}\text{Sn}}^2\gamma_{^{13}\text{C}}^2\hbar^2}{r_{\text{C-Sn}}^6} \tau_{\text{C}}(\text{C-Sn})$$

however the second term is very small and may be neglected because of the smaller $\gamma_{^{119}\text{Sn}}$ vs. $\gamma_{^1\text{H}}$ and the much greater distance of $r_{\text{C-Sn}}$ vs. $r_{\text{C-H}}$. Using the appropriate constants and intermolecular distances given in Table 4-2 one obtains,

$$(4-2) \quad R_{1\text{intra}}^{\text{dd}} = 6.48 \times 10^{10} \tau_{\text{C}}(^{13}\text{C-H})$$

From the ^{13}C T_1 at $+40^\circ\text{C}$ along with $\eta = 1.26$ (NOE factor) at $+40^\circ\text{C}$ we may separate $R_{1\text{intra}}^{\text{dd}}$ from R_1^{SR} at this temperature. Then using Eq. (4-2) we obtain $\tau_{\text{C}}(^{13}\text{C-H}) = 0.68 \times 10^{-12}$ sec at $+40^\circ\text{C}$.

The tensor axis whose reorientation is represented by $\tau_c(^{13}\text{C-H})$ is the same axis as that obtained from the ^2D relaxation data. Therefore making use of $(R_1)_{2\text{D}}$ from Table 4-1 and Figure 4-3 along with the assumed $(e^2qQ/h)_{2\text{D}}$ value for methyl groups of 165 kHz and Eq. (3-10) one obtains values for $\tau_c(^2\text{D})$ and its temperature dependence. The temperature dependence of $\tau_c(^2\text{D})$ and $\tau_c(^{13}\text{C-H})$ must be the same. Thus using our value for $\tau_c(^{13}\text{C-H})$ at $+40^\circ\text{C}$ along with the temperature dependence of the ^2D we obtain the temperature variation of $\tau_c(^{13}\text{C-H})$ shown in Figure 4-4. It has been shown in ND_3/NH_3 (Atkins et al. 1969) and PD_3/PH_3 (Sawyer and Powles 1971) that the molecular reorientation time varies as $I^{\frac{1}{2}}$ therefore,

$$\frac{\tau_c(^2\text{D})}{\tau_c(^{13}\text{C-H})} = \sqrt{\frac{I(\text{Sn}(\text{CD}_3)_4)}{I(\text{Sn}(\text{CH}_3)_4)}} = 1.12$$

Our results show $\tau_c(^2\text{D})/\tau_c(^{13}\text{C-H}) = 1.13$ at $+40^\circ\text{C}$ in excellent agreement with the predicted 1.12. The temperature dependence of $\tau_c(^{13}\text{C-H})$ may now be used along with Eq. (4-2) and our carbon-13 data at three temperatures ($+40$, $+20$ and -20°C) to obtain values for $R_1^{\text{SR}}(^{13}\text{C})$. The results are shown in Figure 4-2. Interpretation of this data and calculation of the spin-rotation constants for ^{13}C will be carried out in a later section.

TABLE 4-1

^{13}C AND ^2D RELAXATION DATA FOR TETRAMETHYL TIN

^{13}C of $\text{Sn}(\text{CH}_3)_4$

T(°K)	R ₁ (sec ⁻¹)
313	0.069
293	0.073
253	0.104

^2D of $\text{Sn}(\text{CD}_3)_4$

T(°K)	R ₁ (sec ⁻¹)
307	0.321
299	0.368
273	0.480
260	0.541
242	0.724

Error in measurement of relaxation rates is $\pm 8\%$

TABLE 4-2

GEOMETRIC PARAMETERS AND MOMENTS OF INERTIA FOR $\text{Sn}(\text{CH}_3)_4$

$r_{\text{C-H}}$	1.09	\AA
$r_{\text{H-H}}$	1.78	
$r_{\text{C-Sn}}$	2.18	**
$\angle \text{H-C-H}$	109.5°	
$\angle \text{C-Sn-C}$	109.5°	

$$I = 344 \times 10^{-40} \text{ gm-cm}^2$$

$$I_{\text{CH}_3} = 5.5 \times 10^{-40} \text{ gm-cm}^2$$

** O. Brockway and H.O. Jenkins, J. Amer. Chem. Soc.,
58,2036 (1936)..

All other values assumed for the molecule. Moments of inertia based on the assumed values.

FIGURE 4-2

Carbon-13 spin lattice relaxation of $\text{Sn}(\text{CH}_3)_4$

and its separation into R_1^{dd} and R_1^{SR} .

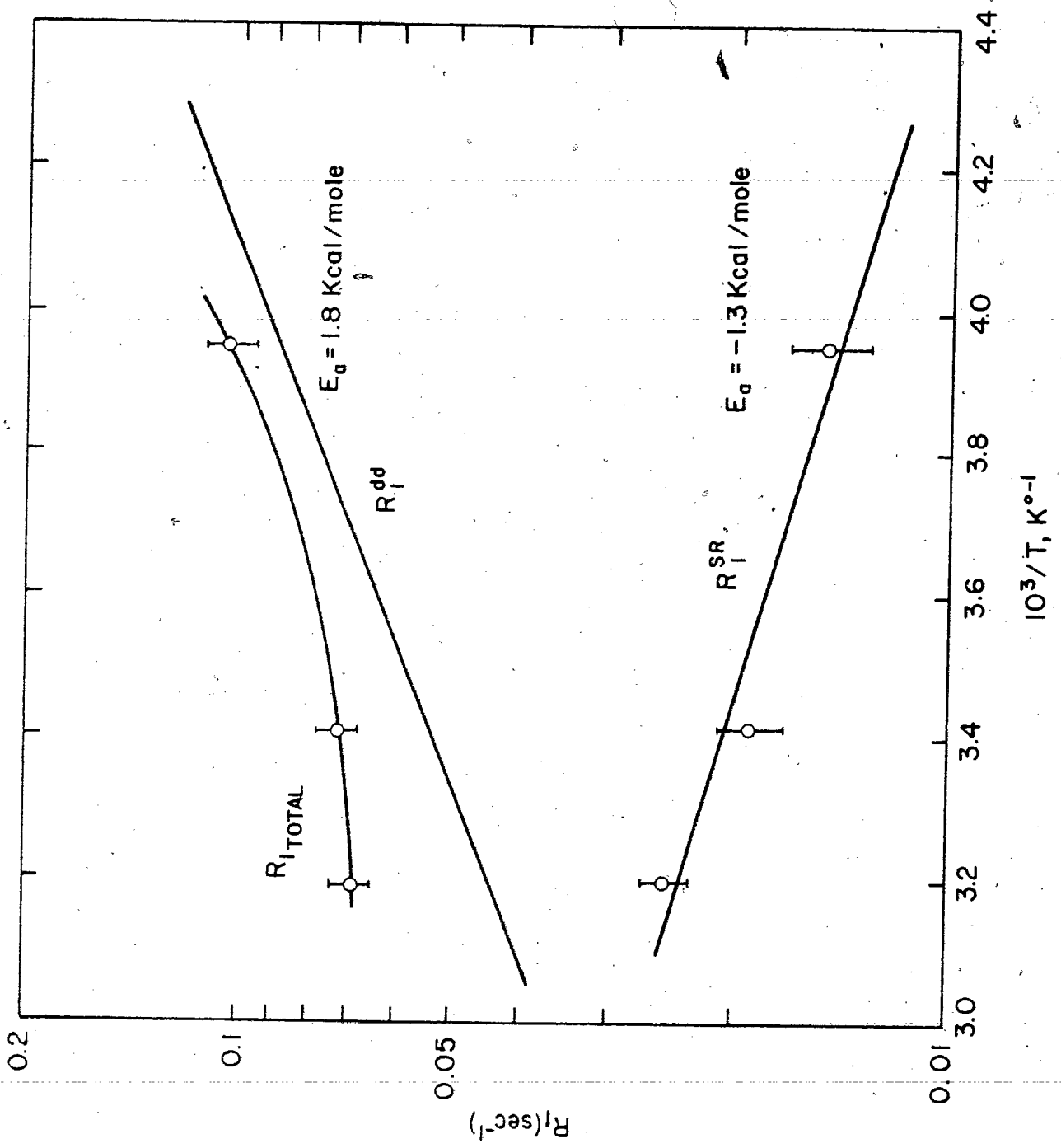


FIGURE 4-3

^{217}Po relaxation in $\text{Sn}(\text{CD}_3)_4$

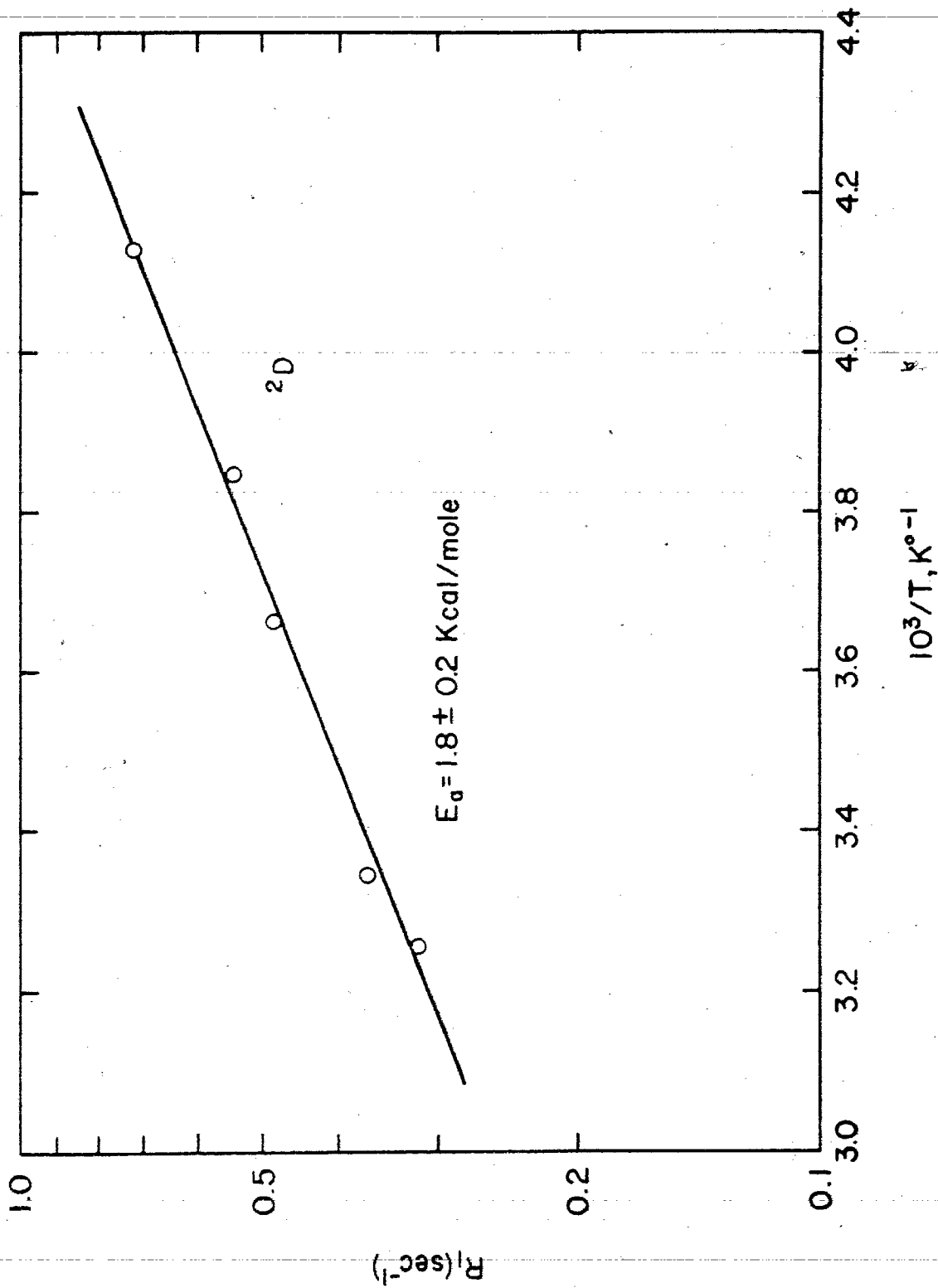
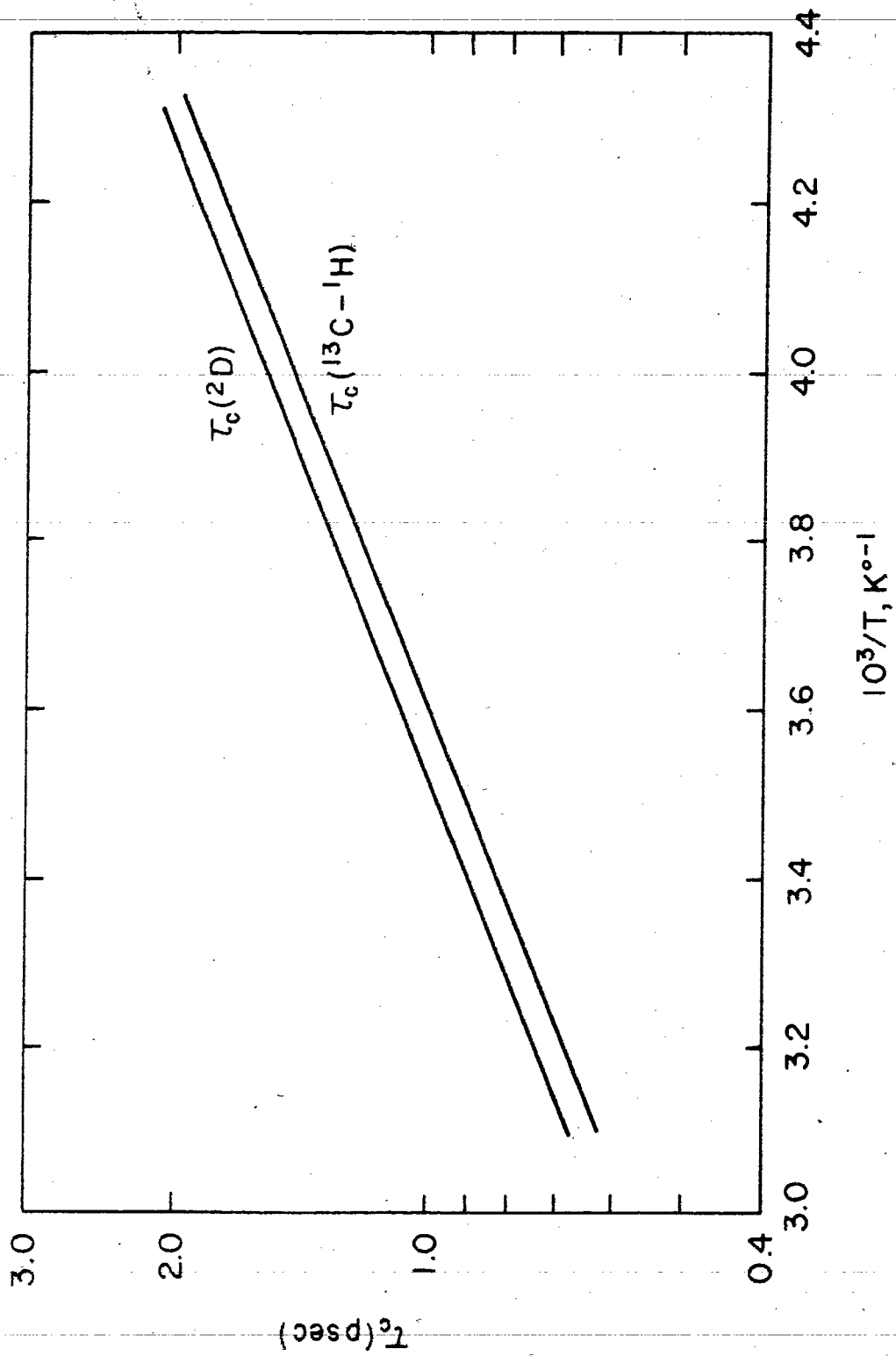


FIGURE 4-4

Temperature dependence of $\tau_c(^2\text{D})$ and $\tau_c(^{13}\text{C}-^1\text{H})$



2. ¹H relaxation

As earlier mentioned the chemical shift anisotropy contribution to the relaxation rate for protons is negligible. Therefore we are left with the separation of the intermolecular and intramolecular contributions.

The temperature dependent proton relaxation times are given in Table 4-3 and Figure 4-5 for pure Sn(CH₃)₄ and for a mixture containing 27 per cent mole fraction Sn(CH₃)₄ in Sn(CD₃)₄. Using the same dilution studies method as used for methyl bromide (Chapter 2) and dimethylmercury (Chapter 3) one may separate the intermolecular contribution from the intramolecular. These results are shown in Figure 4-5. One is then left only with the separation of the intramolecular dipole-dipole from the spin-rotation interaction.

If one first assumes that at 220°K the proton relaxation rate is dominated by the intramolecular dipole-dipole interaction and the spin-rotation contribution is negligible one can obtain the correlation time $\tau_c(\text{H-H})$.

$$(4-3) \quad R_{1\text{intra}}^{\text{dd}} = \frac{3\gamma_{\text{H}}^4 \hbar^2}{r_{\text{H-H}}^6} \tau_c(\text{H-H}) = 5.35 \times 10^{10} \tau_c(\text{H-H})$$

Extrapolation of the proton relaxation rate to 220°K shows $R_{1\text{total}}^{\text{H}} = 0.171 \text{ sec}^{-1}$ which means that $\tau_c(\text{H-H}) = 3.20 \times 10^{-12} \text{ sec}$. The proton correlation time is given by,

$$(4-4) \quad \tau_c(\text{H-H}) = \frac{1}{4}\tau_\theta + \frac{3}{2}(\tau_\theta\tau_M / 4\tau_\theta + \tau_M)$$

where τ_θ is the overall reorientational time for the molecule and τ_M is the internal reorientational time of the methyl group. In terms of rotational diffusion constant $\tau_\theta = 1/6D_\perp$ and $\tau_M = 1/D_{\parallel} - D_\perp$, D_\perp is the rotational diffusion constant for molecular reorientation and D_{\parallel} is for reorientation of the methyl group. Eqs. (4-4) and (4-5) derived from Eq. (2-10).

Extrapolation of the carbon-13 dipole dipole relaxation rate at 220°K allows calculation of the correlation time $\tau_c(^{13}\text{C-H})$ which is 2.29×10^{-12} sec and is given by the following equation,

$$(4-5) \quad \tau_c(^{13}\text{C-H}) = \frac{1}{9}\tau_\theta + \frac{8}{27}(\tau_\theta\tau_M / \tau_\theta + \tau_M) + \frac{16}{27}(\tau_\theta\tau_M / 4\tau_\theta + \tau_M)$$

Thus making use of Eqs. (4-4) and (4-5) along with the values for $\tau_c(\text{H-H})$ and $\tau_c(^{13}\text{C-H})$ at 220°K one obtains:

$$\tau_\theta = 10.88 \times 10^{-12} \text{ sec and } \tau_M = 2.72 \times 10^{-12} \text{ sec}$$

The literature value for the activation energy for methyl rotation in tetramethyl tin is 800 cal/mole (Durig, Craven and Bragin 1970). If we make use of this along with the temperature dependence of $\tau_c(^{13}\text{C-H})$ one obtains the entire temperature dependence for τ_θ shown in Figure 4-6.

TABLE 4-3

 ^1H AND ^{119}Sn RELAXATION DATA FOR LIQUID TETRAMETHYL TIN

^1H of 100% $\text{Sn}(\text{CH}_3)_4$		^1H of 27% $\text{Sn}(\text{CH}_3)_4$		^{119}Sn of 100% $\text{Sn}(\text{CH}_3)_4$	
T(°K)	R_1 (sec $^{-1}$)	T(°K)	R_1 (sec $^{-1}$)	T(°K)	R_1 (sec $^{-1}$)
315	0.105	315	0.085	315	1.733
298	0.126	298	0.100	300	1.324
285	0.132	281	0.120	289	1.293
273	0.150	273	0.122	276	1.029
262	0.177	262	0.135	262	0.786
248	0.205	248	0.150	252	0.740
238	0.256	238	0.175	236	0.512
225	0.309	225	0.208		

FIGURE 4-5

Experimental and derived proton relaxation
rates in tetramethyl tin

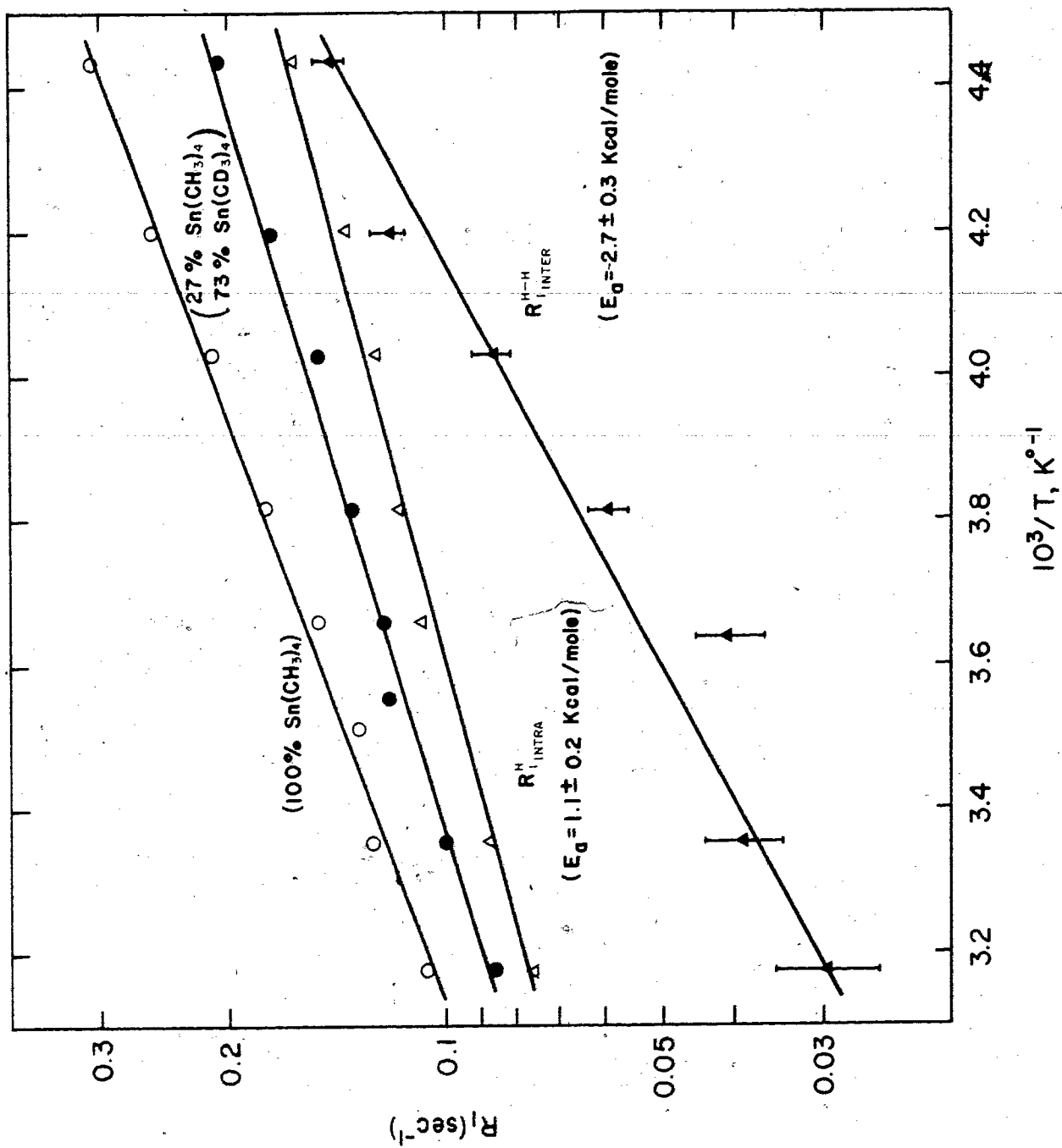
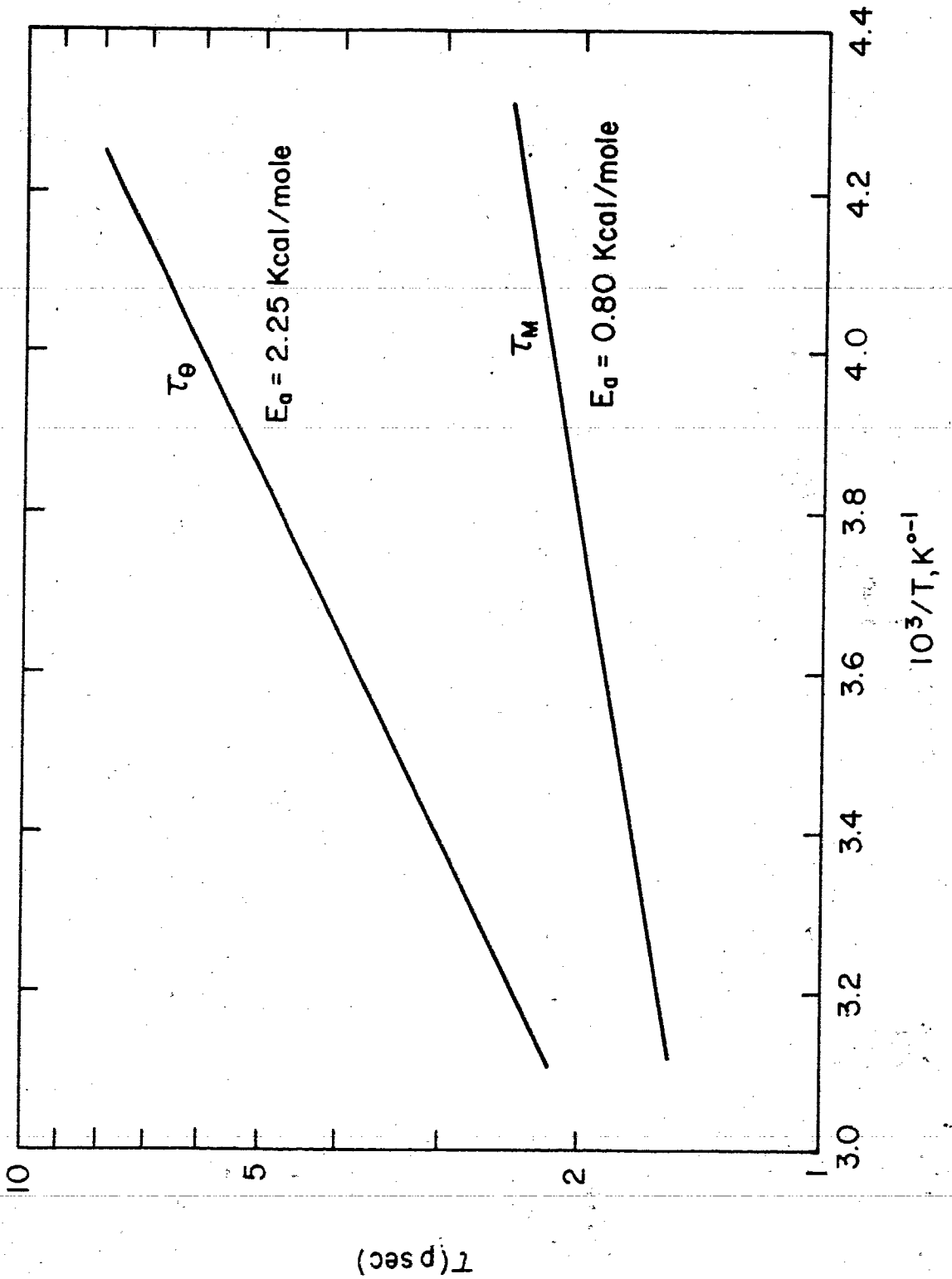


FIGURE 4-6

Temperature dependence of τ_{θ} and τ_M in $\text{Sn}(\text{CH}_3)_4$



The energy of activation for τ_{θ} is 2.25 Kcal/mole in good agreement with the value of 1.9 Kcal/mole obtained for the self-diffusion of neat liquid tetramethyl tin (Kessler, Weiss and Witte 1967). Application of the χ -test at 300°K to the overall molecular reorientation time (τ_{θ}) gives a value of 5.3 for χ at this temperature. This result indicates that we are in the rotational diffusion limit.

A liquid's microviscosity diffusion coefficient is given by,

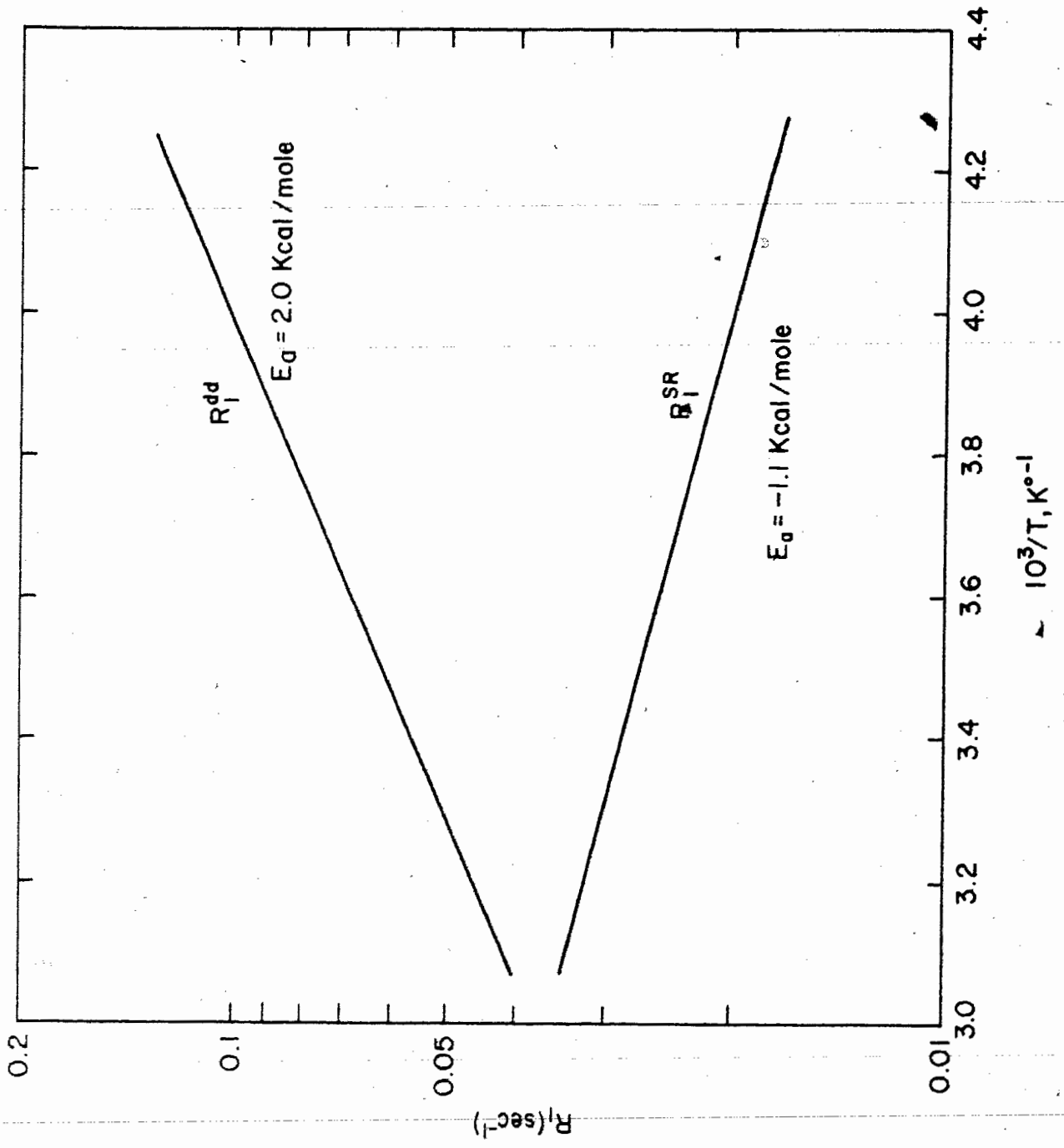
$$(4-6) \quad D_{\mu} = 1.15 \times 10^8 \frac{T\rho}{M_w \eta}$$

where M_w is the molecular weight, ρ is the density and η is the viscosity in poises. For molecules in the rotational diffusion limit the value of D_{μ} is usually of the same magnitude (within 10 per cent) as that obtained from NMR data. For our molecule $D_{\perp} = D$ because the molecule is spherical therefore using viscosity and density data we may calculate D_{μ} and compare it to the NMR value obtained from $\tau_{\theta} = 1/D$. At 300°K $D = 5.9 \times 10^{10}$ from the NMR data and using $\rho = 1.29$ gm/cc and $\eta = 0.41$ cP at 300°K gives a value of $D_{\mu} = 6.1 \times 10^{10}$ in excellent agreement.

The temperature dependence of both τ_{θ} and τ_M allow the calculation of τ_c (H-H) and thus $R_{1\text{intra}}^{\text{dd}}$ by way of Eq. (4-3). This calculation allows the separation of the intramolecular

FIGURE 4-7

Separation of the proton intramolecular
and spin-rotation terms.



and spin-rotation interactions. The results are shown in Figure 4-7. Calculation of the ^1H spin-rotation constant will be discussed in another section.

3. ^{119}Sn relaxation in $\text{Sn}(\text{CH}_3)_4$

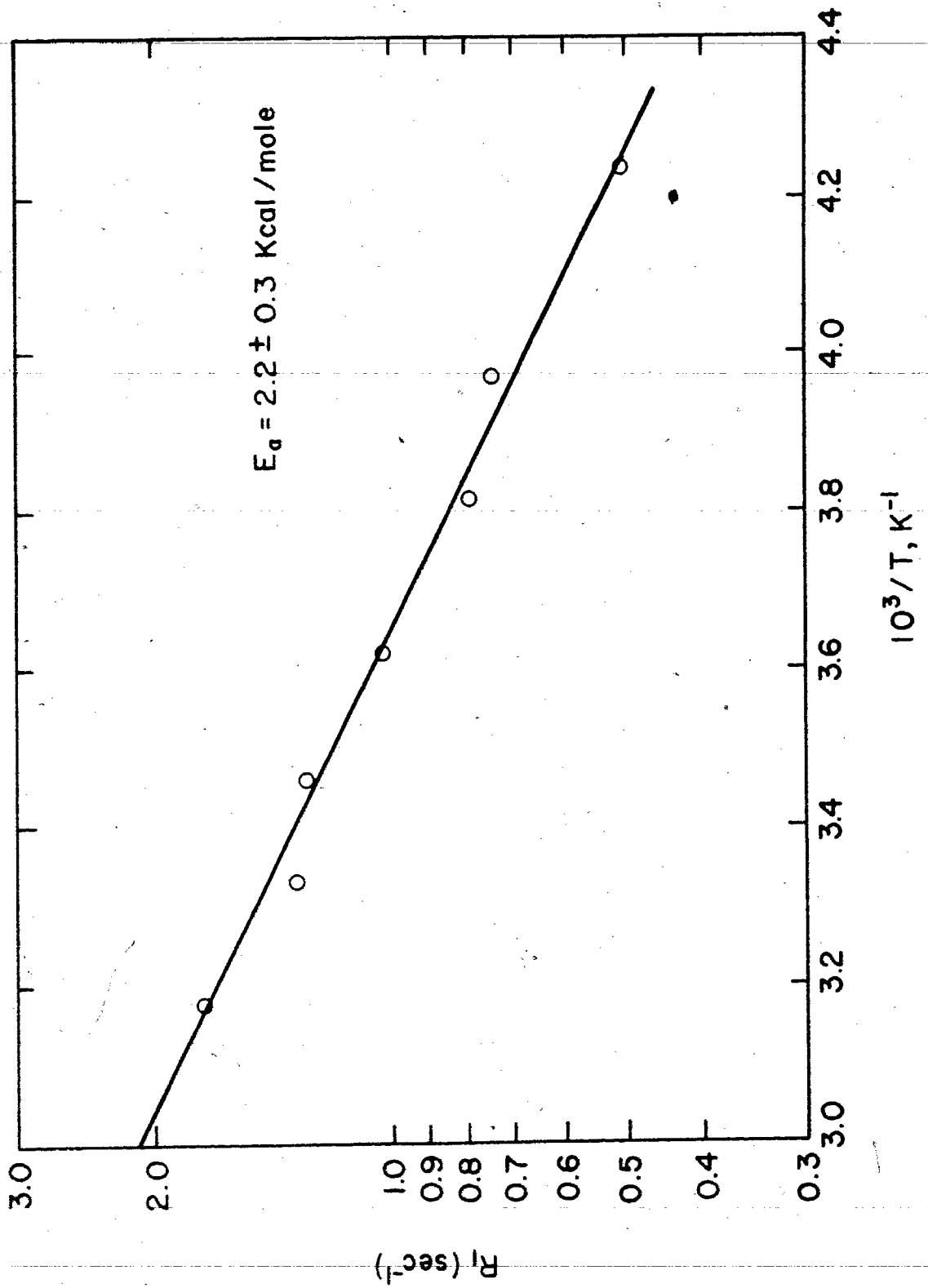
For the ^{119}Sn relaxation it is safe to assume that the intermolecular dipole-dipole relaxation is insignificant. The chemical shift anisotropy term is non-existent because the tin atom lies at the center of a tetrahedral environment. Thus the only operative mechanisms are intramolecular dipole-dipole and spin-rotation. The intramolecular dipole-dipole term is $R_{\text{intra}}^{\text{dd}} \approx 1.5 \times 10^{-9} \text{ sec}^{-1}$ at 300°K . It is rather small since $r_{\text{Sn-H}}$ is quite large and the dependence of the dipolar term on r^{-6} . The intramolecular term due to dipolar coupling is negligible compared to the spin-rotation contribution. The experimental evidence of $R_1(^{119}\text{Sn})$ in Figure 4-8 shows the spin-rotation to be the dominant relaxation mechanism because of its particular temperature dependence. It shows an Arrhenius behaviour with $E_a = -2.2 \pm 0.3 \text{ Kcal/mole}$. This value is in excellent agreement with the energy of activation for overall molecular reorientation ($+2.25 \text{ Kcal/mole}$). From the Hubbard relationship (1963)

(--7)

$$T_1^{-1} = \frac{1}{6kT}$$

FIGURE 4-8

^{119}Sn relaxation in $\text{Sn}(\text{CH}_3)_4$



based on the assumption of rotational diffusion one can immediately see that τ_θ and τ_ω should have the same temperature dependence and because R_1^{SR} depends on τ_ω the dependence should be of opposite sign. This is confirmed from our experimental data again providing evidence that we are in the rotational diffusion limit.

As mentioned earlier in Chapter 3 extension of the diffusion model by Gordon (1965,1966) led to the two models of J- and M-diffusion. McClung (1971,1972) obtained limiting expressions for spherical top molecules

$$(4-8) \quad \tau_\theta \tau_\omega = \frac{\alpha I}{6kT}$$

where $\alpha=1,3$ in J- and M-diffusion respectively.

The spin-rotation relaxation rate for the ^{119}Sn is given by,

$$(4-9) \quad R_1^{SR} = \frac{2IkT}{\hbar^2} (2\pi C_0)^2 \tau_\omega$$

Using Eqs. (4-8) and (4-9) along with $R_1^{SR} = 1.5 \text{ sec}^{-1}$ and $\tau_\theta = 2.82 \times 10^{-12} \text{ sec}$ at 300°K gives the following values for C_0 and τ_ω ,

for J-diffusion $\tau_\omega = 4.9 \times 10^{-14} \text{ sec} \quad |C_0| = 17.7 \text{ kHz}$

for M-diffusion $\tau_\omega = 14.7 \times 10^{-14} \text{ sec} \quad |C_0| = 10.4 \text{ kHz}$

The computed $|C_0|$ values are positive and not negative as had been obtained by Sharp(1972) for SnCl_4 and SnI_4 , because of the neglect of the negative sign of E_I for the ^{119}Sn nucleus in the σ'_p calculation. The tin τ_w is the time between collisions that interrupt the angular velocity of the molecule, and may be compared to the period of free rotation through one radian given by Eq. (2-40). The result is $\tau_f = 0.91$ psec and means that for the J-diffusion model the molecule moves through about a 3° angle jump between collisions.

The magnetic shielding constant has been related to the spin-rotation constant (see Eq. (3-22) by Deverell (1970) and may be used to calculate the second order paramagnetic term σ'_p for the ^{119}Sn nucleus in tetramethyl tin. The results for J-diffusion are $\sigma'_p = -3200$ ppm and for M-diffusion $\sigma'_p = -1900$ ppm. The results for J-diffusion are in excellent agreement with Sharp's (1972) results for $^{119}\text{SnCl}_4$ and $^{119}\text{SnI}_4$. Comparison between the computed σ'_p and observed chemical shifts for SnI_4 , SnCl_4 and $\text{Sn}(\text{CH}_3)_4$ are shown in Table 4-4. The discrepancy between computed and observed chemical shifts for SnCl_4 - $\text{Sn}(\text{CH}_3)_4$ is only about 10 per cent of the total σ'_p for tetramethyl tin and therefore is well within the experimental uncertainties in the measurements of C_0 for SnCl_4 and $\text{Sn}(\text{CH}_3)_4$.

TABLE 4-4

COMPARISON OF COMPUTED σ'_p AND OBSERVED CHEMICAL SHIFTS IN
 $\text{Sn}(\text{CH}_3)_4$, SnCl_4 and SnI_4

$$\sigma'_p (\text{Sn}(\text{CH}_3)_4) = -3200 \text{ ppm}$$

$$\sigma'_p (\text{SnCl}_4) = -2760 \text{ ppm}^a$$

$$\sigma'_p (\text{SnI}_4) = -1480 \text{ ppm}^a$$

$$|\sigma(\text{SnI}_4) - \sigma(\text{Sn}(\text{CH}_3)_4)| = 1720 \text{ ppm computed}$$
$$1698.6 \text{ ppm observed}^b$$

$$|\sigma(\text{SnCl}_4) - \sigma(\text{Sn}(\text{CH}_3)_4)| = 440 \text{ ppm computed}$$
$$147.8 \text{ ppm observed}^b$$

^aR.R. Sharp, J. Chem. Phys., 57, 5321(1972)

^bSee Chapter 6

4. ^{119}Sn relaxation in the series $\text{Sn}(\text{CH}_3)_{4-n}(\text{CD}_3)_n$

It has been demonstrated in ND_3/NH_3 (Atkins et al. 1969) and PD_3/PH_3 (Sawyer and Powles 1971) that molecular reorientation times vary as $I^{\frac{1}{2}}$. Therefore if the Hubbard relationship (rotational diffusion) is valid it would lead to a spin-rotational relaxation time which varies directly as $I^{\frac{1}{2}}$.

With this in mind and having synthesized the molecules in the series $\text{Sn}(\text{CH}_3)_{4-n}(\text{CD}_3)_n$ we decided to test this point. The experiments were carried out at $+28^\circ\text{C}$ and 15.05 MHz. The results are shown in Table 4-6. Looking at Table 4-5 it is seen that substitution of $-\text{CD}_3$ groups for $-\text{CH}_3$ groups does not alter the moments of inertia greatly, in fact going from the fully protonated to the fully deuterated molecule results in only a 26 per cent increase in I . This being the case the expected change in the T_1 of the ^{119}Sn would be small. As seen from our results the observed agreement between theoretical and experimental is excellent considering the difficulties in the measurement of such small differences.

The ^{119}Sn chemical shifts for this series has been measured (Chapter 5) and is only 3 ppm for $\text{Sn}(\text{CH}_3)_4$ - $\text{Sn}(\text{CD}_3)_4$. This result with the already derived value of σ'_p ($\text{Sn}(\text{CH}_3)_4$) of -3200 ppm indicates that full deuteration of the molecule causes only a 0.1 per cent change in the paramagnetic term of the total shielding constant. The value of σ'_p for each

TABLE 4-5

MOMENTS OF INERTIA FOR THE MOLECULES OF THE SERIES $\text{Sn}(\text{CH}_3)_{4-n}(\text{CD}_3)_n$

Molecule	I_{xx}	I_{yy}	I_{zz}	\bar{I}
$\text{Sn}(\text{CH}_3)_4$	344	344	344	344
$\text{Sn}(\text{CH}_3)_3(\text{CD}_3)$	379	379	349	369
$\text{Sn}(\text{CH}_3)_2(\text{CD}_3)_2$	402	384	359	382
$\text{Sn}(\text{CH}_3)(\text{CD}_3)_3$	397	397	430	408
$\text{Sn}(\text{CD}_3)_4$	435	435	435	435

All values $\times 10^{40}$ gm-cm². Values for I_{ii} for all molecules based on the following values: $\angle\text{H-C-H(D)}$, $\angle\text{Sn-C-H(D)}$ and $\angle\text{C-Sn-C}$ all 109.5° , $r_{\text{C-H}} = 1.09 \text{ \AA}$ and $r_{\text{Sn-C}} = 2.18 \text{ \AA}$.

TABLE 4-6

 $T_1(^{119}\text{Sn})$ FOR THE MOLECULES $\text{Sn}(\text{CH}_3)_{4-n}(\text{CD}_3)_n$

Molecule	T_1 (msec)	$\frac{T_1(\text{Sn}(\text{CH}_3)_{4-n}(\text{CD}_3)_n)}{T_1(\text{Sn}(\text{CH}_3)_4)}$	$\sqrt{\frac{I(\text{Sn}(\text{CH}_3)_{4-n}(\text{CD}_3)_n)}{I(\text{Sn}(\text{CH}_3)_4)}}$
$\text{Sn}(\text{CH}_3)_4$	577 ± 16	1.000	1.000
$\text{Sn}(\text{CH}_3)_3(\text{CD}_3)$	592 ± 16	1.026 ± 0.059	1.036
$\text{Sn}(\text{CH}_3)_2(\text{CD}_3)_2$	599 ± 16	1.038 ± 0.058	1.054
$\text{Sn}(\text{CH}_3)(\text{CD}_3)_3$	606 ± 16	1.050 ± 0.057	1.088
$\text{Sn}(\text{CD}_3)_4$	621 ± 16	1.076 ± 0.056	1.124

All T_1 's measured at +28°C.

member of this series along with the \bar{I} (Table 4-5) allows calculation of C_o for each species. The results shown in Table 4-7 indicate that $C_o \propto 1/I$ for a nucleus in a molecule which has undergone isotopic substitution. Calculation of τ_w for each species by use of Eq. (4-9) along with the measured relaxation times and C_o values shows that τ_w varies inversely as $I^{\frac{1}{2}}$ within experimental error.

TABLE 4-7

Molecule	σ'_p (ppm)	C_o (kHz)
$\text{Sn}(\text{CH}_3)_4$	-3200	+17.7
$\text{Sn}(\text{CH}_3)_3(\text{CD}_3)$	-3200	+16.4
$\text{Sn}(\text{CH}_3)_2(\text{CD}_3)_2$	-3200	+15.9
$\text{Sn}(\text{CH}_3)(\text{CD}_3)_3$	-3200	+14.8
$\text{Sn}(\text{CD}_3)_4$	-3200	+13.9

5. Carbon-13 spin-rotation interaction

Although the tetramethyl tin molecule is spherical, treatment of the carbon-13 spin and proton spins is based on the assumption that we may treat the $-CH_3$ group as a symmetric top. As in the methyl bromide case (Chapter 2) we may use ^{13}CO as the basis for an absolute carbon-13 chemical shift scale. The value of σ'_p for ^{13}CO is -256.3 ppm and since $-^{13}CH_3$ in tetramethyl tin is 190.6 ppm upfield from carbon monoxide, σ'_p is -65.7 ppm for tetramethyl tin. Using Deverell's method (1970),

$$(4-10) \quad \sigma'_p(^{13}C) = 2.59 \times 10^{30} (2I_{\perp}C_{\perp} + I_{\parallel}C_{\parallel})$$

As mentioned by Lyerla, Grant and Wang (1971) and also found in the methyl bromide case the (IC) tensor for carbon-13 spins in many non-linear molecules is near isotropic because the anisotropic chemical shift ($\Delta\sigma$) is small compared to σ'_p . For our case it results in $(IC)_t = 8.46 \times 10^{-36}$ and therefore $C_{\perp} \cong 0.25$ kHz and $C_{\parallel} \cong 15.4$ kHz.

For a symmetric top molecule whose nucleus is on the symmetry axis its relaxation rate is given by (Bender and Zeidler 1971; Lyerla Jr. et al. 1971),

$$(4-11) \quad R_1^{SR} = \frac{8\pi^2 kT}{3h^2} \left[(I_{\parallel}C_{\parallel})^2 \frac{\tau_{w\parallel}}{I_{\parallel}} + 2(I_{\perp}C_{\perp})^2 \frac{\tau_{w\perp}}{I_{\perp}} \right]$$

$\tau_{\omega_{\perp}}$ can be obtained from τ_{θ} for the overall reorientation of the molecule and the Hubbard relationship. The value obtained is $\tau_{\omega_{\perp}} = 5.47 \times 10^{-14}$ sec at 313°K. Using Eq. (4-11) along with $R_1^{SR} = 0.025 \text{ sec}^{-1}$ and $\tau_{\omega_{\perp}}$ at 313°K and the value for $I_{\parallel} C_{\parallel} \cong I_{\perp} C_{\perp} \cong (IC)_t$ yields a value of 3.41×10^{26} for $\tau_{\omega_{\parallel}}/I_{\parallel}$. Since we are treating the $-\text{CH}_3$ as a symmetric top I_{\parallel} has the value of $5.5 \times 10^{-40} \text{ gm-cm}^2$ (typical for a methyl group) and therefore $\tau_{\omega_{\parallel}} = 1.88 \times 10^{-13}$ sec. If this angular momentum correlation time is compared to the period of free rotation through one radian given by

$$(4-12) \quad \tau_{\parallel, f} = (I_{\parallel}/kT)^{\frac{1}{2}} = 1.13 \times 10^{-13} \text{ sec}$$

the result is that the molecule makes about a 95° angle jump for this reorientational motion. This is in agreement with the methyl bromide results and with other results on methyl groups which undergo a large angle jump because of their relatively small moments of inertia.

From our relatively limited data the energy of activation for the carbon-13 spin-rotation interaction is -1.3 Kcal/mole. Calculation of E_a for D_{\parallel} (rotational diffusion constant for reorientation of the methyl group about the Sn-C bond) one obtains a value of + 0.95 Kcal/mole. Therefore although our value of -1.3 Kcal/mole is a little high it is well within reason considering our limited data for the carbon-13 relaxation.

All of this data provides further evidence that the carbon-13 spin-rotation relaxation in methyl groups is dominated by methyl group reorientation about the figure axis.

6. Proton spin-rotation interaction

Separation of the intramolecular dipole-dipole and spin-rotation has already been described in Section B2 of this chapter. The energy of activation was found to be -1.1 Kcal/mole.

Since very few ¹H spin-rotation constants have been reported in the literature we now wish to estimate them from our spin-rotation data. Using Deverell's method(1970) along with molecular beam data for the spin-rotation constants for CH₄ (Wofsy, Muentner and Klemperer 1970) and the fact that the protons in (CH₃)₄Sn are 0.1 ppm upfield from methane we can obtain an average value for \bar{C} ,

$$\bar{C} = \frac{(2C_{\perp}I_{\perp} + C_{\parallel}I_{\parallel})}{\frac{1}{3}(2I_{\perp} + I_{\parallel})} = 0.76 \text{ kHz}$$

Using the same treatment as for the protons in the methyl bromide case we may use Eq. (2-44) along with the obtained value for \bar{C} and other molecular constants and reorientational times listed in Table 4-8 to calculate C_{\parallel} and C_{\perp} .

TABLE 4-8

NECESSARY VALUES TO CALCULATE THE PROTON SPIN-ROTATION
CONSTANTS AT 313°K

$R_1^{SR} = 0.032 \text{ sec}^{-1}$	$\theta = 35.3^\circ$
$I_{\perp} = 344 \times 10^{-40} \text{ gm-cm}^2$	$I_{\parallel} = 5.5 \times 10^{-40} \text{ gm-cm}^2$
$\tau_{\omega_{\perp}} = 5.47 \times 10^{-14} \text{ sec}$	$\tau_{\omega_{\parallel}} = 1.88 \times 10^{-13} \text{ sec}$
$D_{\parallel} = 70 \times 10^{10}$	

Two possible solutions are obtained: (a) $C_{\perp} = +0.31 \text{ kHz}$, $C_{\parallel} = -7.45 \text{ kHz}$ and (b) $C_{\perp} = +0.19 \text{ kHz}$, $C_{\parallel} = +8.04 \text{ kHz}$. Substitution of these values into Eq. (2-44) shows that 70% of the spin-rotation interaction is due to the parallel motion (i.e. reorientation of the methyl group about the Sn-C bond) and the other 30% is due to the perpendicular or overall molecular reorientation at 313°K. Since as previously mentioned $E_a(D_{\parallel})$ is +0.95 Kcal/mole and $E_a(D_{\perp})$ is +2.25 Kcal/mole our obtained value of -1.1 Kcal/mole for the proton spin-rotation interaction is in excellent agreement with previous evidence showing that methyl group reorientation about the figure axis is the major source of the proton spin-rotation interaction.

CHAPTER 5

DEUTERIUM ISOTOPE EFFECTS IN THE ^1H , ^{13}C AND ^{119}Sn
NMR SPECTRA FOR THE SERIES $\text{Sn}(\text{CH}_3)_{4-n}(\text{CD}_3)_n$

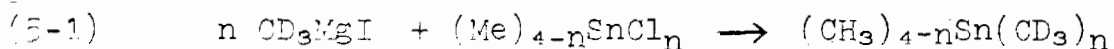
A. Introduction

The existence of isotope effects on chemical shifts in NMR spectroscopy has been known for some time (Batiz-Hernandez and Bernheim 1970). The first experimental isotope shift was measured for $\text{H}_2(\text{HD})$ by Wilmott (1953). Since then it has been observed in ^{19}F resonances of deuterated molecules (Tiers 1957); proton resonances of deuterated methanes (Lavery and Bernheim 1965) and acetone (Gutowsky 1959); ^1H and ^{15}N resonances of deuterated ammonias (Bernheim and Batiz-Hernandez 1964; Litchman et al. 1969). More recently the solvent isotope effect has been observed on chemical shifts of ions in aqueous solution (Lauterbur et al. 1968) by observing the NMR signal of the various alkali halide ions. However the available data on the deuterium isotope effects on ^{13}C NMR are very limited (Fraenkel and Burlant 1965; Maciel et al. 1967; Grishin et al. 1971; Gold et al. 1973). The same is true about the higher Z nuclei. There has been a study by Lauterbur (1965) on the effect of ^{13}C and ^{15}N substitution on the ^{59}Co resonance in $\text{K}_3\text{Co}(\text{CN})_6$.

With this in mind we decided to study the effect of deuterium substitution in $\text{Sn}(\text{CH}_3)_4$ on the ^1H , ^{13}C and ^{119}Sn nuclear magnetic resonance spectra. By studying these nuclei we may see the isotope effect on these various NMR signals, in particular the ^{119}Sn nucleus which has a large paramagnetic contribution to the total shielding of the tin-119 nucleus. We have observed the deuterium isotope effects on both the chemical shifts and spin-spin coupling constants.

B. Experimental

The various members of the series $\text{Sn}(\text{CH}_3)_{4-n}(\text{CD}_3)_n$ were prepared by reacting a Grignard reagent with the appropriate organotin chloride salt (Eq. 5-1). The compounds were further purified using preparative vapor phase chromatography.



The proton spectra were obtained on a Varian A56/60 high resolution spectrometer at $+42^\circ\text{C}$. The ^{13}C spectra were obtained at 15.063710 MHz and $+30^\circ\text{C}$ without proton decoupling (Figures 5-1 to 5-4); the ^{13}C spectra were also obtained at 25.1 MHz with proton decoupling on a Varian X1-100 spectrometer equipped with FT transform capabilities. The ^{119}Sn spectra were obtained at 15.044368 MHz using FT techniques (Figures 5-5 to 5-8). All samples were degassed by the usual freeze-pump-thaw cycles under vacuum.

FIGURES 5-1 to 5-4

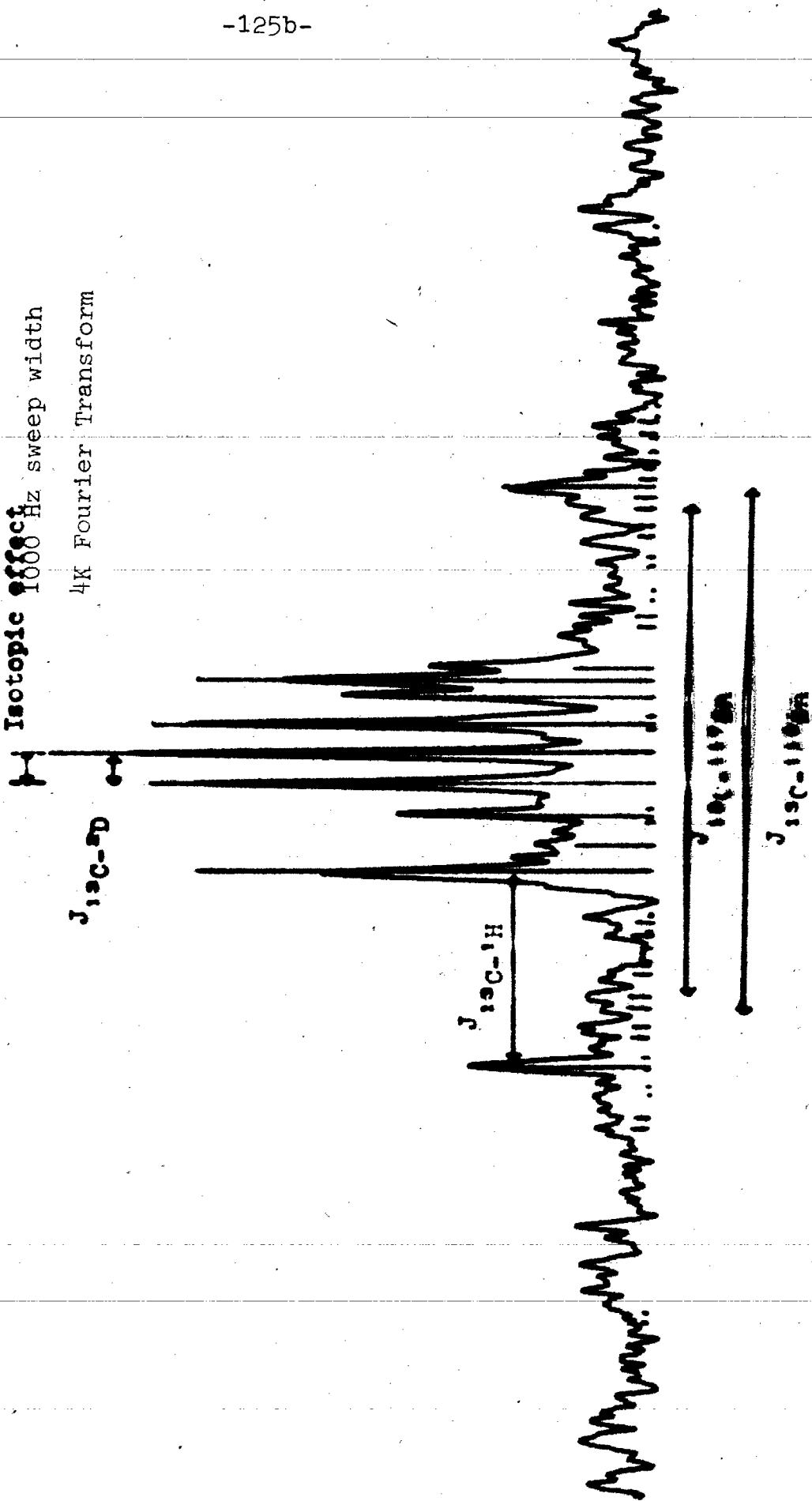
Simulated (transparency) and experimental
 ^{13}C NMR spectra at 15.063710 MHz for the
series $\text{Sn}(\text{CH}_3)_{4-n}(\text{CD}_3)_n$

^{13}C of mixture of $\text{Sn}(\text{CH}_3)_4$ and $\text{Sn}(\text{CD}_3)_4$
at 15.063710 MHz

2250 scans (rep. rate 20 sec)

Isotopic effect
1000 Hz sweep width

4K Fourier Transform



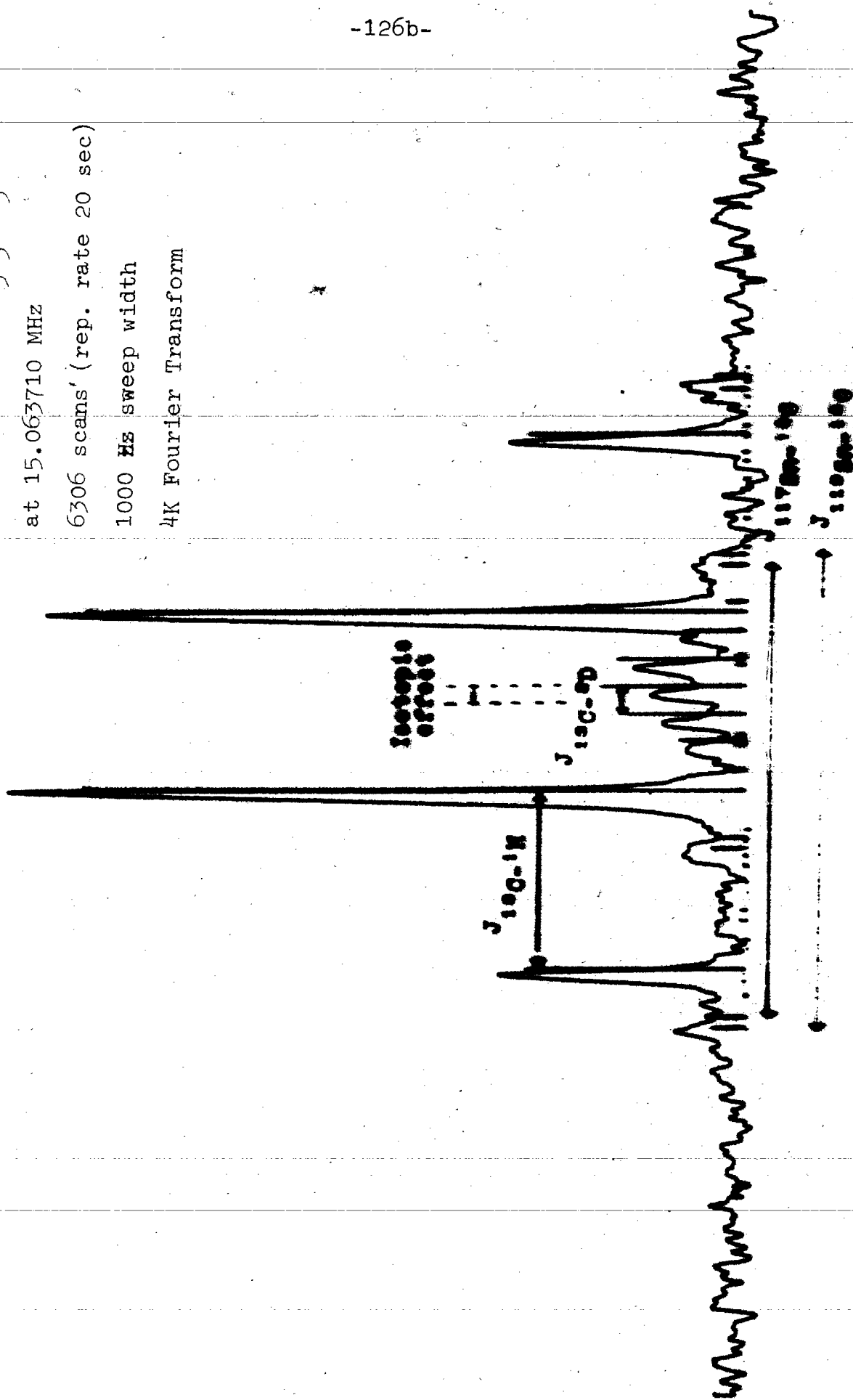
^{13}C of neat $\text{Sn}(\text{CH}_3)_3(\text{CD}_3)$

at 15.063710 MHz

6306 scans' (rep. rate 20 sec)

1000 Hz sweep width

4K Fourier Transform



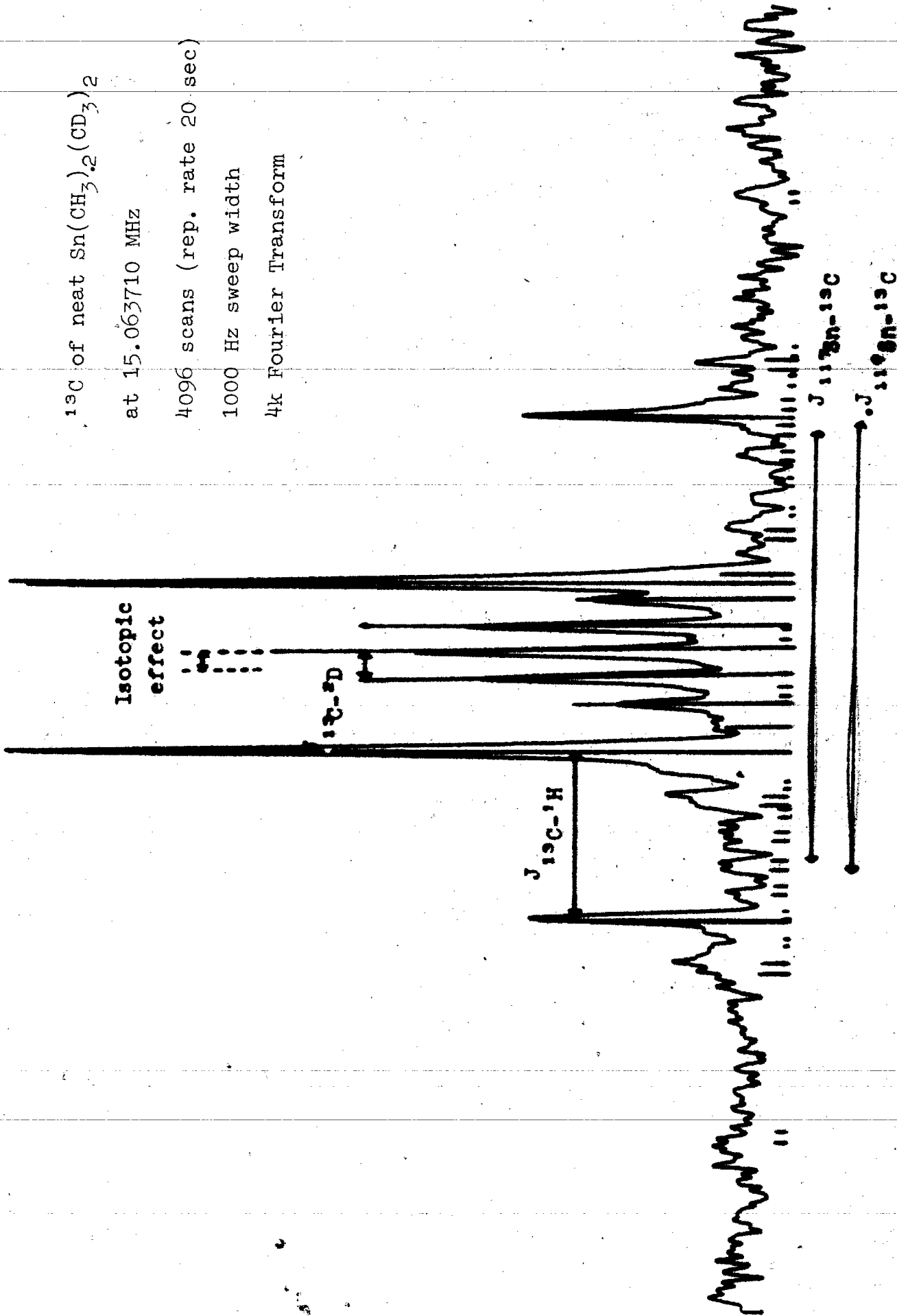
^{13}C of neat $\text{Sn}(\text{CH}_3)_2(\text{CD}_3)_2$

at 15.063710 MHz

4096 scans (rep. rate 20 sec)

1000 Hz sweep width

4k Fourier Transform



Isotopic effect

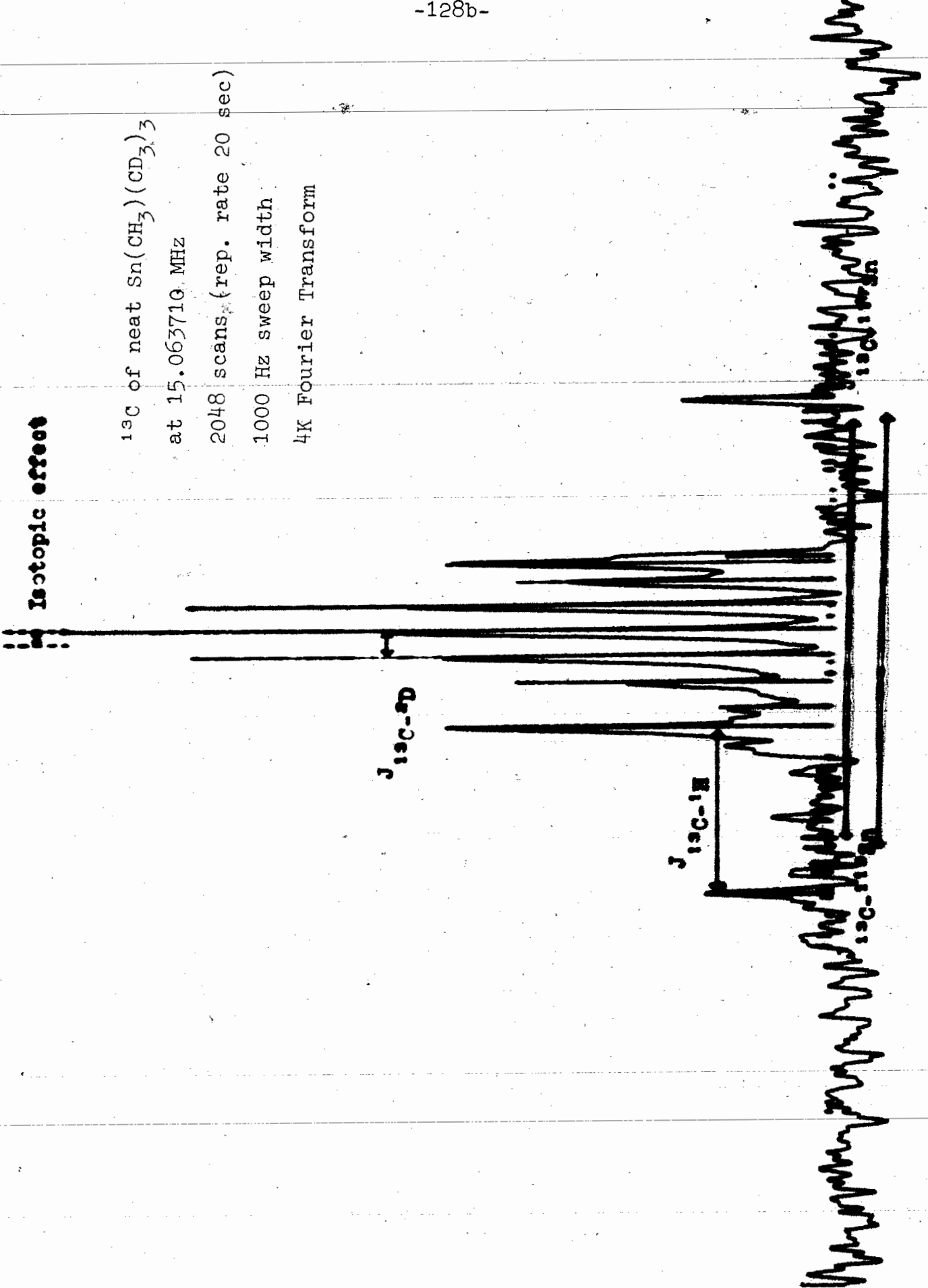
^{13}C of neat $\text{Sn}(\text{CH}_3)(\text{CD}_3)_3$

at 15.063710 MHz

2048 scans (rep. rate 20 sec)

1000 Hz sweep width

4K Fourier Transform



FIGURES 5-5 to 5-8

Simulated (transparency) and experimental
 ^{119}Sn NMR spectra at 15.044368 MHz for the
series $\text{Sn}(\text{CH}_3)_{4-n}(\text{CD}_3)_n$

Isotopic effect

^{119}Sn of mixture of
 $\text{Sn}(\text{CH}_3)_4$ and $\text{Sn}(\text{CD}_3)_4$

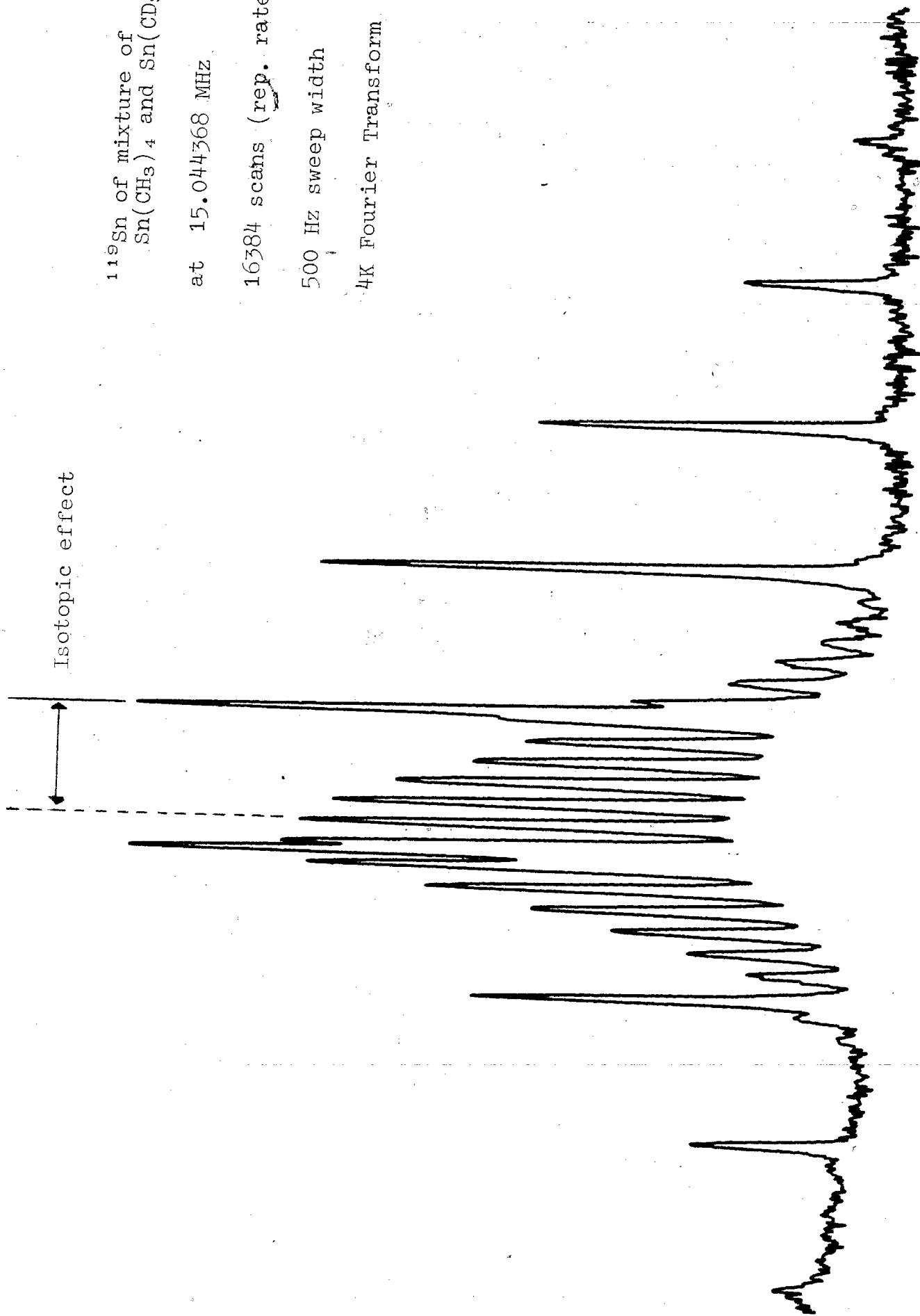
at 15.044368 MHz

16384 scans (rep. rate 1.1 sec)

500 Hz sweep width

4K Fourier Transform

-129b-



^{119}Sn of neat $\text{Sn}(\text{CH}_3)_3(\text{CD}_3)$

at 15.044368 MHz

10,000 scans (rep. rate 1.1 sec)

500 Hz sweep width

4K Fourier Transform

-130b-



^{119}Sn of neat $\text{Sn}(\text{CH}_3)_2(\text{CD}_3)_2$

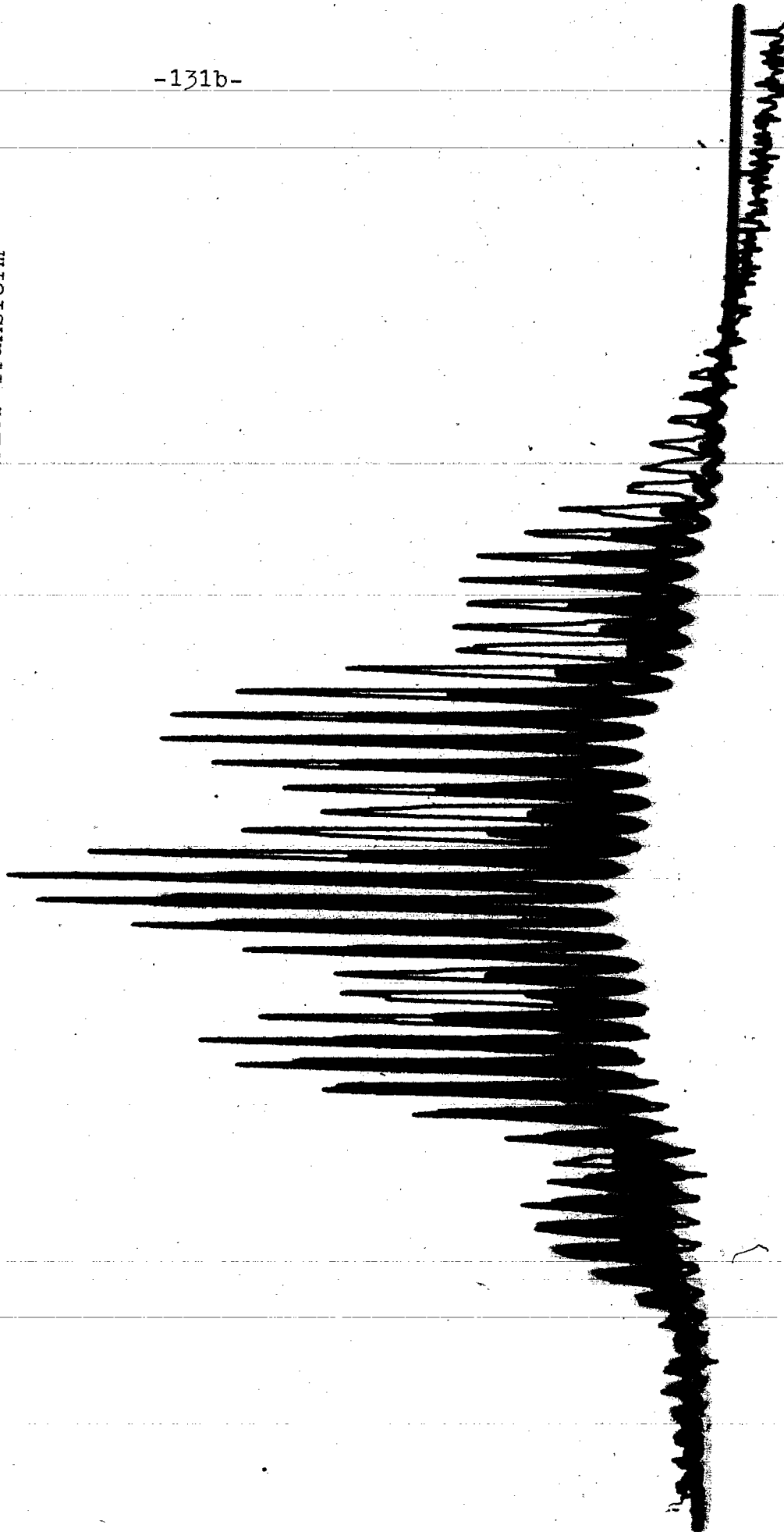
at 15.044368 MHz

37,400 scans (rep. rate 1.1 sec)

500 Hz sweep width

4K Fourier Transform

-131b-



^{119}Sn of neat $\text{Sn}(\text{CH}_3)(\text{CD}_3)_2$

at 15.044368 MHz

57,256 scans (rep. rate 1.1 sec)

500 Hz sweep width

4K Fourier Transform

-132b-



C. Results

1. Proton Nuclear Magnetic Resonance

The proton chemical shifts and J_{1H-2D} are shown in Table 5-1. The geminal coupling constants $J_{1H-2D} = 1.90 \pm 0.05$ Hz indicate that the \angle H-C-D is 109.5° as is the case in CH_4 where $J_{1H-1H} = 12.4$ Hz and thus using the relationship $J_{1H-2D} = (\gamma_D/\gamma_H^*) J_{1H-1H}$ we obtain $J_{1H-2D} = 1.91$ Hz. It has been shown by Gutowsky, Karplus and Grant (1959) that the geminal coupling constant is very sensitive to changes in the \angle H-C-D bond (e.g. in CH_2DI \angle H-C-D is 111.4° and $J_{1H-2D} = 1.50 \pm 0.05$ Hz while for methane \angle H-C-D = 109.5° and $J_{1H-2D} = 1.91$ Hz.

The proton chemical shift is sensitive to isotopic substitution H(D) which appears to produce an upfield linear shift with the number of D substituted for H. These results are in agreement with other deuterium isotope effects on the proton NMR of methanes (Bernheim and Lavery 1965), acetone (Gutowsky 1959) and ammonia (Bernheim and Batiz-Hernandez 1964). For most compounds it appears that geminal H(D) substitution causes a rather small chemical shift difference (~ 0.02 ppm/ D) since the proton chemical shift scale is rather small ~ 20 ppm and thus the paramagnetic contribution term to the total shielding is also rather small.

Although no quantitative treatment has been done on the isotope effect except for H_2 (HD) a number of qualitative explanations have been brought forward. One of these is Gutowsky's

TABLE 5-1

 ^1H Chemical shifts and Spin-spin Coupling Constants

<u>Compounds</u>	$J_{\text{H-D}}$ (Hz)	$\delta(-\text{CH}_3)$ (ppm)	$\delta(-\text{CDH}_2)$ (ppm)	$\delta(-\text{CD}_2\text{H})$
$\text{Sn}(\text{CH}_3)_3(\text{CDH}_2)$		(0)	0.015 ± 0.002	-
$\text{Sn}(\text{CH}_3)_3(\text{CD}_2\text{H})$	1.90 ± 0.05	(0)	-	0.030 ± 0.002
$\text{Sn}(\text{CH}_3)_2(\text{CD}_3)(\text{CDH}_2)$		(0)	0.017 ± 0.002	-
$\text{Sn}(\text{CH}_3)_2(\text{CD}_3)(\text{CD}_2\text{H})$	1.85 ± 0.05	(0)	-	0.034 ± 0.002
$\text{Sn}(\text{CH}_3)(\text{CD}_3)_2(\text{CDH}_2)$		(0)	0.017 ± 0.002	-
$\text{Sn}(\text{CH}_3)(\text{CD}_3)_2(\text{CD}_2\text{H})$	1.90 ± 0.05	(0)	-	0.034 ± 0.002
$\text{Sn}(\text{CD}_3)_3(\text{CDH}_2)$		0	0.020 ± 0.002	-
$\text{Sn}(\text{CD}_3)_3(\text{CD}_2\text{H})$	1.94 ± 0.05	0	-	0.038 ± 0.002

Note: All of these compounds are low abundance impurities. Each pair of compounds is referenced to the methyl group (CH_3) within the same molecule except for the last pair which is referenced to an internal sample of $\text{Sn}(\text{CH}_3)_4$.

(1959) theory that a deuterium neighbor has a smaller zero-point vibrational amplitude than a hydrogen neighbor and thus results in less electrostatic deformation in the applied H_0 field, i.e. reduces the molecular polarizability and thus the paramagnetic shielding. Another explanation has been offered by Bernheim and Lavery (1965) who suggest that one must consider also changes in the bond length (C-H) and possibly a change in the hybridization of the C-H bond contributing to the increased proton magnetic shielding produced by deuterium substitution.

2. ^{13}C Nuclear Magnetic Resonance

To our knowledge this is the first reported case in which a thorough study has been undertaken to examine the deuterium isotope effect on the ^{13}C NMR as the number of $-CH_3$ groups is substituted for $-CD_3$ groups. As is seen from the ^{13}C spectra at 15.05 MHz (Figures 5-1 to 5-4) we have also clearly observed the coupling constants between ^{13}C and 2D (a septet of intensity 1:3:6:7:6:3:1) in all deuterated members of this series. These values for $J_{^{13}C-^2D}$ are some of the few that have been reported in the literature. The ratio $J_{^{13}C-^1H} / J_{^{13}C-^2D}$ is always quite close to the value predicted from the gyromagnetic ratio ($\gamma_H / \gamma_D = 6.5144$). On the average the values of $J_{^{13}C-^1H}$ are slightly higher than $6.5144 J_{^{13}C-^2D}$ ($\Delta J = +0.5 \pm 0.2$ Hz), although within our experimental error. These results are in agreement with those of Gold et al.

(1973) but in contrast to Fraenkel's report (1965) that the J_{13C-1H} in $>CHD$ groups are 3-5 Hz greater than J_{13C-1H} in $>CH_2$ groups.

We have also observed the $J_{13C-119Sn}$ and $J_{13C-117Sn}$ involving $^{117,119}Sn-^{13}CH_3$ in all species containing $-CH_3$ groups and also for $^{117,119}Sn-^{13}CD_3$ in $Sn(CH_3)(CD_3)_3$. The results in Table 5-3 show that the coupling constants are quite insensitive to the isotopic substitution even when the $^{13}CD_3$ is directly involved. Our results are in good agreement with McFarlane's (1967) value of $J_{13C-119Sn} = -340$ Hz.

Isotopic substitution of $-CD_3$ for $-CH_3$ shows some very interesting effects on the ^{13}C NMR, both on the ^{13}C due to $-^{13}CH_3$ and $-^{13}CD_3$. Both carbon-13 signals due to $-^{13}CH_3$ and $-^{13}CD_3$ are shifted upfield relative to $-^{13}CH_3$ in $Sn(CH_3)_4$. The isotopic shift for the $-^{13}CH_3$ is linear and increases by 0.088 ppm/ $-CD_3$ group added. However the isotopic shift due to the $-^{13}CD_3$ group on the ^{13}C of the $-^{13}CD_3$ is 0.700 ppm + 0.088 ppm/ $-CD_3$ group on the molecule (i.e. the chemical shift difference between the $-^{13}CH_3$ and $-^{13}CD_3$ in the same molecule is always 0.700 \pm 0.012 ppm). These results seem to show a primary isotope effect for the ^{13}C directly bonded to the D and a secondary isotope effect for the neighbouring $-^{13}CH_3$. The ^{13}C chemical shifts are given in Table 5-2 and plotted in Figure 5-9.

TABLE 5-2

δ_{13C} for the $\text{Sn}(\text{CH}_3)_{4-n}(\text{CD}_3)_n$ series

<u>Compounds</u>		δ_{13C} (ppm)
1. $\text{Sn}(\text{CH}_3)_4$	$-\text{}^{13}\text{CH}_3$	(0)
2. $\text{Sn}(\text{CH}_3)_3(\text{CD}_3)$	$-\text{}^{13}\text{CH}_3$	0.088 ± 0.012
	$-\text{}^{13}\text{CD}_3$	0.777 ± 0.012
3. $\text{Sn}(\text{CH}_3)_2(\text{CD}_3)_2$	$-\text{}^{13}\text{CH}_3$	0.175 ± 0.012
	$-\text{}^{13}\text{CD}_3$	0.876 ± 0.012
4. $\text{Sn}(\text{CH}_3)(\text{CD}_3)_3$	$-\text{}^{13}\text{CH}_3$	0.263 ± 0.012
	$-\text{}^{13}\text{CD}_3$	0.964 ± 0.012
5. $\text{Sn}(\text{CD}_3)_4$	$-\text{}^{13}\text{CD}_3$	1.052 ± 0.012

All values obtained at both 15.1 MHz and 25.1 MHz at temperatures of $+30^\circ\text{C}$ and $+38^\circ\text{C}$ respectively.

TABLE 5-3

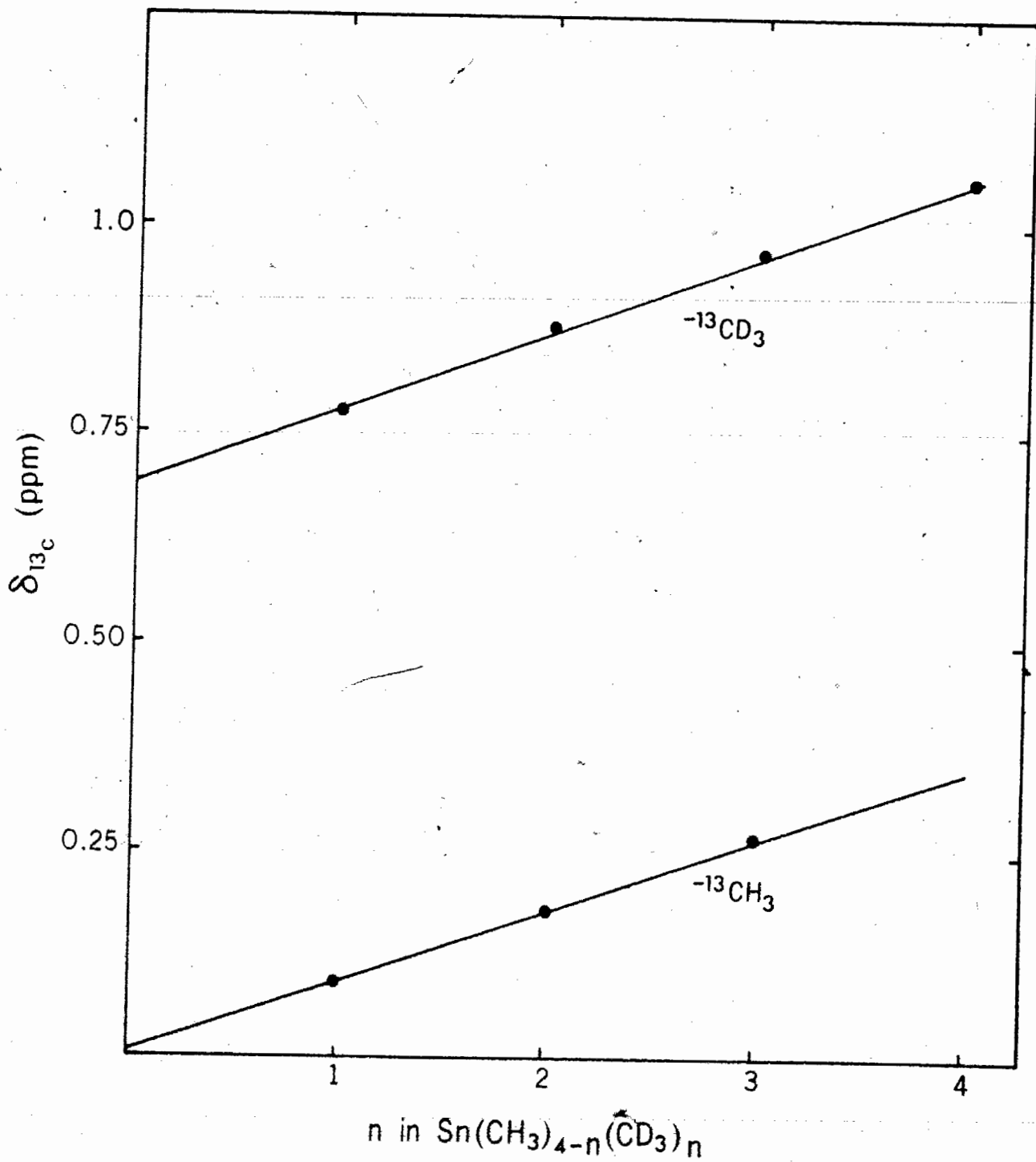
J's involving ^{13}C in the $\text{Sn}(\text{CH}_3)_{4-n}(\text{CD}_3)_n$ series

Compounds	**		
	$J_{^{13}\text{C}-^{119}\text{Sn}}$	$J_{^{13}\text{C}-^{117}\text{Sn}}$	$J_{^{13}\text{C}-^1\text{H}}$
1. $\text{Sn}(\text{CH}_3)_4$	338.4 ± 0.3	323.2 ± 0.3	127.7 ± 0.2
2. $\text{Sn}(\text{CH}_3)_3(\text{CD}_3)$			
a. $-\text{}^{13}\text{CH}_3$	338.6 ± 0.3	323.2 ± 0.3	127.5 ± 0.2
b. $-\text{}^{13}\text{CD}_3$	a	a	a
3. $\text{Sn}(\text{CH}_3)_2(\text{CD}_3)_2$			
a. $-\text{}^{13}\text{CH}_3$	338.6 ± 0.3	323.5 ± 0.3	127.6 ± 0.2
b. $-\text{}^{13}\text{CD}_3$	a	a	a
4. $\text{Sn}(\text{CH}_3)(\text{CD}_3)_3$			
a. $-\text{}^{13}\text{CH}_3$	338.4 ± 0.3	323.2 ± 0.3	127.3 ± 0.2
b. $-\text{}^{13}\text{CD}_3$	338.1 ± 0.3	324.0 ± 0.3	-
5. $\text{Sn}(\text{CD}_3)_4$	a	a	a

** From ^1H spectrum at 60 MHz. All other values from proton decoupled ^{13}C spectra at 25.1 MHz. a Not apparent in spectrum.

FIGURE 5-9

Plot $\delta(^{13}\text{C})$ vs. n in $\text{Sn}(\text{CH}_3)_{4-n}(\text{CD}_3)_n$



Our results indicate that although the coupling constant is not very sensitive to isotopic substitution this is not the case for chemical shifts. Also the isotopic shifts in ^{13}C NMR are much greater than in proton NMR; this is presumably a reflection of the larger size of σ'_p (i.e. the chemical shift window in ^{13}C is ~ 600 ppm while in ^1H only ~ 20 ppm).

3. ^{119}Sn Nuclear Magnetic Resonance

We have measured the coupling constants $J_{^{119}\text{Sn}-^1\text{H}}$ in the proton NMR spectra and $J_{^{119}\text{Sn}-^2\text{D}}$ in the ^{119}Sn NMR spectra. These values are given in Table 5-4. Once again for negligible geometry change the gyromagnetic ratios ($\gamma_{\text{H}}/\gamma_{\text{D}} = 6.5144$) should be quite close to the values for the coupling constants. Our results show that the values of $J_{^{119}\text{Sn}-^1\text{H}}$ are slightly greater than $6.5144 J_{^{119}\text{Sn}-^2\text{D}}$ ($\Delta J = +1.9 \pm 1.5$ Hz) although close to the limits of experimental error.

The effect of substitution of $-\text{CD}_3$ groups for $-\text{CH}_3$ groups on the chemical shift of the ^{119}Sn is quite large (see Figure 5-10 and Table 5-4). The tin-119 chemical shift in going from $\text{Sn}(\text{CH}_3)_4$ to $\text{Sn}(\text{CD}_3)_4$ is 2.86 ± 0.03 ppm which is very large considering that the D's are not directly bonded to the tin atom. The reason for this appears to be that the paramagnetic term (σ'_p) of the shielding tensor is rather large in ^{119}Sn (-3200 ppm for $^{119}\text{Sn}(\text{CH}_3)_4$) and thus a shift of ~ 3 ppm reflects only a change of 0.1 per cent in the paramagnetic term.

TABLE 5-4

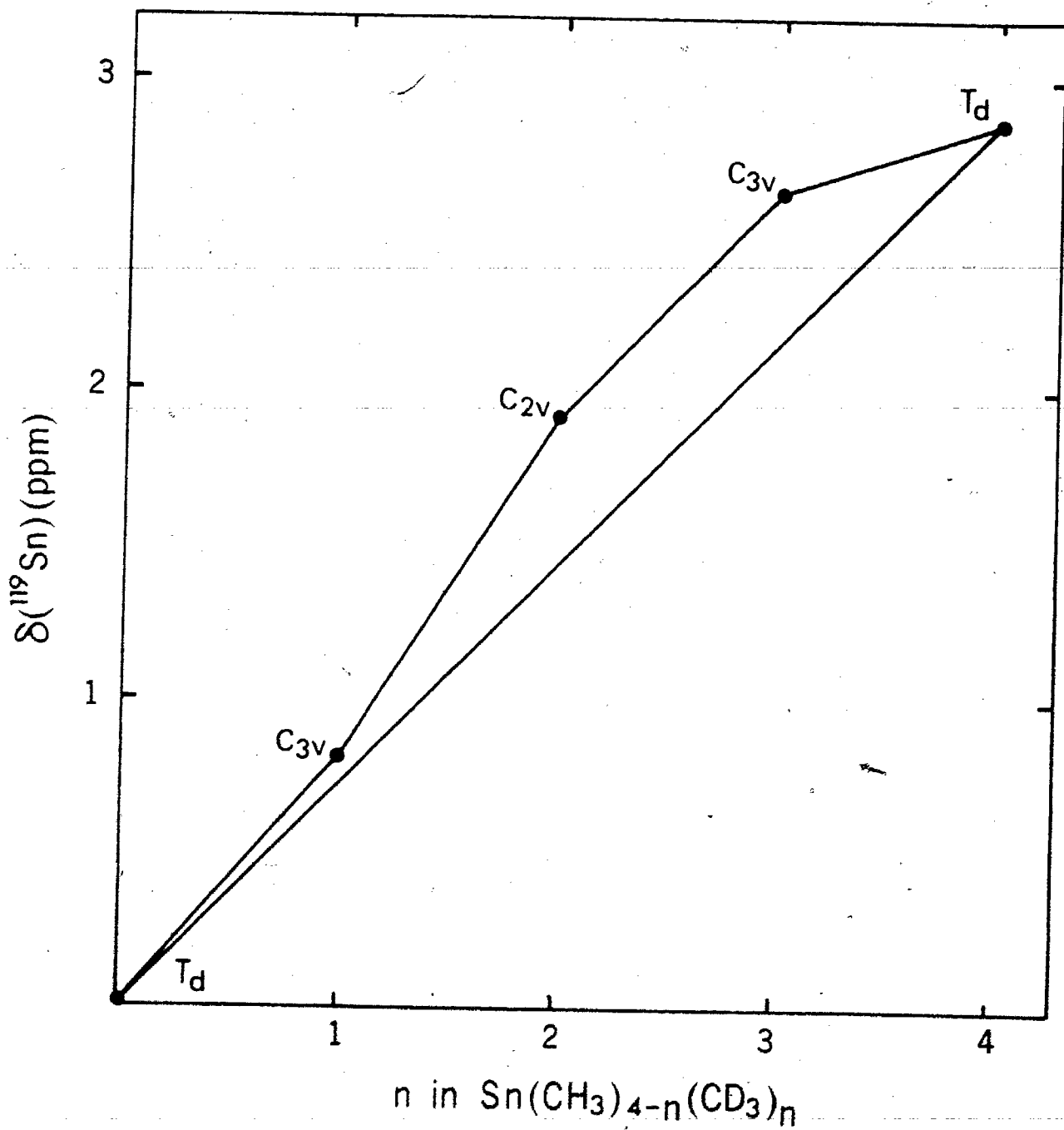
 ^{119}Sn Chemical shifts and Coupling Constants

Compounds	$\delta_{^{119}\text{Sn}}$ (ppm)	^a $J_{\text{H-}^{119}\text{Sn}}$ (Hz)	$J_{\text{D-}^{119}\text{Sn}}$ (Hz)
$\text{Sn}(\text{CH}_3)_4$	(0)	54.0 ± 0.2	-
$\text{Sn}(\text{CH}_3)_3(\text{CD}_3)$	0.80 ± 0.03	54.0 ± 0.2	8.0 ± 0.2
$\text{Sn}(\text{CH}_3)_2(\text{CD}_3)_2$	1.91 ± 0.03	54.1 ± 0.2	8.0 ± 0.2
$\text{Sn}(\text{CH}_3)(\text{CD}_3)_3$	2.63 ± 0.03	$53.8 (\pm 0.2)$	8.0 ± 0.2
$\text{Sn}(\text{CD}_3)_4$	2.86 ± 0.03	-	8.0 ± 0.2

^a Obtained from the ^1H spectra at 60 MHz.

FIGURE 5-10

Plot $\delta(^{119}\text{Sn})$ vs. n in $\text{Sn}(\text{CH}_3)_{4-n}(\text{CD}_3)_n$



In Figure 5-10 the straight line from point 0 ($\text{Sn}(\text{CH}_3)_4$) to point 4 ($\text{Sn}(\text{CD}_3)_4$) is between molecular configurations of identical overall symmetry. This dependence reflects both bond length changes on D substitution and possible angle changes at the C centers along with associated changes in electron density. From this figure it is apparent that $\text{Sn}(\text{CH}_3)_2(\text{CD}_3)_2$ with C_{2v} symmetry and $\text{Sn}(\text{CH}_3)(\text{CD}_3)_3$ with C_{3v} symmetry deviate from the straight line relationship. This then represents effects due to symmetry distortion around the Sn atom. Thus there appears to be at least two effects causing this deviation: i) the size effect of the average electron cloud and ii) a symmetry effect.

Theoretical calculations of isotopic chemical shifts should be useful in the testing of shielding theories. There have been a number of approaches used. Gutowsky (1959) tried to use the idea of an intramolecular electric field which varied with isotopic substitution. This was followed by more accurate calculations involving internuclear distances and averaging over the zero-point vibrational functions of the molecules (Hindermann and Cornwell 1968). Bernheim and Batiz-Hernandez (1966) considered shielding as a function of small variations in bond hybridization caused by isotopic substitution. However, all of these calculations are restricted to simple molecules.

Thus far there is no good quantitative approach which predicts chemical shifts upon isotopic substitution because the calculations involve the use of electronic wavefunctions which require knowledge of bond angles and bond lengths along with possible contributions of excited vibrational states to the magnetic shielding. Therefore having obtained the geometrical structures of isotopically substituted molecules one might then obtain a clear explanation of the isotope shift and thus possibly be able to use the isotope shift as a tool for determining molecular structure.

CHAPTER 6

HIGH RESOLUTION ^{119}Sn NMR STUDIES BY PULSE FOURIER TRANSFORM

A. Survey of Chemical Shifts and T_1 's

The ^{119}Sn isotope ($I = 1/2$) is the most abundant isotope of tin and the one most frequently studied in NMR investigations. Previous measurements of ^{119}Sn chemical shifts had been done under rapid passage dispersion mode (Burke and Lauterbur 1961) and also absorption mode signals involving proton decoupling (Hunter and Reeves 1968). However now that Fourier transform is readily available a number of heavy nuclei may be studied with greater ease. We report the results of signal-averaged pulse Fourier transform experiments on ^{119}Sn in a variety of tin compounds. All spectra were obtained on natural abundance (8.68 per cent) ^{119}Sn samples in 10 mm tubes at 15.05 MHz, using a modified NMR-Specialties spectrometer with a home-built crossed coil, external water-lock probe (Wells, Higgs and Brooke). The sample was not spun. Fourier transformation of the free induction decay (FID) was accomplished using a Nicolet 1082 FT system. Spin-lattice relaxation times were obtained by the usual $180^\circ - \tau - 90^\circ$ pulse sequence. All chemical shifts are given relative to the reference $\text{Sn}(\text{CH}_3)_4$.

All tin compounds were obtained commercially except for SnCl_2 , SnBr_2 , $\text{SnCl}_4 \cdot 2\text{CH}_3\text{OH}$ and $\text{SnCl}_4 \cdot 2\text{CH}_3\text{CN}$. Both stannous chloride and bromide were prepared by reacting stannous oxide with concentrated HCl and HBr respectively. Both stannic chloride adducts were prepared by reacting methanol and acetonitrile with cold SnCl_4 (anhydrous) producing immediately a white precipitate of $\text{SnCl}_4 \cdot 2\text{CH}_3\text{OH}$ and $\text{SnCl}_4 \cdot 2\text{CH}_3\text{CN}$. The melting points of these adducts are in agreement with those reported in the literature (Negita et al. 1968).

B. Results and Discussion

1. Chemical shifts

The large range of chemical shifts observed shows that the major contributory term to the shielding of the tin-119 nucleus is the paramagnetic term. This has been shown to be the case for ^{13}C chemical shifts (see Chapter 2) and also ^{119}Sn (Chapter 4; Sharp 1972). The diamagnetic term contribution to the total shielding constant remains essentially constant and it is the changes in the paramagnetic term which cause the changes in chemical shift for a particular nucleus. The chemical shift data is tabulated in Table 6-1.

The variation in chemical shift for the series $\text{CH}_3\text{SnCl}_{4-n}$ is the same as that observed for $(n\text{-butyl})_n\text{SnCl}_{4-n}$ (Burke and Lauterbur 1961; Hunter and Reeves 1968) and

similarly suggests that there are two important factors opposing each other in the shielding of the tin nuclei of this series: (a) an inductive effect resulting in the increased shielding by the addition of alkyl groups and (b) an opposite effect due to (p, d) π bonding between the Sn-Cl. The tin chemical shifts and coupling constants $J_{\text{Sn-C-H}}$ are very dependent on the concentration and type of solvent used, in good agreement with the results of Hunter and Reeves (1968), and suggesting specific solvation effects. A typical high resolution ^{119}Sn spectrum is shown in Figure 6-1.

2. Linewidths or T_2 relaxation

The linewidth is indicative of the various possible spin-spin relaxation mechanisms contributing to the transverse relaxation time T_2 . The possible mechanisms are: a) experimental i.e. magnet inhomogeneity, b) scalar relaxation, and c) exchange which could be determined from the temperature dependence. The T_2 values measured for the various ^{119}Sn compounds are listed in Table 6-1.

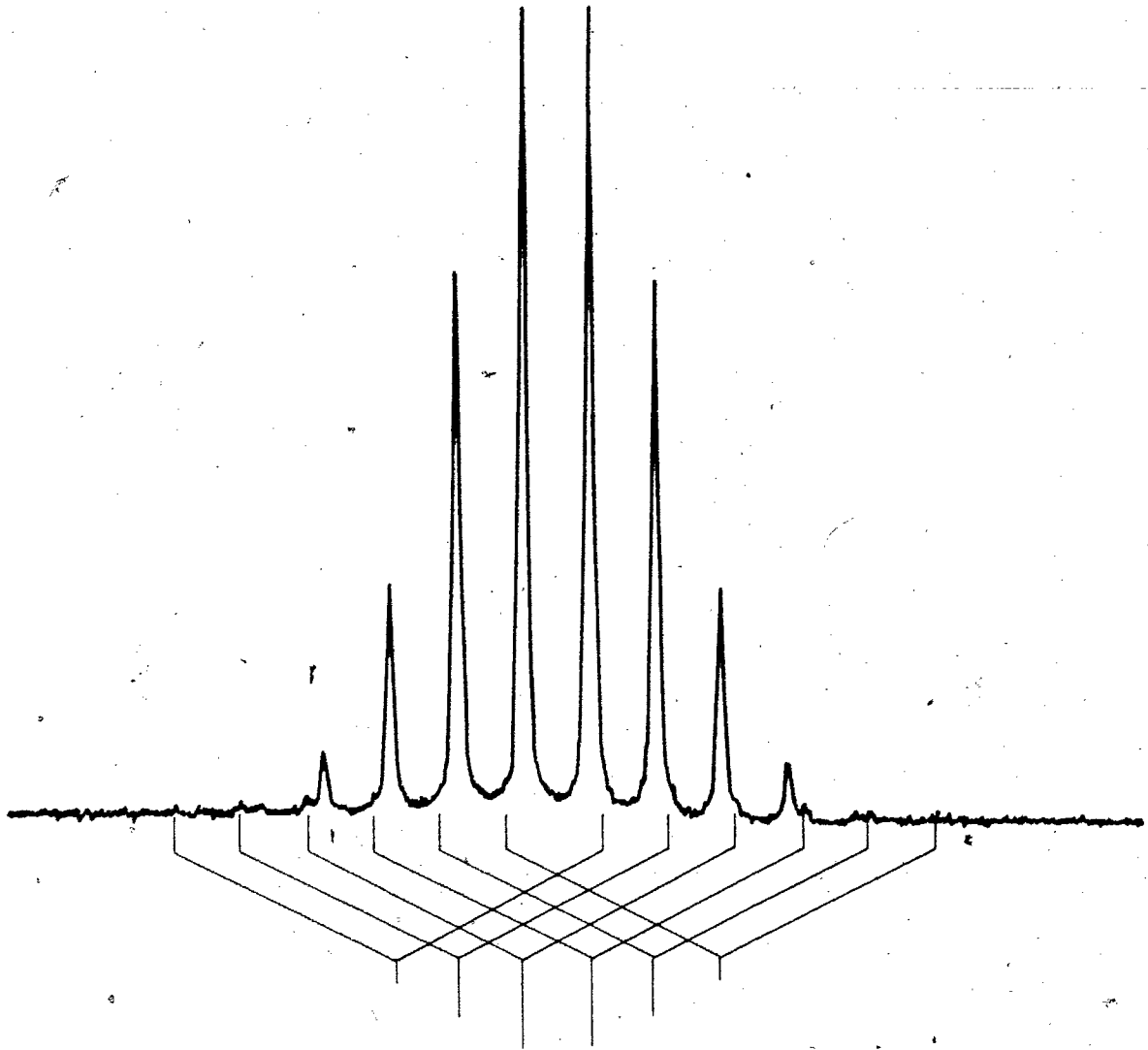
SnCl_4 , SnBr_4 and SnI_4 (Sharp 1972, 1973) all have a T_2 dominated by scalar relaxation of the second kind (Abragam 1961), to the geminal halogen nuclei assumed to be relaxing independently,

$$(6-1) \quad R_2^{SC} = \frac{1}{T_2} = \frac{4\pi^2 J^2 S(S+1)}{3} \left[T_{1Q} + \frac{T_{2Q}}{1 + (\omega_I - \omega_S)^2 T_{2Q}^2} \right] N_S$$

FIGURE 6-1

High Resolution ^{119}Sn NMR spectra at 15.05 MHz
of 5M $\text{Sn}(\text{CH}_3)_3\text{Cl}$ in CCl_4

(8000 scans at a rate of 1 scan/sec. The dominant splitting is due to the $^2J_{^{119}\text{Sn}-^1\text{H}} = 59.9$ Hz. Further splitting of each of these lines into a doublet ($J_{^{119}\text{Sn}-^{13}\text{C}} = 387$ Hz) is caused by the 1.1% ^{13}C)



where J is the scalar coupling constant between nuclei I and S; S is the spin of the quadrupolar nucleus, usually $T_{1Q} = T_{2Q}$ for liquids and N_S is the number of quadrupolar nuclei involved. The large scalar coupling constants (Sharp 1972, 1973) in all three compounds along with the fairly short T_2 of the quadrupolar halogens produce a relatively efficient transverse relaxation in ^{119}Sn .

The series of methyltin chlorides shows decreasing linewidths as the number of chlorines is decreased. Again this is attributed to the scalar contribution to T_2 by the rapidly relaxing chlorines scalar coupled to the tin nucleus. The scalar contribution to T_2 depends on the number of chlorine atoms in the molecule and therefore as the number of chlorines is decreased the linewidth is also decreased.

The two adducts of stannic chloride ($\text{SnCl}_4 \cdot 2\text{CH}_3\text{OH}$ and $\text{SnCl}_4 \cdot 2\text{CH}_3\text{CN}$) have a smaller linewidth than the anhydrous SnCl_4 . This may be a reflection of the decrease in s character of the tin nucleus in going from a tetrahedral (sp^3) geometry to a cis-octahedral (sp^3d^2) geometry (Webster and Blayden 1969; Cunningham et al. 1972). This decrease in s character of the nucleus would cause the $J_{^{119}\text{Sn}-\text{Cl}}$ to be smaller than the reported 470 Hz by Sharp (1972), and therefore would make a smaller contribution to T_2^{SC} (see Eq. (6-1)) making the tin-119 linewidth smaller. Also the change to the octahedral species increases the moment of inertia, lowering

τ_{θ} and raising τ_{θ} , assuming rotational equipartition. This shortens T_{1Q} and also decreases the scalar R_p at the Sn in the fast relaxation limit.

3. Spin-lattice relaxation times (T_1)

The wide range of T_1 's shows that a number of spin-lattice mechanisms may be operative. The possible mechanisms are: a) dipole-dipole, b) scalar relaxation, c) spin-rotation and in some cases d) chemical shift anisotropy. The last case is only found in the compounds which do not have T_d or O_h symmetry and thus may contain an anisotropic shielding for the tin-119 nucleus. However this contribution would be very small and may be neglected in our discussion.

For tetramethyl tin, T_1 is strictly dominated by the spin-rotation interaction (Chapter 4). The T_1 of SnCl_4 is also dominated by spin-rotation as has been demonstrated by Sharp (1972). However in SnBr_4 (Sharp 1973) and SnI_4 (Sharp 1972) the spin-lattice relaxation rate is a mixture of both spin-rotation and scalar relaxation. For SnBr_4 Sharp (1973) has obtained a decomposition of the T_1 ; he obtained $T_1^{\text{SR}} = 7$ sec $T_1^{\text{SC}} = 1.8$ sec at 300°K . For the SnI_4 case Sharp (1972) has obtained data at 477°K however extrapolation of his data back to 300°K yields $T_1^{\text{SR}} = 10$ sec and $T_1^{\text{SC}} = 0.38$ sec. Our T_1 data for the various Sn(IV) halides are in excellent agreement with Sharp's (1972,1973) reported values. We were only able to measure the T_1 of one SnCl_4 adduct ($\text{SnCl}_4 \cdot 2\text{CH}_3\text{OH}$)

because the signal of the acetonitrile adduct was very weak. The $\text{SnCl}_4 \cdot 2\text{CH}_3\text{OH}$ adduct most probably relaxes by spin-rotation, its T_1 (7.3 sec) is much longer than SnCl_4 ($T_1 = 1.6$ sec) probably because of a smaller angular correlation time (τ_w) due to increased moment of inertia along with a smaller spin-rotation constant (C_0) related to the smaller paramagnetic shielding. All of the tin compounds containing protons most probably are also dominated by the spin-rotation interaction with the dipole-dipole relaxation being negligible because of the r^{-6} dependence. Both Sn(II) dihalides in their respective acids have similar T_1 values (4 sec). These solutions are most likely a mixture of SnX_3^- and SnX_4^{--} species in very rapid halide exchange. From the data in Table 6-1 there is a trend showing that with increasing chemical shift there is also an increase in the T_1^{SR} . The reason for this is that the paramagnetic term of the shielding tensor becomes smaller with the upfield shift in going from $\text{Sn}(\text{CH}_3)_4$ to SnI_4 and thus the spin-rotation constant becomes smaller, also the value of τ_w decreases with increasing moment of inertia causing overall a less effective spin-rotation interaction and therefore the T_1^{SR} values become longer.

The rather short relaxation times make ^{119}Sn a useful nucleus for further studies using signal-averaged pulse Fourier transform NMR.

TABLE 6-1

 ^{119}Sn CHEMICAL SHIFTS, T_1 's AND T_2 's

Compound	(ppm) ^a	$J_{\text{H-}^{119}\text{Sn}}$ (Hz)	T_2 (msec)	T_1 (sec)
SnI_4 (2M in CS_2)	1698.6	940 ^b	10	$T_1^{\text{SC}} = 0.38$ $T_1^{\text{SR}} = 10$
$\text{SnCl}_4 \cdot 2\text{CH}_3\text{CN}$ (satd. in CH_3CN)	775.0	-	4	*
SnBr_4 (5M in CS_2)	631.6	920 ^c	3	$T_1^{\text{SC}} = 1.8$ $T_1^{\text{SR}} = 7$
$\text{SnCl}_4 \cdot 2\text{MeOH}$ (satd. in MeOH)	602.1	-	8	7.3
$\text{Na}_2\text{Sn}(\text{OH})_6$ (aq)	591.0	-	64	**
SnCl_2 (satd. in HCl)	388.1	-	80	4.2
SnBr_2 (satd. in HBr)	385.0	-	21	3.8
SnCl_4 (neat)	147.8	470 ^d	1.5	1.6
$\text{Sn}(\text{CH}_3)_4$ (neat)	0	54.0 ^e	106	0.6
$\text{Sn}(\text{CH}_3)(\text{Cl})_3$ (5M in CCl_4)	-15.2	99.7 ^e	3	2.0
$\text{Sn}(\text{CH}_3)_2\text{Cl}_2$ (acetone)	-19.6	86.2 ^e	21	1.0
$\text{Sn}(\text{CH}_3)_2\text{Cl}_2$ (satd. in CCl_4)	-141.2	71.0 ^e	11	*
$\text{Sn}(\text{CH}_3)_3\text{Cl}$ (5M in CCl_4)	-160.0	59.9 ^e	40	0.66

* Not measured owing to weakness of signal. ** Not measured. ^a Precision ± 0.1 ppm
 Instrumental linewidth 3 Hz. All spectra recorded at 301°K. ^b $J_{^{119}\text{Sn-I}}$; ^c $J_{^{119}\text{Sn-Br}}$
^d $J_{^{119}\text{Sn-Cl}}$. ^e Measured on a Varian A56/60 High resolution NMR spectrometer by
 observing proton spectrum.

C. STUDY OF HYDROLYSIS EQUILIBRIA PRODUCTS OF Sn(IV)Cl₄
BY ¹¹⁹Sn NMR

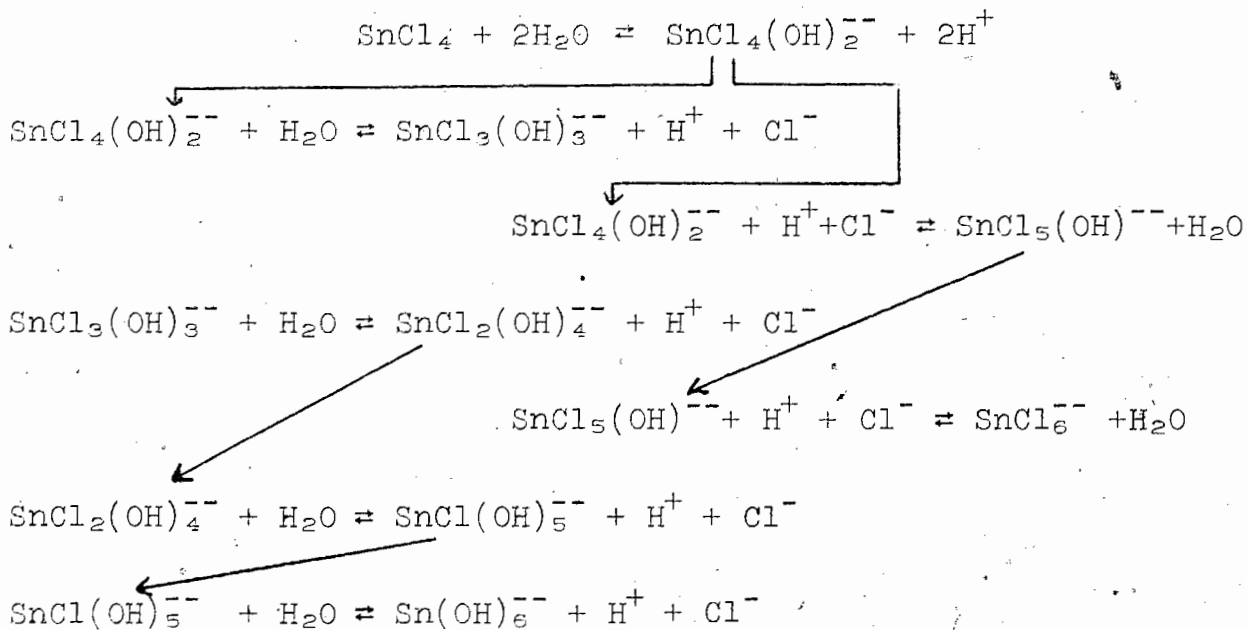
NMR exchange studies have usually employed the ¹H or ¹⁹F nucleus as the probe because of high natural abundance and easily observable NMR signal. For nuclei of low natural abundance and spin 1/2 the relatively narrow linewidth and low sensitivity have been in the past a problem in detection of the NMR signal. However now with the advent of signal-averaging and Fourier Transform this problem has been eliminated and we are able to detect the NMR signals of nuclei such as ¹¹³Cd, ¹¹⁹Sn, ¹⁹⁹Hg and ²⁰⁷Pb much more easily.

There have been several NMR studies involving metal halide species in organic liquids. These have involved the use of the metal nuclei as the NMR probe in the identification of the various mixed metal halide complexes. The nuclei in these studies were: ⁹³Nb (Kidd and Spinney 1973), ⁷³Ge (Kidd and Spinney 1973) and ⁴⁹Ti (Kidd, Matthews and Spinney 1972). Evans and Dean (1968) have characterized in solution some 100 anions of the type SnF_{6-n}X_n⁻ using ¹⁹F NMR. They have also obtained equilibrium constants for the displacement of F⁻ from SnF₆⁻ by chloride, bromide and hydroxide ions. We planned to study the hydrolysis of SnCl₄ by a fresh and novel approach, that of utilizing the ¹¹⁹Sn nucleus as the NMR probe.

1. Hydrolysis

The mechanism for the hydrolysis of a covalent halide such as SnCl₄ has to be different from the hydrolysis of an

ionic halide. The first step in the hydrolysis of SnCl_4 may involve the coordinate addition of two water molecules. This seems logical since the Sn(IV) is coordinatively unsaturated and thus the addition of two molecules of water enable it to attain its stable coordination maximum number of six. Compounds such as CCl_4 , SF_6 and OsF_8 do not hydrolyze because the central element has already attained its maximum coordination number and therefore the initial addition step does not occur. However a compound such as WCl_6 can be hydrolyzed because the maximum coordination number of tungsten is eight. A possible mechanism for the hydrolysis of SnCl_4 may be as follows:



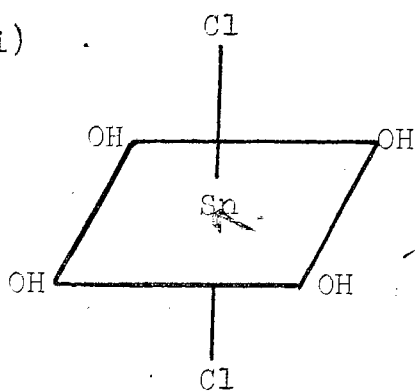
One may notice that there exists the possibility of cis and trans structural isomers for three of these proposed species.

FIGURE 6-2

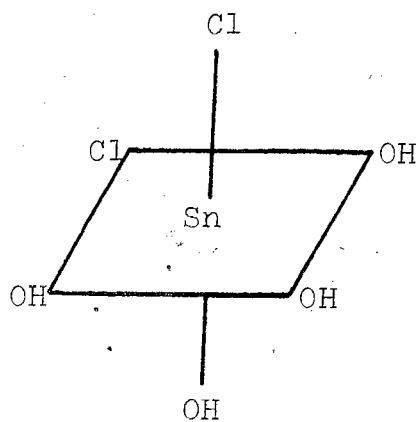
Possible cis and trans Isomers of the
dichloro, trichloro and tetrachloro
tin species

trans

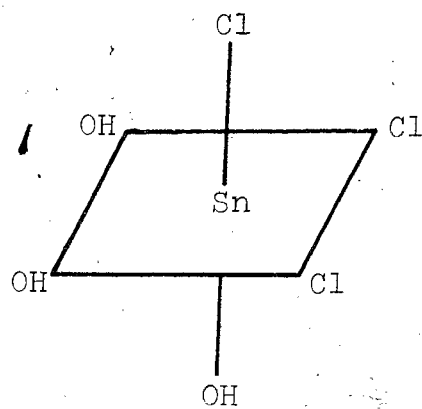
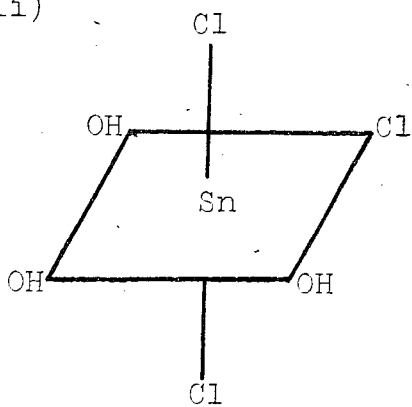
(i)



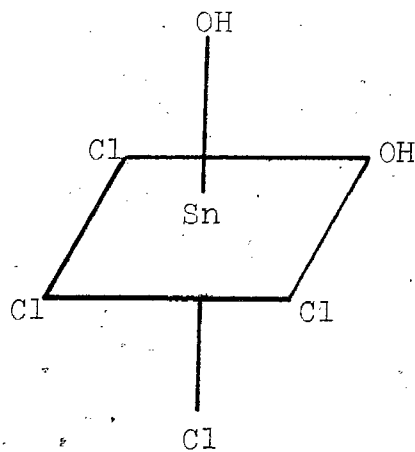
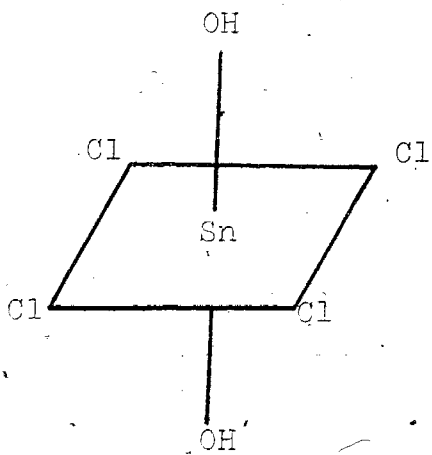
cis



(ii)



(iii)



Previous attempts at finding the ^{119}Sn NMR signal in aqueous solutions of tin tetrachloride (Lauterbur and Burke 1961) have failed. Possibly it was because of the early crude techniques used to observe these "exotic" nuclei i.e. rapid passage dispersion mode spectra. However now with FT techniques at hand it is much easier and less time consuming to observe the rather weak signals of such "exotic" nuclei as ^{199}Hg , ^{113}Cd , ^{119}Sn and other nuclei. In preliminary work we have been able to observe a number of ^{119}Sn signals in aqueous tin tetrachloride solutions. We believe these to be the signals of the various chlorotin(IV) species in solution. By variation of the concentration of SnCl_4 , pH and chloride concentration we have observed what we believe are all seven of the species, $\text{SnCl}_n(\text{OH})_{6-n}^-$. The possible existence of this complete series of chlorohydroxo tin species had been discussed by de la Puente (1922). However direct proof of their existence has never been reported in the literature.

2. Characterization of the species

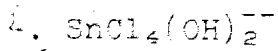
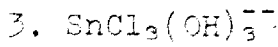
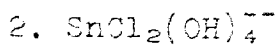
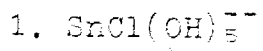
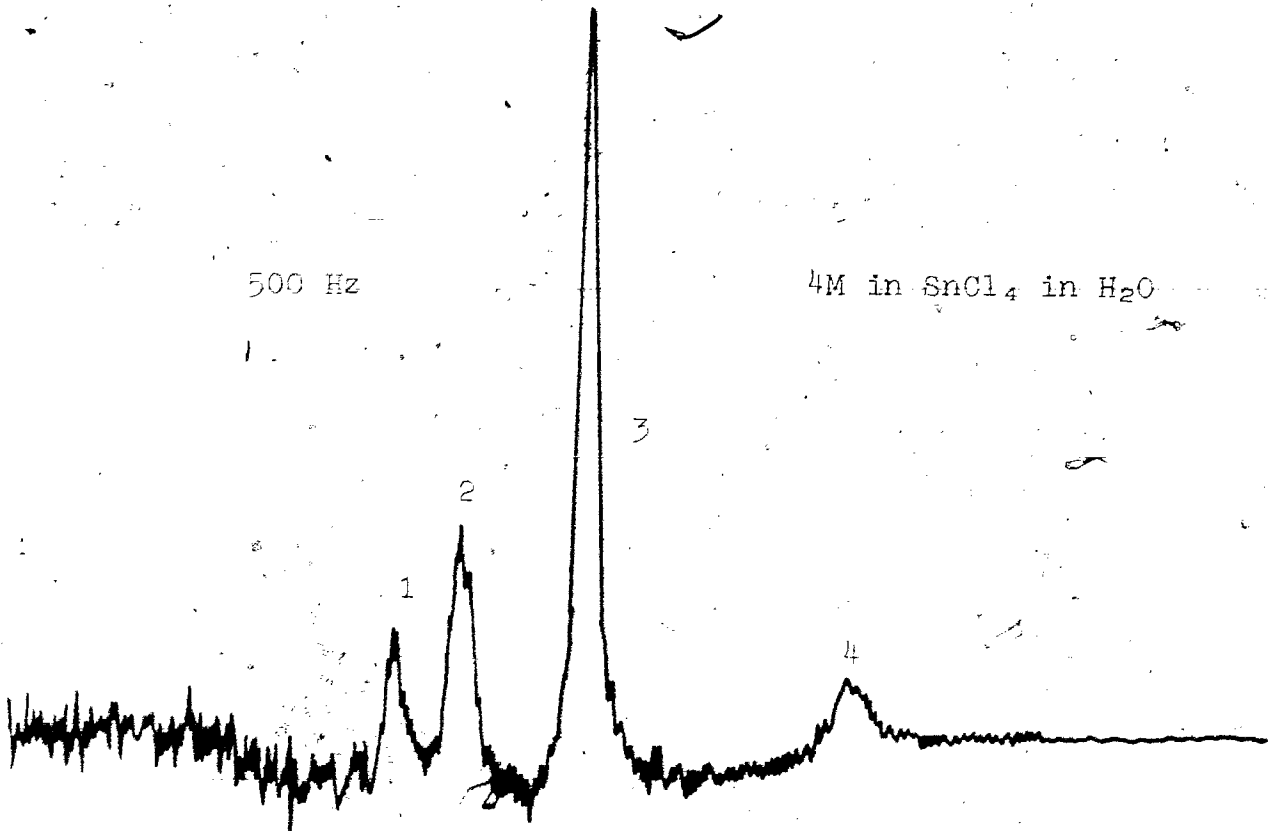
The various measured chemical shifts and linewidths are given in Table 6-2 relative to $^{119}\text{Sn}(\text{CH}_3)_4$ as the reference standard. A representative spectrum is also shown in Figure 6-3. This is the first reported instance in which the various chlorohydroxo tin species have been individually observed. The only other species which had been previously identified are SnCl_6^- and SnBr_6^- by Raman spectroscopy (Woodward and Anderson 1957).

FIGURE 6-3

Typical ^{119}Sn NMR spectra of chlorhydroxo-tin species

500 Hz

4M in SnCl₄ in H₂O



4M in SnCl₄ in 2.5M HCl

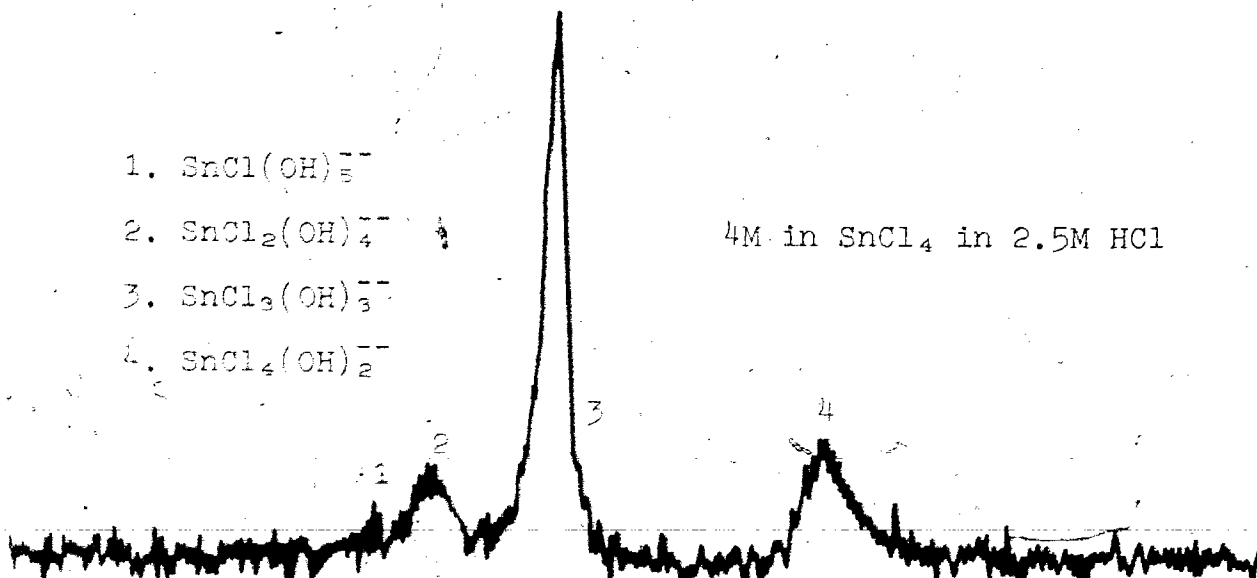


TABLE 6-2

ASSIGNED CHEMICAL SHIFTS AND LINEWIDTHS FOR THE VARIOUS
 $^{119}\text{SnCl}_n(\text{OH})_{6-n}^{--}$ SPECIES

Species	Concentration	δ^a (ppm)	$\Delta\nu_{\frac{1}{2}}$ (Hz)
$\text{Sn}(\text{OH})_6^{--}$	Satd. in NaOH	589.5 \pm 0.5	5
$\text{SnCl}(\text{OH})_5^{--}$	4M	622 \pm 1	35
$\text{SnCl}_2(\text{OH})_4^{--}$	4M	629 \pm 1	40
$\text{SnCl}_3(\text{OH})_3^{--}$	4M	644 \pm 1	35
$\text{SnCl}_4(\text{OH})_2^{--}$	4M	675 \pm 2	70
$\text{SnCl}_5(\text{OH})^{--}$	4M in 6M HCl	684 \pm 2	150
SnCl_6^{--}	Satd. in conc HCl	692 \pm 2	400

^aAll spectra taken at 26°C. All shifts to high field
 from $^{119}\text{Sn}(\text{CH}_3)_4$ as external standard.

From the spectra in Figure 6-3 and our assignment of each ^{119}Sn signal it seems that we do not observe the structural isomers, cis and trans for the dichloro, trichloro and tetrachloro tin species. Two possible reasons for this are; (a) one of the structural isomers is more stable thermodynamically than the other and thus we only observe either the cis or trans isomer as is the case for the SnCl_4 adducts with acetonitrile (Cunningham et al. 1972), acetone (Beattie et al. 1963) and POCl_3 (Branden 1963) whose stereochemistry as determined by X-ray diffraction in the solid state and by IR spectroscopy in solutions is cis; (b) the other possible reason may be the possibility of rapid ligand exchange giving us an average signal for the two isomers. Our proposed species is octahedral; for the exchange to occur would necessitate the complex to go through some type of five-coordinate intermediate via an $\text{S}_{\text{N}}1$ dissociation. But then we are led to the paradox of fast $\text{S}_{\text{N}}1$ dissociation to accommodate rapid structural interconversion, but slow intermolecular exchange of ligands at the same intermediate.

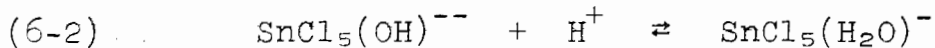
Studies have been conducted by Neuman (1954) on the Sb(V) in HCl system. By analyzing the UV spectra of various solutions of Sb(V) in HCl solutions ranging from 2 to 12M, he determined the kind and amounts of species present. With decreasing acidity he showed the presence of Sb(OH)Cl_5^- , $\text{Sb(OH)}_2\text{Cl}_4^-$,etc. and measured the amounts present for

various acidities. The $\text{Sb}(\text{OH})\text{Cl}_5^-$ is the predominant form in 8M HCl, $\text{Sb}(\text{OH})_2\text{Cl}_4^-$ in 6M acid and below 5M acid he found $\text{Sb}(\text{OH})_3\text{Cl}_3^-$ and the more hydrolyzed species are the most important.

A similar study to Neuman's has been conducted by Inoue et al. (1959) on the UV determination of quadrivalent tin in the HCl acid medium. They believe they have identified the SnCl_6^{--} and $\text{Sn}(\text{OH})\text{Cl}_5^{--}$ species in 6M HCl solution. Their results indicate that the hydronium ion gives a large effect on the system because it expedites the formation of chloro-complex from stannic hydroxo-complexes which exist in low acidity. Thus our system could be analogous and consist of our proposed species of the type $\text{SnCl}_n(\text{OH})_{6-n}^{--}$.

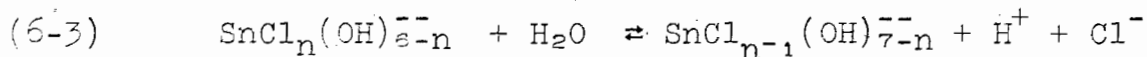
Neuman (1954) observed that there was no retention of antimony on cation-exchange resins and complete retention on anion-exchangers. Boner (1949) also conducted migration studies on the $\text{Sb}(\text{V})$ -HCl system which indicated that all of the species containing antimony were anionic. In a similar manner we may investigate the Sn(IV) system to determine if the species present are really negatively charged particles such as $\text{SnCl}_n(\text{OH})_{6-n}^{--}$.

It is also quite possible that at high acid concentrations the species present could be chloroaquo-tin species (e.g. $\text{SnCl}_5(\text{H}_2\text{O})^{--}$) since at such high acid concentrations it could be quite easy to protonate an OH^- group.



We could seek evidence of this by studying the pH dependence of SnCl_4 in water using a strong acid such as HClO_4 . At low $[\text{H}^+]$ where the major species would be in the form $\text{SnCl}_5(\text{OH})^{--}$, we would hopefully see the chemical shift characteristic of this species while at high $[\text{H}^+]$ the predominant species would be in the form $\text{SnCl}_5(\text{H}_2\text{O})^-$ and thus we would see the chemical shift for this particular species, while in between one would see only an average chemical shift proportional to the relative amounts of each species ($\text{SnCl}_5(\text{OH})^{--}$ or $\text{SnCl}_5(\text{H}_2\text{O})^-$) present.

Another possible approach to the identification of the species present in this system is to assume that each species is a particular type and thus see if reasonable equilibrium constants can be obtained. If we assume the species present are members of the series $\text{SnCl}_{n-1}(\text{OH})_{6-n}^{--}$ then the equilibrium relating these species, is given by

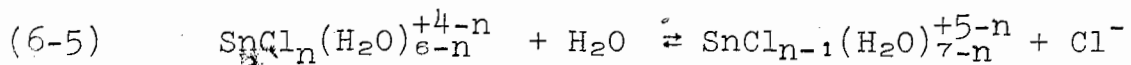


and the equilibrium constant is given by,

$$(6-4) \quad K = \frac{[\text{SnCl}_{n-1}(\text{OH})_{7-n}^{--}] (a_{\text{H}^+})(a_{\text{Cl}^-})}{[\text{SnCl}_n(\text{OH})_{6-n}^{--}] (a_{\text{H}_2\text{O}})}$$

where $n = 1, \dots, 6$

However if the species present are of the type $\text{SnCl}_n(\text{H}_2\text{O})_{6-n}^{+4-n}$ then*,



and

$$(6-6) \quad K = \frac{[\text{SnCl}_{n-1}(\text{H}_2\text{O})_{7-n}^{+5-n}] [\text{Cl}^-]}{[\text{SnCl}_n(\text{H}_2\text{O})_{6-n}^{+4-n}] [\text{H}_2\text{O}]}$$

where a_{H^+} , a_{Cl^-} , and $a_{\text{H}_2\text{O}}$ are the activities of H^+ , Cl^- , and water. The activities of H_2O can be calculated from data of Akerlof and Teare (1937) and the activities of a_{H^+} and a_{Cl^-} can be measured by using a standard hydrogen cell along with a Ag/AgCl electrode system and the following relationship,

$$(6-7) \quad E_{\text{cell}} = E_{\text{H}_2/\text{H}^+}^\circ - E_{\text{Ag}/\text{AgCl}}^\circ - 0.0592 \log (a_{\text{H}^+})(a_{\text{Cl}^-})$$

The only assumption involved in the calculation of Eq. (6-4) is that the activity coefficient of the chlorohydroxo-tin species are the same.

* Note that in Eq. (6-4) we deal with activities while in Eq. (6-6) we have written the equilibrium constant in terms of concentrations. The reason for this is that we cannot measure the activity of Cl^- alone.

Because of this problem about the a_{Cl^-} in Eq. (6-6) we must be careful in the handling of data in this part of the problem.

The amounts of the tin species is determined by using ^{119}Sn FT high resolution NMR (i.e. integration of the signal from each species along with the known total concentration of $Sn(IV)$ in solution).

Once the equilibrium constants have been obtained the changes in heat content, free energy and entropy of these reactions can be calculated in the usual manner. From the equilibrium constant and the expression,

$$(6-8) \quad \Delta G = -RT \ln K$$

we obtain the free energy. Then by studying the temperature dependence of the equilibrium constant and using the following equation we obtain ΔH ,

$$(6-9) \quad \frac{d \ln K}{d(1/T)} = - \frac{\Delta H}{R}$$

From these two quantities it is then trivial to obtain the entropy ΔS .

D. FURTHER WORK

Our characterization of each member of the series is not quite complete and this must be verified before proceeding with the determination of the equilibrium constants for the various reactions. The direct observation of the ^{119}Sn signals due to the various chlorohydroxo-tin species should allow the determination of the OH/Cl displacement rates to be much more easily obtained than if ^{35}Cl were used as the probe nucleus. This should serve to show the fertility of not only this system but of many other systems involving metal nuclei in which one may use the metal nucleus as the NMR probe.

CHAPTER 7

SYMMETRY EFFECTS IN ^{13}C T_1 RELAXATION IN METHYL GROUPSA. Results

We have recently observed a differential T_1 effect in the ^{13}C spin-lattice relaxation of the members of the quartet in methyl groups. This observed behaviour has never been previously reported in the literature. We have observed the undecoupled ^{13}C spectrum of $^{13}\text{CH}_3\text{CN}$ and $\text{Hg}(^{13}\text{CH}_3)(\text{CH}_3)$ at 301°K both at 15.0 and 25.1 MHz using pulse FT techniques. The results obtained are as follows: (a) Figure 7-1 shows the ^{13}C quartet due to the coupled protons in $^{13}\text{CH}_3\text{CN}$ and it is plainly seen that the quartet remains in a ratio 1:3:3:1 as τ is varied in the $180^\circ\text{-}\tau\text{-}90^\circ$ pulse sequence, (b) Figure 7-2 shows the ^{13}C quartet in $\text{Hg}(\text{CH}_3)_2$ (the quartet is broader than in the acetonitrile case because of the unresolved $^3J_{^{13}\text{C-H}} = 1.3$ Hz), the ratio of this quartet begins and ends at 1:3:3:1 ratios but near the null point it does not remain in this ratio. This result is better illustrated in Figure 7-3 and 7-4. Figure 7-3 shows the ^{13}C spectrum of $\text{Hg}(\text{CH}_3)_2$ at $\tau = 8.5$ sec for the $180^\circ\text{-}\tau\text{-}90^\circ$ sequence. The only apparent members are the two inner lines while the outer two lines appear nulled out. Figure 7-4 shows again the ^{13}C spectrum

of $\text{Hg}(\text{CH}_3)_2$ at $\tau = 8.7$, 8.8 , and 9.0 sec showing examples where the outer wings are positive and the inner members negative, outer members positive and inner members nulled out, and finally the outer wings larger than the inner lines.

We then decided to measure both the spin-lattice relaxation times (T_1) in proton decoupled conditions. We also measured the nuclear Overhauser enhancement factor (η) for both compounds. The results are as follows at 301°K :

$^{13}\text{CH}_3\text{CN}$	$T_1 = 19.7 \pm 0.7$ sec	$\eta = 0.70 \pm 0.10$
$(^{13}\text{CH}_3)(\text{CH}_3)\text{Hg}$	$T_1 = 13.0 \pm 0.5$ sec	$\eta = 1.40 \pm 0.10$

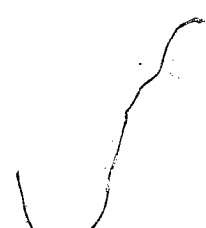
The nuclear Overhauser enhancement factor (η) for a heteronuclear system where both spins are $1/2$ is given by,

$$(7-1) \quad \eta_{I-\{S\}} = \frac{1}{2} \frac{\gamma_S}{\gamma_I} \frac{R_1(\text{dipolar})}{R_1(\text{total})}$$

therefore if $I = ^{13}\text{C}$ and $S = ^1\text{H}$ Equation (7-1) becomes,

$$(7-2) \quad \eta_{^{13}\text{C}-\{^1\text{H}\}} = 1.988 R_1(\text{dipolar}) / R_1(\text{total})$$

Using this equation along with the measured η and $T_1(^{13}\text{C})$ we can calculate the contribution from dipole-dipole interactions (DD) and the contribution from other mechanisms, in this case spin-rotation (SR).



-167 a-

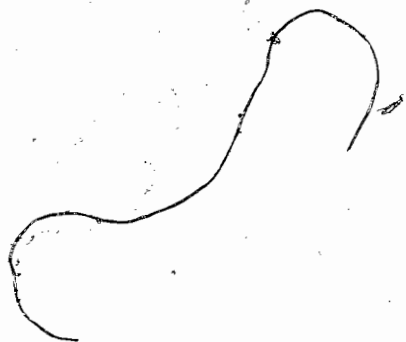
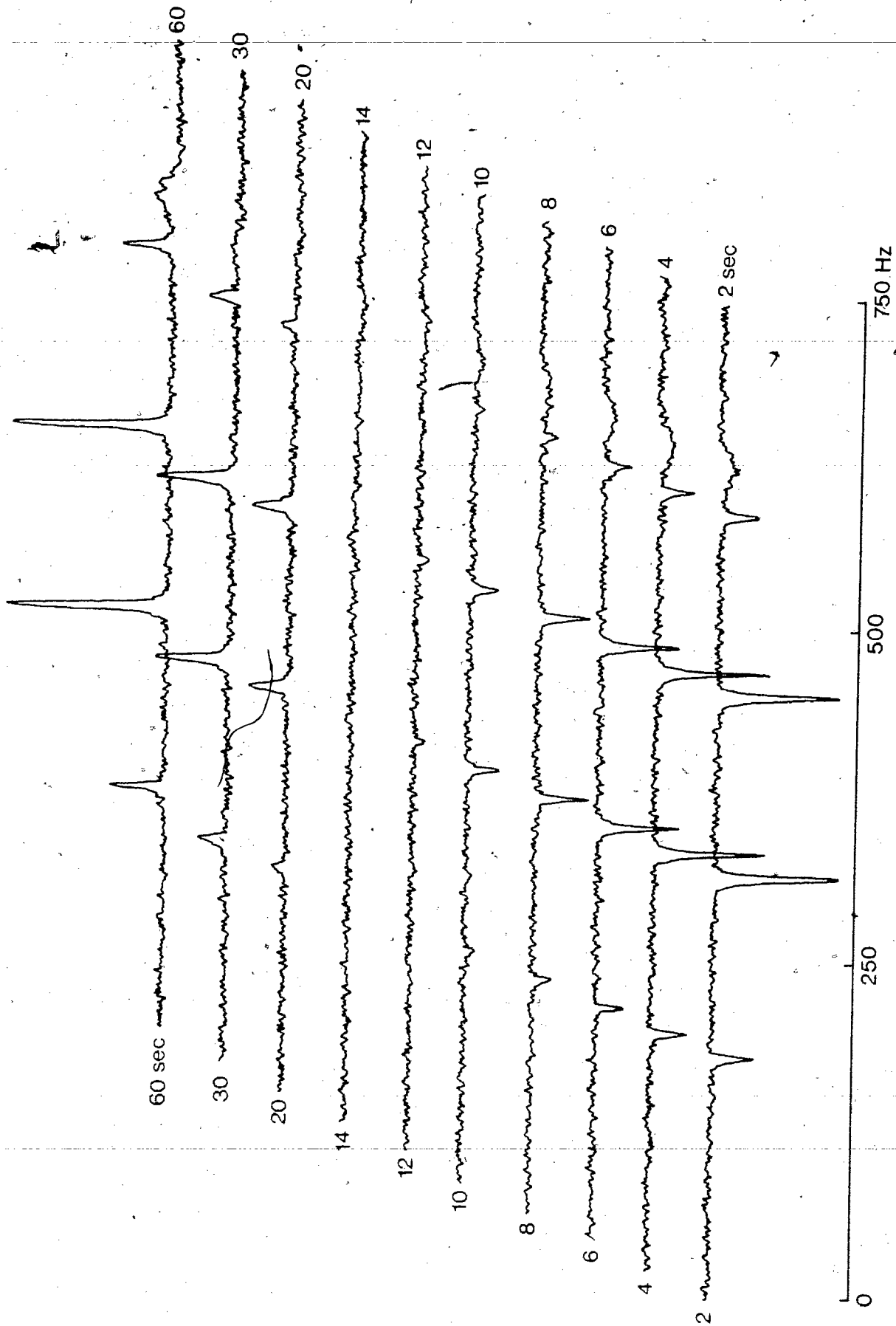


FIGURE 7-1

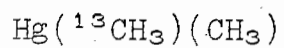
Plot of 180° - τ - 90° pulse sequence in the proton uncoupled ^{13}C quartet of natural abundance $^{13}\text{CH}_3\text{CN}$



-168 a-

FIGURE 7-2

Plot of 180° - τ - 90° pulse sequence in the proton
undecoupled ^{13}C quartet of natural abundance.



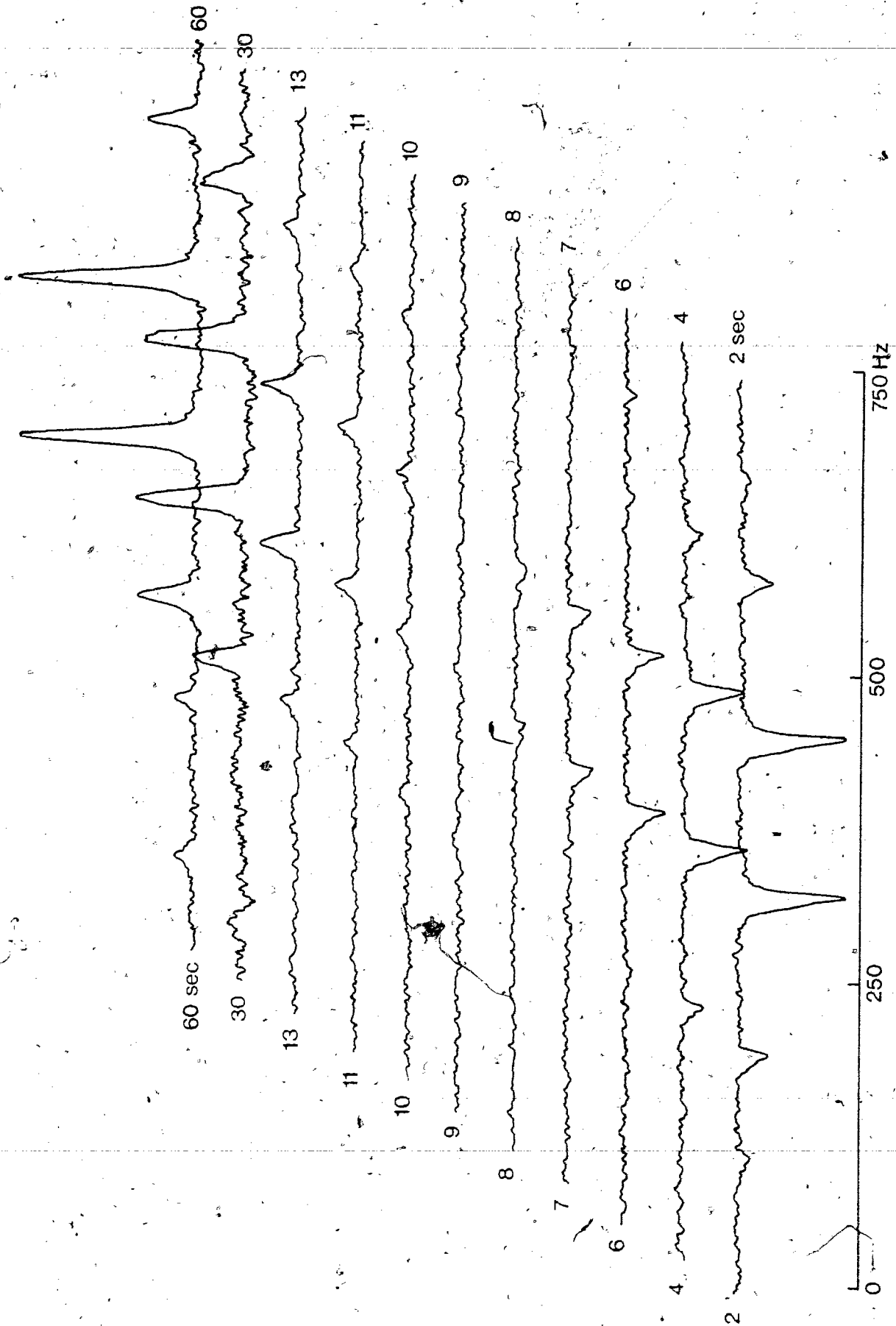
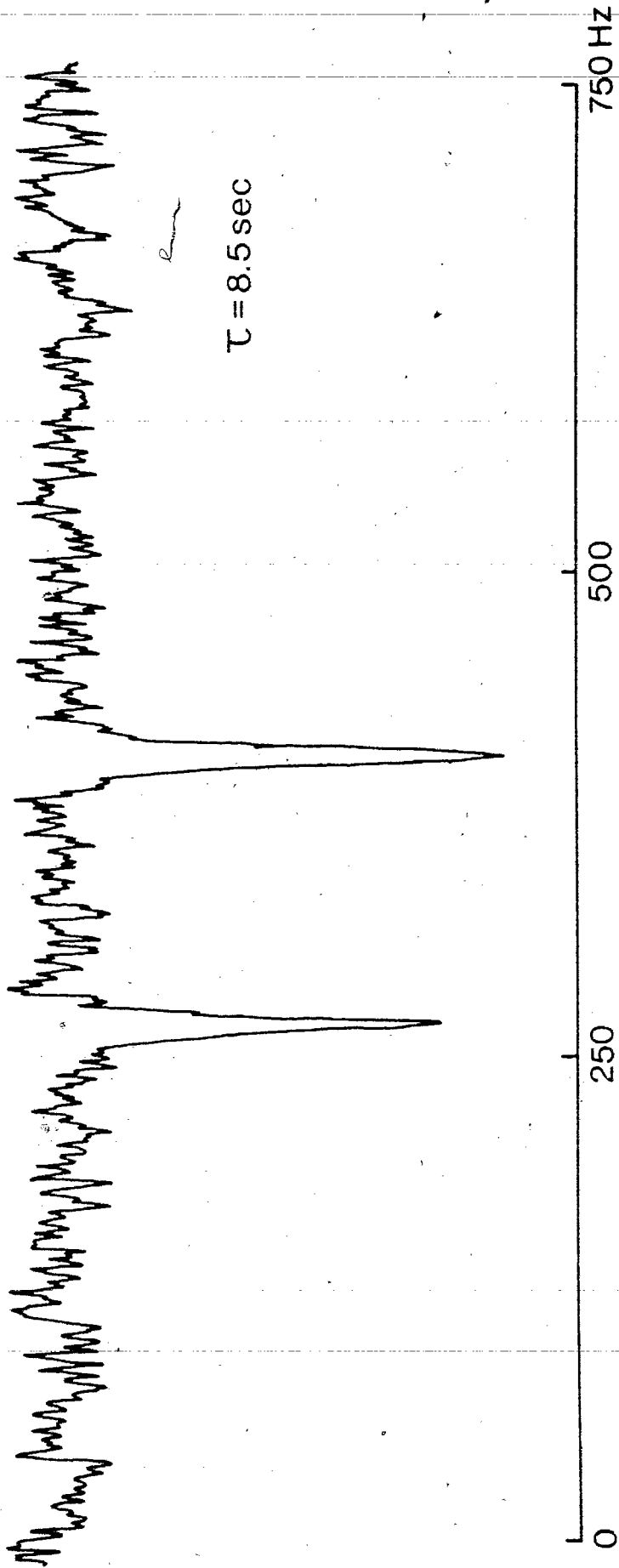


FIGURE 7-3

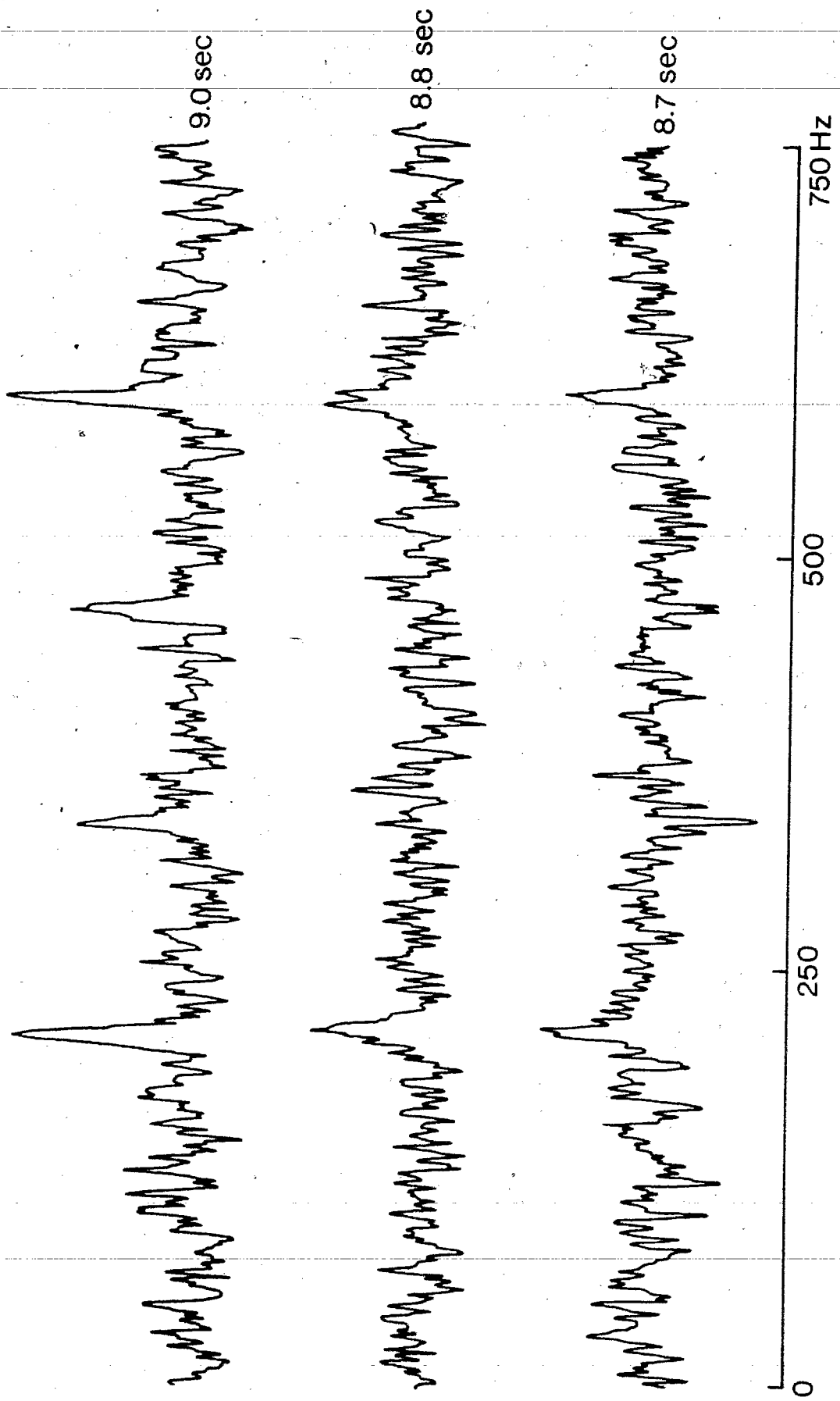
Plot of 180° - τ - 90° sequence for $\tau = 8.5$ sec in the
 ^{13}C quartet of $\text{Hg}(\text{CH}_3)_2$. (cycle time 90 sec; 1000 scans)



Handwritten mark resembling a checkmark or the letter 'e'.

FIGURE 7-4

Plot of $180^\circ\text{-}\tau\text{-}90^\circ$ sequence for $\tau=8.7;8.8;\text{and }9.0$ sec. in the ^{13}C quartet of $\text{Hg}(\text{CH}_3)_2$. (360 scans)



In neither case did we observe any non-exponential behaviour in carbon-13 T_1 experiments. Although there may have been such behaviour it was well within our possible experimental observation errors.

Using Eq. (7-2) we may calculate the DD and SR contributions for both acetonitrile and dimethyl mercury. The results are as follows: (a) $^{13}\text{CH}_3\text{CN}$ T_1 is 35% DD and 65% SR and (b) $(^{13}\text{CH}_3)(\text{CH}_3)\text{Hg}$ T_1 is made up of 70% DD and 30% SR. The same effect has been observed in the ^{13}C T_1 recovery of the ^{13}C quartet in $\text{Sn}(\text{CH}_3)_4$, where at the same temperature in Chapter 4 it was shown that the ^{13}C relaxation mechanism is about 30% SR and 70% DD.

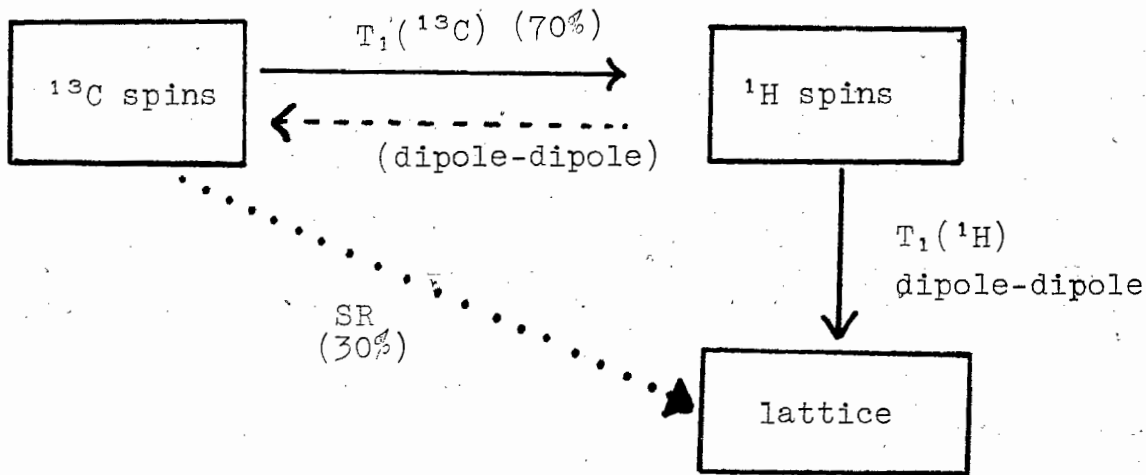
B. Discussion

This data identifies the ^{13}C to ^1H dipole-dipole relaxation interaction as responsible for the observed relaxation rate differences of the multiplet members. A qualitative explanation is that there is a feeding of energy between the ^{13}C spins and the ^1H spin reservoir (see Figure 7-5). For the ^{13}C dipole-dipole case there is an exchange of energy between the carbon-13 and proton spins before the energy goes out to the lattice while for the spin-rotation case the energy is directly transferred to the lattice and thus by-passing the interaction with the ^1H spins and effectively short-circuiting this effect of differential T_1 's.

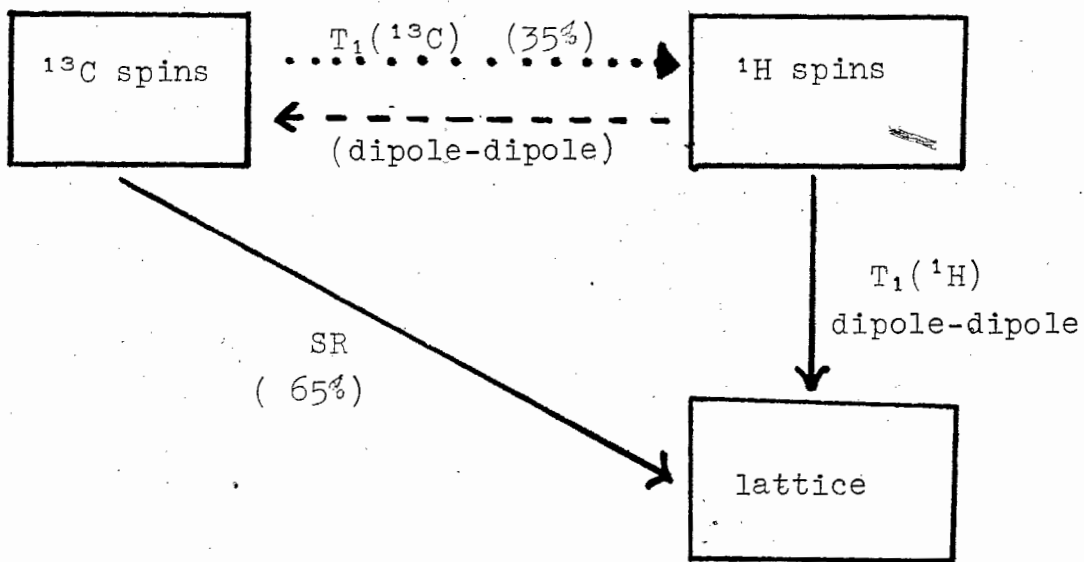
FIGURE 7-5

Sketch showing the possible processes for energy transfer to the lattice in a) CH_3CN and b) $\text{Hg}(\text{CH}_3)_2$

^{13}C Dipole-Dipole case ($\text{Hg}(\text{CH}_3)_2$)



^{13}C Spin-rotation case (CH_3CN)



When dipolar coupling occurs between two unlike spins I and S then the change in magnetization of the I and S spins is given by a set of coupled equations (Abragam 1961),

$$(7-3) \quad \frac{d\langle S_z \rangle}{dt} = - \frac{1}{T_1^{SS}} (\langle S_z \rangle - S_0) - \frac{1}{T_1^{SI}} (\langle I_z \rangle - I_0)$$

$$(7-4) \quad \frac{d\langle I_z \rangle}{dt} = - \frac{1}{T_1^{II}} (\langle I_z \rangle - I_0) - \frac{1}{T_1^{IS}} (\langle S_z \rangle - S_0)$$

This means that when an r.f. field is applied at frequency ω_S it will affect $\langle I_z \rangle$ while it acts on $\langle S_z \rangle$. These so called "cross-relaxation" terms T_1^{SI} and T_1^{IS} cause a non-exponential behaviour in the recovery of the S_z magnetization. We would of course observe this behaviour if we proton decoupled our $\text{Hg}(\text{CH}_3)_2$ ^{13}C quartet since it would recover at a rate which would be a mixture of the outer and inner lines which have different T_1 values. We did not observe non-exponentiality in the proton decoupled T_1 measurement of $\text{Hg}(\text{CH}_3)_2$ because this non-exponentiality is too small and within any experimental uncertainties in measurement. It seems that these above equations have something missing that is they are for a non-selective T_1 experiment. However our T_1 experiments are selective since we observe each component of the quartet separately. This leads to the conclusion that one must symmetrize the various members of the quartet.

The quartet for the undecoupled $^{13}\text{CH}_3$ system of local nuclear space symmetry C_{3v} has the following symmetry components.

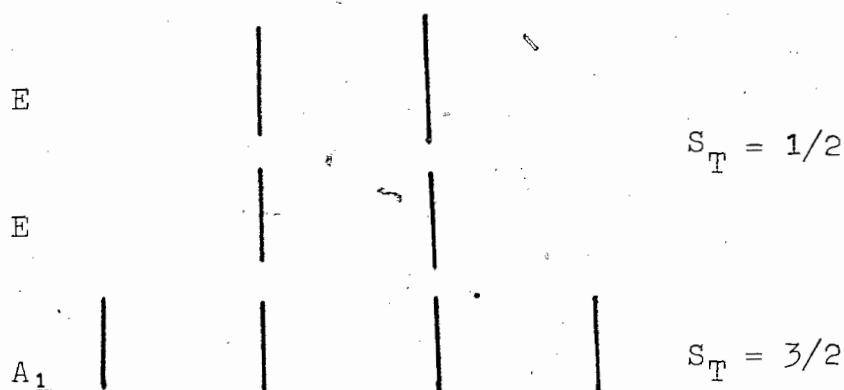


Figure 7-6. I-Spin Resonance Quartet.

It is quite possible that this symmetry effect is the cause of this non-equivalent relaxation behaviour in the $\text{Hg}(\text{CH}_3)_2$ case where T_1 is dominated by DD but not in the CH_3CN case where T_1 is dominated by the SR interaction. Each outer component of the quartet having $A_1(^1\text{H})$ symmetry has an effective T_1 of 12.1 sec while the E components have T_1 of 13.0 sec (we observe an average T_1 for the degenerate inner lines).

Apparently this effect had never been noticed before possibly for two reasons: (a) most ^{13}C T_1 measurements are obtained under proton decoupled conditions, (b) it is very difficult to observe the effect except near the null point of the 180° - τ - 90° sequence where this effect is best observed and thus requires very long term signal-averaging since the ^{13}C T_1 's are fairly long.

APPENDIX A

Isotope	NMR frequency in 10 kGauss field (MHz)	Natl. Abundance %	Spin
^1H	42.5759	99.9844	$\frac{1}{2}$
^2D	6.53566	0.0156	1
^{13}C	10.705	1.108	$\frac{1}{2}$
^{35}Cl	4.172	75.4	$\frac{3}{2}$
^{37}Cl	3.472	24.6	$\frac{3}{2}$
^{79}Br	10.667	50.57	$\frac{3}{2}$
^{81}Br	11.499	49.43	$\frac{3}{2}$
^{115}Sn	13.92	0.35	$\frac{1}{2}$
^{117}Sn	15.17	7.67	$\frac{1}{2}$
^{119}Sn	15.87	8.68	$\frac{1}{2}$
^{199}Hg	7.60	16.86	$\frac{1}{2}$
^{201}Hg	2.80	13.24	$\frac{3}{2}$

Varian Associates, NMR Table (Fifth edition)

APPENDIX B

1. Determination of $T_1(^{201}\text{Hg})$

$$(R_1)_Q = \frac{3\pi^2 (2I + 3)}{10I^2(2I-1)} (e^2qQ/h)_Q^2 \tau_c$$

Since the ^{201}Hg atom ($I = 3/2$) lies on the main symmetry axis in $\text{Hg}(\text{CH}_3)_2$ and $\theta = 0$ then $\tau_c = 1/6D_{\perp}$.

$$(R_1)_{^{201}\text{Hg}} = \frac{\pi^2}{15D_{\perp}} (e^2qQ/h)_{^{201}\text{Hg}}^2$$

At $+40^\circ\text{C}$ $D_{\perp} = 2.5 \times 10^{10}$. However we do not know the value for $(e^2qQ/h)_{^{201}\text{Hg}}$. However we can estimate this value from the known values for $^{79,81}\text{Br}$ in CH_3HgBr (Gordy et al. 1953),

$$(e^2qQ/h)_{^{79}\text{Br}} = 325 \text{ MHz}$$

$$(e^2qQ/h)_{^{81}\text{Br}} = 270 \text{ MHz}$$

We also know that for

^{79}Br	$I = 3/2$	$eQ = 0.335$
^{81}Br	$I = 3/2$	$eQ = 0.280$
^{201}Hg	$I = 3/2$	$eQ = 0.5$

Therefore $(e^2qQ/h)_{^{201}\text{Hg}} \cong (0.5/0.335)(325 \text{ MHz}) \cong 500 \text{ MHz}$.

This is an upper limit value since the procedure is not really valid because of the different eQ 's for Br and Hg and in fact eQ is probably less at the Hg than at the Br.

Using this value for $(e^2qQ/h)_{201\text{Hg}}$ along with D_{\perp} at $+40^{\circ}\text{C}$ we obtain,

$$T_1(^{201}\text{Hg}) \cong 1.5 \times 10^{-7} \text{ sec}$$

2. ^{201}Hg Scalar contribution to $R_{2\text{H}}$ in $\text{Hg}(\text{CH}_3)_2$

$$R_2^{\text{SC}} = \frac{4\pi^2}{3} J_{\text{H}-^{201}\text{Hg}}^2 (I_{\text{Hg}}+1) I_{\text{Hg}} \left[T_{1\text{Hg}} + \frac{T_{2\text{Hg}}}{1+(\omega_{\text{H}}-\omega_{\text{Hg}})^2 T_{1\text{Hg}}^2} \right]$$

Since $(\omega_{\text{H}}-\omega_{\text{Hg}})^2 T_{1\text{Hg}}^2 \gg 1$ the above equation reduces to,

$$R_2^{\text{SC}} = \frac{4\pi^2}{3} J_{\text{H}-^{201}\text{Hg}}^2 \left(\frac{3}{2}\right) \left(\frac{5}{2}\right) T_{1\text{Hg}}$$

From our measurement we know that $J_{\text{H}-^{199}\text{Hg}} = 101.5 \text{ Hz}$ thus

$$J_{\text{H}-^{201}\text{Hg}} \cong \frac{\gamma_{^{201}\text{Hg}}}{\gamma_{^{199}\text{Hg}}} \times J_{\text{H}-^{199}\text{Hg}} \cong 38 \text{ Hz}$$

Therefore at $+40^{\circ}\text{C}$ $R_2^{\text{SC}} \cong 10^{-2} \text{ sec}^{-1}$. At this temperature $R_{1\text{H}} \cong 0.088 \text{ sec}^{-1}$ so that for the 13.24% natural abundance $^{201}\text{Hg}(\text{CH}_3)_2$ $R_{2\text{H}} = R_{1\text{H}} + R_2^{\text{SC}} \cong 0.098 \text{ sec}^{-1}$ and for the remaining 69.9% Hg isotopes with $I=0$, $R_{1\text{H}} = R_{2\text{H}}$. This means that the average $R_{2\text{H}}$ value for the resonance due to Hg isotopes with $I=0$ and ^{201}Hg ($I=3/2$) collapsed resonance would be 0.090 sec^{-1} . Thus we see that the R_2^{SC} contribution of the $^{201}\text{Hg}(\text{CH}_3)_2$ is negligible.

BIBLIOGRAPHY

- Abraham, A., "The Principles of Nuclear Magnetism", Clarendon Press, 1961
- Akerlof, G., and J.W. Teare, J. Amer. Chem. Soc., 59, 1855(1937)
- Allerhand, A., J. Chem. Phys., 52, 3596(1970)
- Armstrong, R.L., and J.A. Courtney, Can. J. Phys., 50, 1262(1972)
- Atkins, P.W., A. Lowenstein, Y. Margalit, Mol. Phys., 17, 329 (1969)
- Bartoli, T.J., and T. A. Litovitz, J. Chem. Phys., 56, 404(1972)
- Bartoli, T.J., and T.A. Litovitz, J. Chem. Phys., 56, 413(1972)
- Batiz-Hernandez, H., and R.A. Bernheim, Progress in NMR Spect., 3, 63(1970)
- Beattie, I.R., G.P. McQuillan, L. Rule and M. Webster, J. Chem. Soc., 1514(1963)
- Bender, H.J., and M. Zeidler, Ber. Bunsenges. Phys. Chem., 75, 236(1971)
- Bernheim, R.A., and H. Batiz-Hernandez, J. Chem. Phys., 40, 3446(1964)
- Bernheim, R.A., and H. Batiz-Hernandez, J. Chem. Phys., 45, 2261(1966)
- Blayden, H.E., and M. Webster, J. Chem. Soc. (A), 2443(1969)
- Elicharski, J.S., Acta. Phys. Pol., 24, 817(1963)
- Bloch, F., Phys. Rev., 70, 460(1946)
- Bloembergen, N., E. Purcell and R.V. Pound, Phys. Rev., 73, 679(1948)
- Bloom, M., "Magnetic Resonance and Relaxation", ed. R. Blinc, North Holland, Amsterdam, 1967, p.65
- Bonera, G., and A. Rigamonti, J. Chem. Phys., 42, 171(1965)
- Bonner, N.A., J. Amer. Chem. Soc., 71, 3909(1949)

- Bopp, T., J. Chem. Phys., 47, 3621(1967)
- Brandon, C.I., Acta.Chem.Scand., 17, 759(1963)
- Bull, T.E., and J. Jonas, J.Chem.Phys., 52, 4553(1970)
- Caesar, G.P., and B.P. Dailey, J.Chem.Phys., 50, 4200(1969)
- Caspary, W.J., F. Millett, M. Reichbach and B.P. Dailey, J.Chem.Phys., 51, 623(1969)
- Carrington, A., and A.P. McLachlan, "Introduction to Magnetic Resonance", Harper and Row, 1967
- Chan, S.O., PhD. Thesis, Simon Fraser University (1969)
- Cukler, R.I. and K. Lakatos-Lindenberg, J. Chem.Phys., 57, 3427(1972)
- Cunningham, D., M.J.Frazer and J.D. Donaldson, J. Chem. Soc., 1647(1972)
- Dailey, B.P., and P.K. Bhattacharyya, Mol. Phys., 26, 1388(1973)
- Debye, P., "Polar Molecules", Dover (1929)
- Deverell, C., Mol. Phys., 18, 319(1970)
- Donaldson, J.D., D. Cunningham and M.J.Frazer, J. Chem. Soc. (A) 1647(1972)
- Durig, J.R., S.M. Craven, and J. Bragin, J. Chem. Phys., 52, 2046(1970)
- Egelstaff, P.A., D.I. Page and J.G. Powles, Mol. Phys., 20, 281(1971)
- Evans, D.F., and P.A.W. Dean, J. Chem. Soc. (A), 1154(1968)
- Farrar, T.O., S.J. Bruck, R.R. Shoup and E.D. Becker, J. Amer. Chem. Soc., 94, 699(1972)
- Fitzman, M., and K. Rider, J. Chem. Phys., 51, 2425(1969)
- Flygare, W.H., J. Chem. Phys., 41, 793(1964)
- Fraenkel, M., and W. Burlant, J. Chem. Phys., 42, 3724(1965)
- Freeman, R. and H.D. Hill, 5th Conference on Molecular Spectroscopy, England, Sept. 1971

- Gierer, A., and K. Wirtz, *Z. Naturforsch.*, A8, 532(1953)
- Gillen, K.T., and J.H. Noggle, *J. Chem. Phys.*, 53, 801(1970)
- Gillen, K.T., M. Schwartz and J.H. Noggle, *Mol. Phys.*, 20, 899(1971)
- Gillen, K.T., and J. E. Griffiths, *Chem. Phys. Lett.*, 17, 359(1972)
- Gillen, K.T., D.C. Douglas, M.S. Malmberg and A.A. Maryott, *J. Chem. Phys.*, 57, 5170(1972)
- Gillen, K.T., J.H. Noggle and T.K. Leipert, *Chem. Phys. Lett.*, 17, 505(1972)
- Gillen, K.T., J.H. Noggle and T.K. Leipert, *J. Mag. Res.*, 13, 158(1974)
- Gilman, H., and R.E. Brown, *J. Amer. Chem. Soc.*, 51, 928(1929)
- Gold, W., H.N. Colli, and J.E. Pearson, *J.C.S. Chem. Comm.*, 408(1973)
- Goldberg, H.S., and P.S. Pershan, *J. Chem. Phys.*, 58, 3816(1973)
- Gordy, W., W.V. Smith and R.F. Trambarulo, "Microwave Spectroscopy", Dover (1953)
- Gordon, R.G., *Advances in Magnetic Resonance*, 3, 1 (1968)
- Gordon, R.G., *J. Chem. Phys.*, 44, 1830(1966)
- Grant, D.M., K.F. Kuhlmann, and R.K. Harris, *J. Chem. Phys.*, 52, 3439(1970)
- Grant, D.M., K.F. Kuhlmann, and R.K. Harris, *J. Phys. Chem.*, 75, 585(1971)
- Grant, D.M., K.F. Kuhlmann, and C.H. Wang, *J. Chem. Phys.*, 55, 4676(1971)
- Grishin, Yu.K., N.M. Sergeev and Yu. A. Ustynyuk, *Mol. Phys.*, 22, 711(1971)
- Gutowsky, H.S., and D.E. Woessner, *Phys. Rev.*, 104, 843(1956)
- Gutowsky, H.S., *J. Chem. Phys.*, 31, 1683(1959)
- Gutowsky, H.S., M. Karplus and D.M. Grant, *J. Chem. Phys.*, 31, 1278(1959)

- Hawk, R., Ph D. Thesis, University of Michigan (1973)
- Hertz, H.G., "Progress in NMR Spectroscopy", Vol. III, Pergamon press, Chapter 5, 1967
- Higasi, K., K. Bergmann and G.P. Smyth, J. Phys. Chem., 64, 880(1960)
- Hindermann, D.K. and C.D. Cornwell, J. Chem. Phys., 48, 4148(1968)
- Hubbard, P.S., Phys. Rev., 131, 1155(1963)
- Huntress Jr., W.T., J. Chem. Phys., 48, 3524(1968)
- Huntress Jr., W.T., Advances in Mag. Resonance, 4, 1(1970)
- Ishibashi, M., Y. Yamamoto and Y. Inoue, Bull. Inst. Chem. Res. Kyoto University, 37, 39(1959)
- Ivanov, E.N., Sov. Phys. JETP, 18, 1041(1964)
- Jonas, J., and J.M. DiGennaro, J. Chem. Phys., 50, 2392(1969)
- Kessler, V.D., A. Weiss and H. Witte, Ber. Bunsenges. Phys. Chem., 71, 3(1967)
- Kidd, R.G., R.W. Matthews and H.G. Spinney, J. Amer. Chem. Soc., 94, 6686(1972)
- Kidd, R.G., and H.G. Spinney, J. Amer. Chem. Soc., 95, 88(1973)
- Kidd, R.G., and H.G. Spinney, Inorganic Chemistry, 12, 1967(1973)
- Kivelson, D., and T. Keyes, J. Chem. Phys., 57, 4599(1972)
- Kuhlmann, K.F., D.M. Grant and R.K. Harris, J. Chem. Phys., 52, 3439(1970)
- La Puente de, J., Anales Soc. Espan. Fis. Quim., 20, 486(1922)
- Laulicht, I., and S. Meriman, J. Chem. Phys., 59, 252(1973)
- Lauterbur, P.C., J. Chem. Phys., 42, 799(1965)
- Lauterbur, P.C., and J.J. Burke, J. Amer. Chem. Soc., 83, 326(1961)
- Lauterbur, P.C., J.E. Ramirez, A. Loewenstein and M. Shporer, Chem. Comm., 214(1968)

- Lavery, B.J., and R.A. Bernheim, J. Chem. Phys., 42, 1464(1965)
- Levy, G.C., J.C.S. Chem. Comm., 352(1972)
- Litchman, W.M., M. Alei Jr., and A.E. Florin, J. Chem. Phys., 50, 1897(1969)
- Litchman, W.M., and M. Alei Jr., J. Chem. Phys., 56, 5818(1972)
- Lyerla Jr., J.R., D.M. Grant and R.D. Bertrand, J. Phys. Chem., 75, 3967(1971)
- Maciel, G.E., P.D. Ellis and D.C. Hofer, J. Phys. Chem., 71, 2160(1967)
- Maryott, A.A., T.C. Farrar, and M.S. Malmberg, J. Chem. Phys., 54, 64(1971)
- Mitchell, R.W., and M. Eisner, J. Chem. Phys., 33, 86(1960)
- Mc Clung, R.E.D., J. Chem. Phys., 51, 3842(1969)
- Mc Clung, R.E.D., J. Chem. Phys., 57, 5478(1972)
- Mc Farlane, W., J. Chem. Soc. (A), 528(1967)
- Negita, H., S. Ichiba, M. Mishima, and H. Sakai, Bull. Chem. Soc. Japan, 41, 49(1968)
- Neumann, H.M., J. Amer. Chem. Soc., 76, 2611(1954)
- O'Reilly, D.E., J. Chem. Phys., 49, 5416(1968)
- O'Reilly, D.E., J. Chem. Phys., 55, 2155(1971)
- O'Reilly, D.E., J. Chem. Phys., 57, 885(1972)
- O'Reilly, D.E., J. Chem. Phys., 57, 890(1972)
- O'Reilly, D.E., E.M. Peterson and D.L. Hogenboom, J. Chem. Phys., 57, 3969(1972)
- Ozier, I., L.M. Crapo and N.F. Ramsey, J. Chem. Phys., 49, 2314(1968)
- Parker, R.G., and J. Jonas, Rev. of Sci. Inst., 41, 319(1970)
- Pines, A., W.K. Shim and J.S. Waugh, J. Chem. Phys., 54, 5438 (1971)

- Poole, C.P., and H.A. Faracah, "Relaxation in Magnetic Resonance", Academic Press(1970)
- Powles, J.G., Ber. Bunsenges. Phys. Chem., 67, 328(1963)
- Powles, J.G., and D.W. Sawyer, Mol. Phys., 21, 89(1971)
- Ramsey, N.F., "Molecular Beams", Oxford Press (1956)
- Ramsey, N.F., Phys. Rev., 78, 699(1950)
- Reeves, L.W., and B.K. Hunter, Can.J. Chem., 46, 1399(1968)
- Rigny, P. and J. Virlet, J. Chem. Phys., 47, 4645(1967)
- Rothschild, W.G., J. Chem. Phys., 51, 5187(1969)
- Rothschild, W.G., J. Chem. Phys., 53, 3265(1970)A
- Rothschild, W.G., J. Chem. Phys., 53, 990(1970)B
- Rothschild, W.G., J. Chem. Phys., 57, 991(1972)
- Sawyer, D.W., and J.G. Powles, Mol. Phys., 21, 83(1971)
- Sharp, R.R., J. Chem. Phys., 57, 5321(1972)
- Sharp, R.R., 14th NMR Conference, Boulder, Colorado (1973)
- Sharp, R.R., private communication (1974)
- Spriss, H.W., D. Schweitzer, U. Haberlen and K.H. Hausser, J. Mag. Resonance, 5, 101(1971)
- Tiers, G.V.D., J. Amer. Chem. Soc., 79, 5585(1957)
- Van derHart, 14th ENC Conference , Boulder, Colorado (1973)
- Van Geet, A.L., and D.N. Hume, Analytical Chem., 37, 983(1965)
- Tuks, M.F., and I.A. Chernyavskaya, Dokl. Akad. Nauk. USSR, 145, 549(1962)
- Wang, C.H., J. Mag. Res., 9, 75(1973)
- Waring, G.E., and W.S. Horton, J. Amer. Chem. Soc., 67, 540(1945)
- Wells, E.J., and K.H. Abramson, J. Mag. Res., 1, 378(1969)
- Wells, E.J., T.P. Higgs and A. Brooke (unpublished results)

Wimmett, T.F., Phys. Rev., 91, 476(1953)

Woessner, D.E., B.S. Snowden, and E.T. Strom, Mol. Phys., 14, 265(1968)

Wofsy, S.C., J.S. Muentzer and W. Klemperer, J. Chem. Phys., 53, 4005(1970)

Woodward, L.A., and L.E. Anderson, J. Chem. Soc., 1284(1957)

Zeidler, M.D., Ber. Bunsenges. Phys. Chem., 69, 659(1965)